UNIVERSITY OF HAWAII
LIBRARY
JAN 18 '51

The
PHILOSOPHICAL MAGAZINE

FIRST PUBLISHED IN 1798

. 41 SEVENTH SERIES No. 323 December, 1950

A Journal of Theoretical Experimental and Applied Physics

EDITOR
PROFESSOR N. F. MOTT, M.A., D.Sc., F.R.S.

EDITORIAL BOARD
SIR LAWRENCE BRAGG, O.B.E., M.C., M.A., D.Sc., F.R.S.
ALLAN FERGUSON, M.A., D.Sc.
SIR GEORGE THOMSON, M.A., D.Sc., F.R.S.
PROFESSOR A. M. TYNDALL, C.B.E., D.Sc., F.R.S.

PRICE 10s.
Annual Subscription £5 2s. 6d. payable in advance.

D AND PUBLISHED BY TAYLOR & FRANCIS LTD., RED LION COURT, FLEET ST., LONDON, E.C.4.

Early Scientific Publication

DIARY OF ROBERT HOOKE, M.A., M.D., F.R.S.
1672-1680

Edited by **H. W. ROBINSON** and **W. ADAMS**
Recommended for publication by the Royal Societ
London

25/-
net

"This vivid record of the scientific, artistic and soc activities of a remarkable man during remarkable years h too long remained in obscurity."—Extract from foreword Sir Frederick Gowland Hopkins, O.M., President of t Royal Society.

MATHEMATICAL WORK OF JOHN WALLIS, D.D., F.R.S.

By **J. F. SCOTT, Ph.D., B.A.**

12/6
net

"His work will be indispensable to those interested in t early history of The Royal Society. I commend to students of the Seventeenth Century, whether scientific humane, this learned and lucid book."—Extract from fo word by Prof. E. N. da C. Andrade, D.Sc., Ph.D., F.R.S.
Recommended for publication by University of Lond

CORRESPONDENCE AND PAPERS OF EDMOND HALLEY

Arranged and Edited by **EUGENE FAIRFIELD MACPIK**

21/-
net

First published on behalf of The History of Scien Society by Oxford University Press. Now re-issued Taylor & Francis, Ltd.

MEMOIRS OF SIR ISAAC NEWTON'S LIFE

By **WILLIAM STUKELEY, M.D., F.R.S., 1752**
From an Original Manuscript
Now in the possession of the Royal Society, Londo

5/-
net

HEVELIUS, FLAMSTEED AND HALLEY

Three Contemporary Astronomers and their Mutual Relati
By **EUGENE FAIRFIELD MACPIKE**
Published by arrangement with The History of Scien
Society

12/6
net

Established
over 150 years

TAYLOR & FRANCIS, LT
RED LION COURT, FLEET ST., LONDON E.
PRINTERS & PUBLISHERS OF SCIENTIFIC BOO

CONTENTS OF No. 323.

Page

CVII. The Radioactivity of F^{20}.—I. By J. V. JELLEY, Cavendish Laboratory, Cambridge 1199

CVIII. The Radioactivity of F^{20}.—II. By R. M. LITTAUER, Cavendish Laboratory, Cambridge 1214

CIX. The Emission of Short Range Alpha Particles from Light Elements under Proton Bombardment.—IV. The Reaction $^{19}F(p\alpha)^{16}O$. By JOAN M. FREEMAN, Cavendish Laboratory, Cambridge 1225

CX. An Interferometric Study of some Optical Properties of Evaporated Silver Films. By R. C. FAUST, Royal Holloway College. (Plates XXXVI. & XXXVII.) 1238

CXI. The "Velocity" of Brownian Movement. By R. FÜRTH, Birkbeck College, University of London 1255

CXII. The Use of Atmospherics to Study the Propagation of Very Long Radio Waves. By F. F. GARDNER, Cavendish Laboratory, Cambridge 1259

CXIII. The Force Acting on a Body Moving Uniformly through a Gas containing Sound Waves. By F. R. N. NABARRO, Department of Metallurgy, The University of Birmingham 1270

CXIV. A Note on the Decay of Current in Germanium Diodes. By J. R. TILLMAN and H. YEMM, The Post Office Engineering Research Station, London 1281

CXV. Correspondence :—
- Superconductivity of Niobium. By L. C. JACKSON and H. PRESTON-THOMAS, H. H. Wills Physical Laboratory, University of Bristol 1284
- Lattice Sums for Ionic Crystals. By F. C. FRANK, H. H. Wills Physical Laboratory, University of Bristol .. 1287
- Some Extensions in Use of Resistance Thermometry in the Study of Gaseous Explosions. By A. S. LEAH, C. ROUNTHWAITE and D. BRADLEY, University of Leeds 1289

CXVI. Notices of New Books and Periodicals received :—
- J. K. SYRKIN and M. E. DYATKINA'S Structure of Molecules and the Chemical Bond 1292

Index to Volume 1293

With Title-page, Contents, etc.

***All communications for the Philosophical Magazine should be addressed, post-paid, to the Editors, c/o Messrs. TAYLOR AND FRANCIS, LTD., Red Lion Court, Fleet Street, London, England.

CVII. *The Radioactivity of* F^{20}.—I.

By J. V. JELLEY *,
Cavendish Laboratory, Cambridge †.

[Received August 23, 1950.]

SUMMARY.

The beta and gamma radiation emitted by F^{20} has been studied by absorption, coincidence and spectrometer techniques. The upper limit of the beta particle spectrum was found to be $5{\cdot}03 \pm 0{\cdot}05$ MeV. and gamma rays of $1{\cdot}63 \pm 0{\cdot}02$ MeV. and $2{\cdot}45 \pm 0{\cdot}06$ MeV. with an intensity ratio of $(8{\cdot}4 \pm 2{\cdot}6)$ to 1 were also observed. No gamma–gamma coincidences were found, and it is concluded that the predominant mode of disintegration of F^{20} leads to a 1·63 MeV. excited state of Ne^{20}. The total energy release $F^{20}-Ne^{20}$ is $6{\cdot}66 \pm 0{\cdot}05$ MeV., and the mass of F^{20} derived from this value is compared with that obtained from the F^{19} (dp) and F^{19} $(n\gamma)$ reactions.

§ 1. INTRODUCTION.

THE radioactive nucleus F^{20}, of 12 seconds half-life, decays into Ne^{20} with the emission of beta and gamma radiations. Measurements of the energies of these radiations and observations of beta–gamma and gamma–gamma coincidences suggested the decay scheme shown in fig. 1. (Hornyak and Lauritsen 1948, Mattauch and Flammersfeld 1949.)

According to this scheme the emission of a beta-spectrum with an upper limit of 5·1 MeV. leads to the formation of Ne^{20} in an excited state of 2·2 MeV. from which gamma-ray transitions take place either directly to the ground state or via an intermediate state of about 1·6 MeV. Though the lower energy gamma-rays were known to be present (Bower and Burcham 1939, Curran and Strothers 1940), their energy was only inferred from evidence for an excited state of Ne^{20} at 1·6 MeV. obtained in observations on the neutron groups from the reaction F (dn) Ne^{20} (Bonner 1939, and Powell 1940). The total energy release in the decay process on the assumption of this decay scheme is in fair agreement with that derived from the energy release in the reaction F^{19} (dp) F^{20} (Bower and Burcham 1939).

The present experiments were undertaken to improve the energy measurements, to obtain more precise information on the gamma–gamma coincidences, to determine the branching ratio for the two alternative de-excitation modes of the 2·2 MeV. level of Ne^{20} and to detect the

---

[*] Communicated by Dr. W. E. Burcham.

[†] Now at the Atomic Energy Research Establishment, Harwell.

gamma-ray of energy ~0·6 MeV. which must be present according to this decay scheme. In the course of the work it appeared that the decay scheme shown in fig. 1 (decay scheme I.) was incorrect and a revised scheme is presented, together with new measurements of the beta- and gamma-ray energies. A new determination of the energy release in the reaction F^{19} (*dp*) F^{20} was also made.

This work was completed in the summer of 1949, and a preliminary account of it has already appeared (Jelley 1950). It has recently been repeated in part and extended by R. M. Littauer in the Cavendish Laboratory ; his results are presented in the following paper (II.).

Fig. 1.

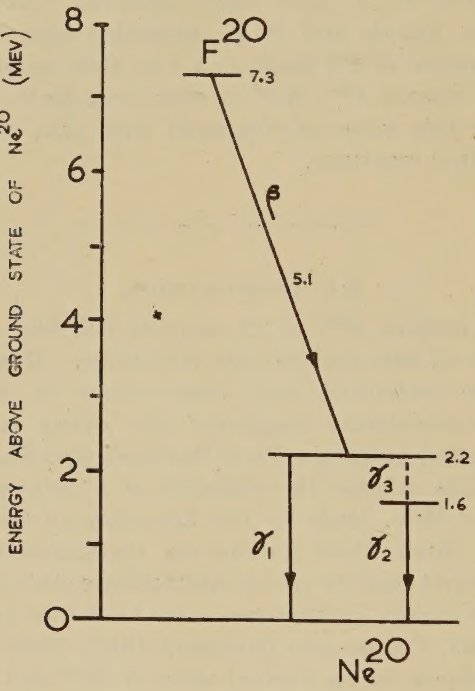

Accepted decay scheme of F^{20} (decay scheme I).

§ 2. Experimental Technique.

(a) *Production of* F^{20}.

F^{20} was produced by irradiating thick barium or calcium fluoride targets with deuteron beams of 1–50 μamps. at bombarding energies between 500 and 930 keV. The beam was interrupted periodically by an electromagnetically operated shutter to give suitable irradiation and decay periods T_i and T_d. During the irradiation periods, the Geiger counters used in measuring and monitoring the beta- and gamma-radiations were electrically suppressed to avoid high counting rates and to eliminate counting of " prompt " radiations from the target.

The essential features of the layout of the shutter box, analysing magnet and target tube have been described elsewhere (Jelley and Paul 1948).

Background counting rates, due to shutter radiations, activities present in the analysing magnet, and target activities of longer period than those due to F^{20}, were obtained by stopping the commutator used to operate the cyclic irradiation procedure, leaving the beam on the shutter and counting after a lapse of time for the F^{20} to decay.

(b) *Beta-ray absorption* (see fig. 2 (*a*)).

Two cylindrical aluminium counters, of diameter 2·2 cm., length 6·0 cm. and wall thickness 0·034 gm./cm.^{2} were mounted in a lead housing as shown, with a partition of thickness 11·6 gm./cm.^{2}. Counter M was used as a monitor while various absorbers were placed in front of counter A.

Fig. 2.

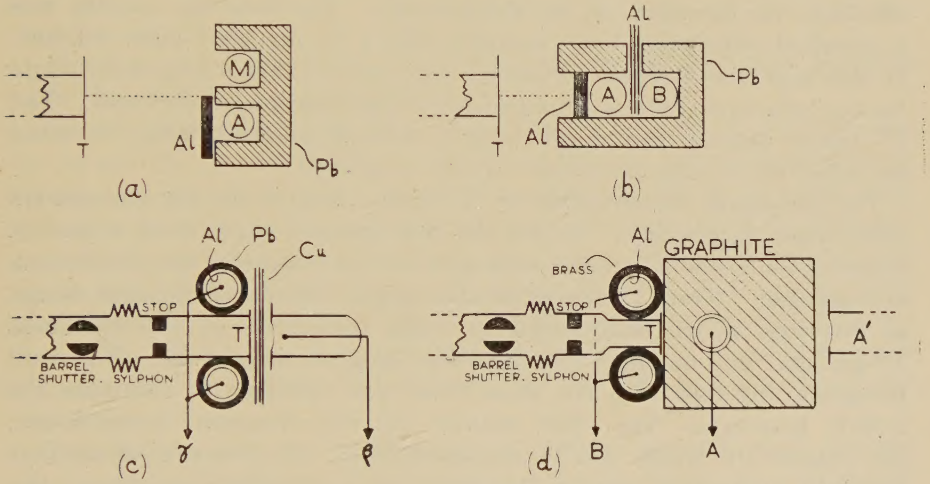

Counter arrangements for study of F^{20} activity.
(*a*) Beta-ray absorption.
(*b*) Gamma-ray absorption.
(*c*) Beta-gamma coincidences.
(*d*) Gamma-gamma coincidences.

The counters were situated 28 cm. from the target, T. In this experiment a beam of 50 μamp. at 750 keV. was used, to irradiate a thick BaF_2 target, and the values for T_i and T_d were 10·7 and 8·8 sec. respectively.

(c) *Gamma-ray absorption* (see fig. 2 (*b*)).

The method of observing the secondary electron absorption (Bothe and Kolhörster 1929) was used to determine the energies of the gamma-rays. The F^{20} gamma-rays from an irradiated BaF_2 target emerged through the 0·64 gm./cm.^{2} brass target support and entered the " thick " aluminium radiator of thickness 3·4 gm./cm.^{2}; the 5 MeV. beta-rays were excluded by the radiator and target support. The secondary electrons produced in the radiator passed through two counters A and B in coincidence, aluminium absorbers being placed between the counters which were of diameter 2·2 cm., active length 6·0 cm., and of wall thickness 34 mg./cm.^{2}. In this experiment $T_i=10{\cdot}7$ sec., $T_d=5{\cdot}2$ sec., and the beam energy and current were 900 keV. and 50 μamp. respectively.

(d) *Beta–gamma and gamma–gamma coincidence experiments.*

The arrangement of counters in the beta-gamma coincidence experiments is shown in fig. 2 (*c*). A CaF_2 target was deposited on a 0·68 gm./cm.^{2} brass support and bombarded by a collimated deuteron beam so that the active F^{20} covered an area 4 × 7 mm.^{2}. To provide increased efficiency and to compensate for fluctuations in beam position, the gamma-rays were detected by two counters connected in parallel. These counters were similar to those used in the absorption experiments, but were surrounded by cylindrical lead converters of thickness (2·9 gm./cm.^{2}) adequate to exclude the 5 MeV. beta-rays while providing the highest efficiency for detection of the gamma-rays. The beta-ray counter was a standard cylindrical brass counter with a 10 mg./cm.^{2} mica window. In this experiment copper absorbers were used so that a large solid angle for the beta-rays could be obtained with large absorption thickness. The F^{20} source activity was chosen to give suitable counting rates ; it could be varied by altering the beam current or energy.

Fig. 2 (*d*) shows the arrangement of counters used in the gamma–gamma coincidence experiment. As for the beta–gamma experiment a pair of counters connected in parallel were used for one channel of the coincidence arrangement. These (B) were two aluminium counters of the same design as described above, surrounded by brass converters of wall thickness 3·9 gm./cm.^{2} and mounted one each side the glass target tube. This wall thickness, together with the glass tube, was sufficient to eliminate the 5 MeV. beta-rays. The other counter (A) was of special construction, the reasons for which will be discussed later. It consisted of another standard aluminium counter immersed in a graphite converter ; the thickness of graphite between the target and counter wall was sufficient to exclude the 5 MeV. beta-rays. A BaF_2 target was used, mounted on a brass support of thickness 0·26 gm./cm.^{2}, the bombarded area of the target was 4 × 5 mm.^{2}. In both these experiments T_i and T_d were set to 1·0 and 2·6 sec. respectively. For the second part of the gamma–gamma coincidence experiment, in which a beta-counter A′ replaces the gamma-ray counter, the counter used in the beta-ray absorption experiment was employed.

Errors resulting from variations in mean source strength during an experiment were minimized by maintaining the single counting rates as nearly constant as possible during a run. Corrections were applied to the observed coincidence rates to allow for the fact that the counting periods were comparable with the half-life of the activity. The coincidence unit was similar to that described elsewhere (Jelley 1948) ; the coincidence resolving time was checked from time to time and had the average value $0{\cdot}63 \pm 0{\cdot}02$ μsec.

(e) *Spectrometer.*

The spectrometer used for the beta- and gamma-ray energy measurements was an iron-cored instrument with 90° focusing, built by R. M. Littauer and described in the following paper (II.). For the beta-ray measurements the spectrometer was connected directly to the target chamber in which the F^{20} was formed. The overall resolving power and geometrical aperture were 3·5 per cent and 0·031 steradians respectively and the instrument was calibrated for the following energies : (i) 148 keV., the energy of the internally converted gamma-ray F-line from ThB ; (ii) 6·8 MeV. which is the maximum energy of the Compton electron distribution from the 6·98 MeV. component of the gamma–radiation from the reaction $F^{19}(p\alpha', \gamma)O^{16}$ (Walker and McDaniel 1948). The calibration for gamma-ray energy measurements is described in II.

§ 3. RESULTS.

(a) *Beta-ray energy.*

Fig. 3 shows the absorption curve in aluminium obtained experimentally with the counter arrangement of fig. 2 (*a*).

The curve is normalized, after correcting to a constant counting rate in the monitor, to an effective intensity of 100 per cent at zero absorber thickness. The gamma-ray background, followed out further than that included in the figure, was extrapolated back and intercepted the intensity axis at 12 per cent. The true beta-absorption curve after subtraction of the background is also shown. To obtain the true origin of this curve a correction term, of 0·509 gm./cm.^{2} must be added to the absorption figures to include absorptions in (i) the BaF_2 target layer, (ii) the brass target support, (iii) the counter wall and (iv) the air path between target and counters.

The beta-ray end-point energy was derived by the method of analysis developed by Bleuler and Zünti (1946), in which curves are constructed relating values of the maximum energy $E_{\beta\max}$ to absorber thicknesses d_n corresponding to reductions in intensity by factors $1/2^n$ of that with no absorber ; the family of curves published by these workers strictly apply only to the case of allowed Fermi spectra from nuclei of Z-value 20. Correcting for the initial absorption mentioned above and using Bleuler and Zünti's curves, values of 4·98, 4·90, 4·92 and 4·86 were obtained for $E_{\beta\max}$, giving a mean value of $4{\cdot}91 \pm 0{\cdot}08$ MeV. A correction term of +1 per cent must be added in transforming from Z=20 to Z=9 and the corrected value for $E_{\beta\max}$ is then $4{\cdot}96 \pm 0{\cdot}08$ MeV.

The relatively small spread among the values obtained suggests that the beta-spectrum consists at least predominantly of one component.

Fig. 4 shows the Kurie plot obtained with the spectrometer; the function $\sqrt{[N(E)/f]}$ is plotted against W, where $f=\sqrt{[W^2-1]}$ and $W=[1+(E/m_0c^2)]$, the total electron energy expressed in units of m_0c^2. N(E) is the relative counting rate per unit energy interval. From the intercept at

$$W=(10{\cdot}85 \pm 0{\cdot}10)m_0c^2$$

the beta-ray end-point energy was found to be

$$E_{\beta\max}=5\cdot03\pm0\cdot05 \text{ MeV}.$$

which agrees with that obtained by the absorption method within the limits of error. The beta spectrum also appears from the Kurie plot to consist predominantly of one component.*

Fig. 3.

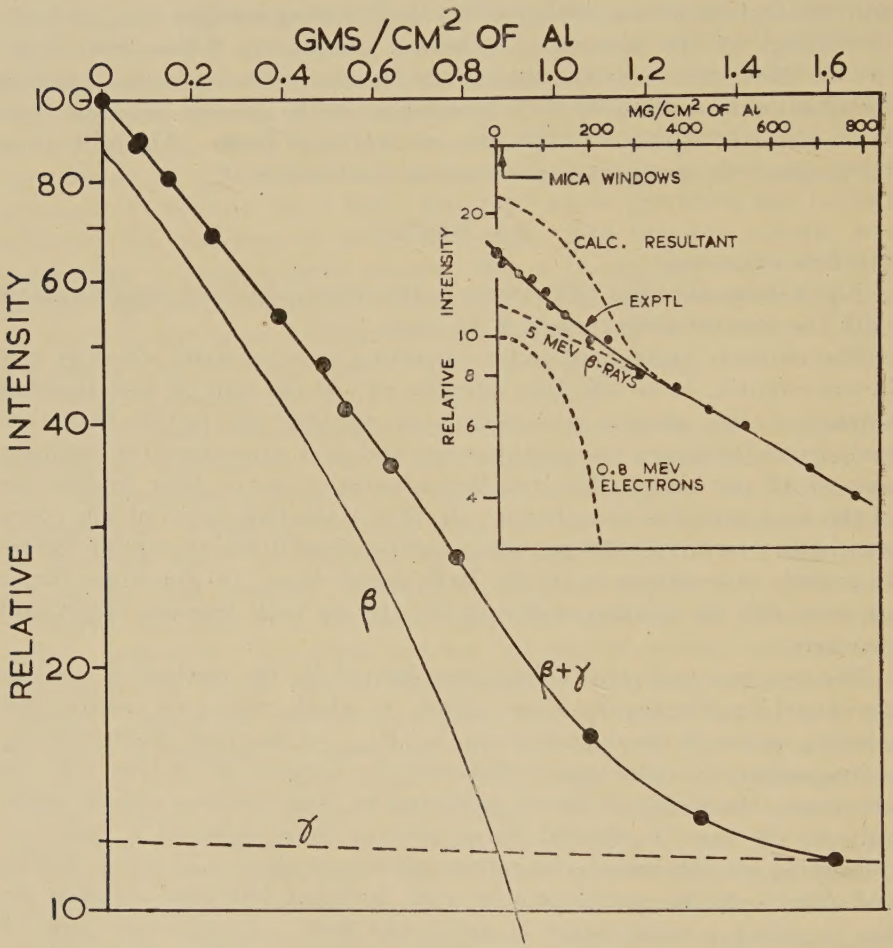

F^{20} beta-radiation absorption curve.
Inset : more detailed survey of low absorption region.

The period of the beta activity was found to be 12·6±0·1 seconds which is rather higher than the value of 10·7±0·2 sec. recently reported (Snowdon 1950).

---

* In the more recent experiments reported in II., the presence of a weak beta component of higher energy was established. A rather higher upper limit (5·3 MeV.) for the main beta spectrum was obtained.

(b) *Gamma-ray energy and intensity.*

Fig. 5 shows the secondary electron absorption curve obtained with the counter arrangement shown in fig. 2 (*b*). The ordinates give relative values of the ratio of coincidences to front counter rates (N_C/N_A) normalized to 100 per cent at zero absorber thickness; the background was obtained from observations with absorber thicknesses greater than those shown in the figure.

Fig. 4.

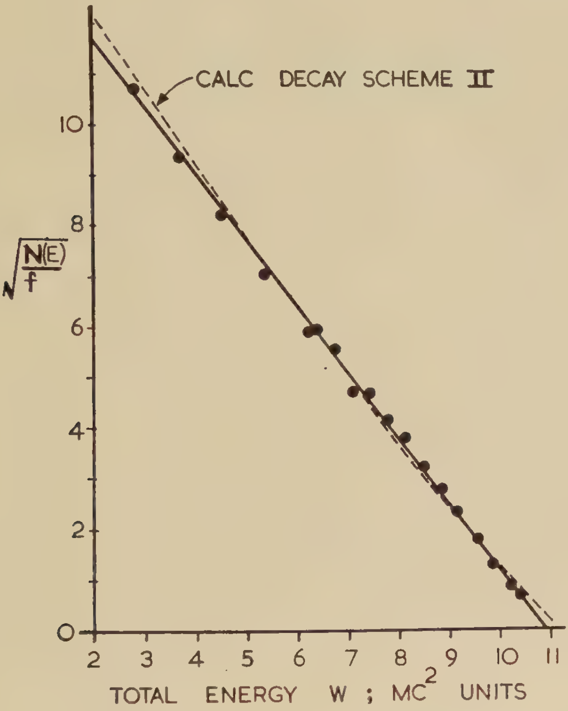

F^{20} beta spectrum. Kurie plot.

It appears from this absorption curve that there are two main components, with an intensity ratio (by inspection) of between 5 and 10 to 1. The energies of these components were derived by the method due to Bleuler and Zünti (1946, fig. 8), assuming that particular intensity ratio (6·6/1), for the two components which gave the minimum spread in the energy values found for the two radiations. The energies so obtained were:

$E_{\gamma 1}$ 1·87, 1·75, 1·68, 1·62, 1·56, 1·51 and 1·47 MeV.

$E_{\gamma 2}$ 2·66, 2·54, 2·41, 2·36, 2·44 and 2·30 MeV.

giving mean values

$$E_{\gamma 1}=1{\cdot}64\pm0{\cdot}05 \text{ MeV.}, \qquad E_{\gamma 2}=2{\cdot}45\pm0{\cdot}06 \text{ MeV.}$$

It was found by experiments with gamma-ray sources of known energy that the ratio of coincidences to front counter rate with no absorber, denoted by $(N_C/N_A)_0$, depended on the incident gamma-ray energy. The ratio of intensities of the two components which gave the best results in the Bleuler–Zünti analysis must therefore be corrected for the energy dependence of the ratio $(N_C/N_A)_0$ to give the true intensity ratio.

Fig. 5.

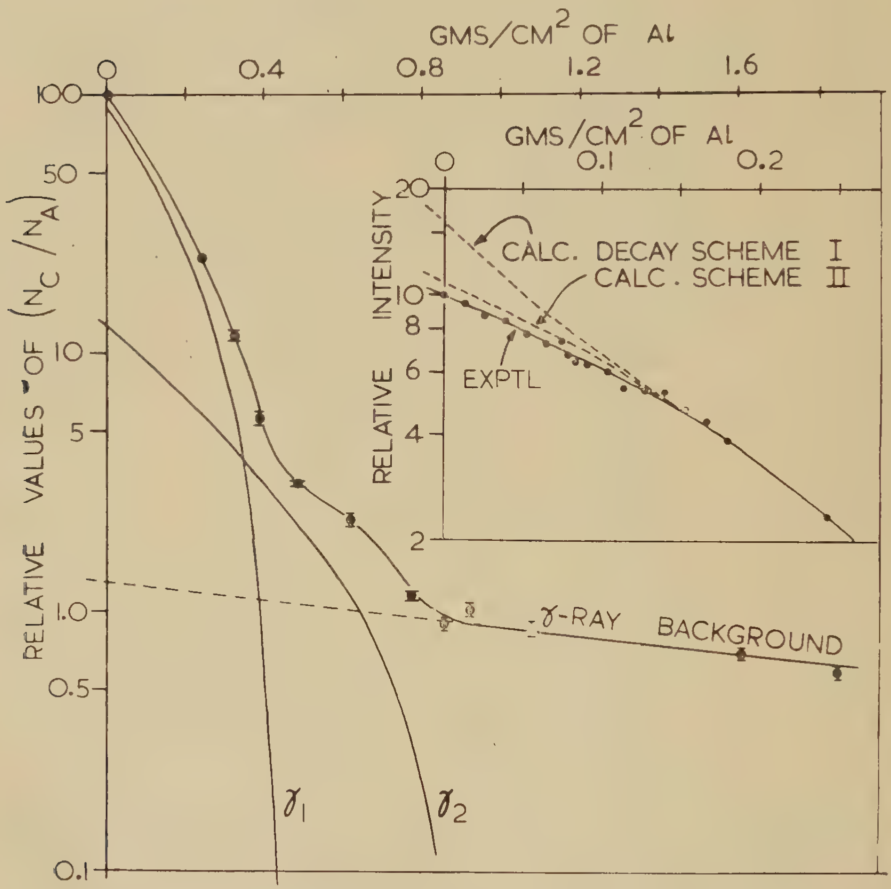

F^{20} gamma-radiation. Absorption of secondary electrons. Inset : more detailed examination of low absorption region.

With this correction, and estimating the errors in extrapolation, it was found that

$$\frac{I_{\gamma 1}}{I_{\gamma 2}} = (8{\cdot}4 \pm 2{\cdot}6)/1,$$

which means relative intensities of 89 per cent and 11 per cent for the soft and hard components respectively.

The results obtained using the spectrometer are described in II. The energy of the hard component could not be measured owing to its low intensity, but that of the softer radiation was found to be $1{\cdot}63 \pm 0{\cdot}02$ MeV., in good agreement with the absorption measurement. The period of the gamma-ray activity was found to be about 12 seconds ; no determination of the periods was made for the two components separately (*cf.* II.).

(c) *Possible existence of a lower energy gamma-ray.*

According to the decay scheme I., fig. 1, there should be a gamma-ray of energy 800 keV. (using present values for the other gamma-ray energies) in cascade with the 1·64 MeV. radiation and of equal intensity. In an attempt to establish the existence of this radiation the low energy region of the curve shown in fig. 5 was studied in detail (see fig. 5 inset) using thin absorbers. Fig. 5 (inset) gives, together with the experimental curve, and fitted to it at the point for 0·15 gm./cm.^{2}, the calculated curve for decay scheme I., fig. 1. Comparison of these two curves shows that there is no 800 keV. gamma-radiation present in intensity comparable with that of the 1·64 MeV. component.

The possibility of total internal conversion of the 800 keV. radiation* was investigated by observing the beta-ray absorption curve carefully over the region 0–800 mgm./cm.^{2} of aluminium. Thin windows were used on the target chamber and counters. The curve obtained is shown inset in fig. 3, together with the curve calculated assuming that each quantum of 1·64 MeV. radiation is accompanied by a 800 keV. internal conversion electron. The curves given by Bleuler and Zünti were used for the beta-ray absorption and the data published by Marshall and Ward (1937) for the homogeneous conversion electrons ; the calculated and experimental curves are fitted at the 400 mgm./cm.^{2} point. Comparison of the two curves shows that there are no internal conversion electrons of 800 keV. in the right intensity ; the slight concave rise at low absorption occurred with other beta-ray sources.

(d) *Beta–gamma coincidences.*

Curran and Strothers (1940) found coincidences between beta- and gamma-rays in the decay of F^{20} and and showed that the absorption of beta-gamma coincidences followed closely that of the beta-rays. Their conclusion that the dominant beta and gamma-ray components are coupled, was confirmed using the counter arrangement shown in fig. 2(*c*). Observation of the single counter rates N_β, N_γ, and the coincidence rate $N_{\beta\gamma}$ were made ; the latter was corrected for chance rate N_c using the relation $N_c = 2\tau N_\beta N_\gamma$. A background correction, obtained by observations with a thick absorber, was made to the observed values of N_β to obtain the true counting rate in the β-counter due to F^{20} beta-rays ; this correction became very large near the end-point of the beta-ray absorption curve.

---

* The author is grateful to Professor S. Devons for suggesting this possibility.

In fig. 6 is shown a plot of the values of the ratio $N_{\beta\gamma}/N_\beta$ versus absorber thickness, the corrections discussed above having been applied. On this figure are also included the cut-off points corresponding to the two beta-ray energies involved in the alternative decay scheme to be presented later. Owing to the poor statistics it was impossible to obtain evidence in favour of a particular decay scheme, though the result was consistent with the previous evidence that at least the dominant beta ray component proceeds to an excited state of Ne^{20}.

(e) *Gamma–gamma coincidences.*

Owing to the high energy of the beta-radiation from F^{20}, some or all of the gamma–gamma coincidences observed by Curran and Strothers (1940) in their arrangement, in which lead-walled counters were used, may have been due to bremsstrahlung. With this in mind it was decided to use the counter arrangement of fig. 2 (*d*), in which one counter was constructed of graphite, in a study of gamma–gamma coincidences.

Fig. 6.

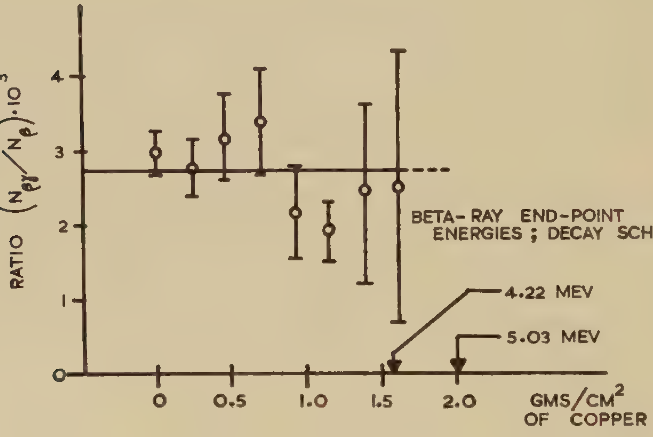

Results of beta-gamma coincidence experiment.

It is essential to carry out a gamma–gamma coincidence experiment on a quantitative basis if the resulting evidence is to be used to assist in the designation of a particular decay scheme. With this aim in view, a method originally proposed by Dunworth (1940) and more recently developed by Wiedenbeck (1947), was applied to a study of gamma–gamma coincidences from F^{20}. Essentially the method consists firstly of carrying out a gamma–gamma coincidence experiment and, secondly, repeating it after one of the gamma-ray counters has been replaced by a beta-ray counter; the single and beta-gamma and gamma–gamma coincidences are measured, from which various ratios can be set up; these ratios, which are different for different decay schemes, are then compared with calculated values, using measured values of counter efficiencies.

With the arrangement already described, sets of gamma–gamma and beta–gamma coincidence runs were carried out, counter A being replaced by the beta-counter A′ for the beta–gamma runs, taking care not to disturb the geometry of the counters B. Ten gamma–gamma and four beta–gamma runs were made. As before, the individual and coincidence rates were found from the number of irradiation cycles and counting periods, after a predetermined number of coincidences had accumulated; these figures were set at 200 and 400 for gamma–gamma and beta–gamma runs respectively.

Correcting the single counter rates for backgrounds and the observed coincidence rates for chance coincidences, the following ratios were obtained after compounding the ten gamma–gamma and four beta–gamma runs :—

$$\left.\begin{array}{ll}\text{From the } \gamma\gamma \text{ runs } N_{\gamma\gamma}/N_{A\gamma} & =(3{\cdot}03\pm0{\cdot}23)\times10^{-4}. \\ \text{From the } \beta\gamma \text{ runs } N_{A'\beta}/N_{\beta\gamma} & =523\pm40.\end{array}\right\}$$

The errors quoted here are standard deviations calculated from the spread among the ratios of the varoius rates in the two types of runs.

From the above figures, the value obtained for the ratio R, defined by

$$R=\frac{N_{\gamma\gamma}}{N_{A\gamma}}\cdot\frac{N_{A'\beta}}{N_{\beta\gamma}}$$

is

$$R_{\text{obs}}=0{\cdot}16\pm0{\cdot}02.$$

R is a function of the gamma-counter efficiences and the branching ratio of the altenative gamma-transitions; inserting the various values for these quantities, the derivations of which are discussed in Appendix A, the value of R for decay scheme I (fig. 1) is found to be

$$R_{\text{calc}}=0{\cdot}47.$$

It will be seen that the experiment gives too low a gamma–gamma coincidence rate for decay scheme I. and, furthermore, it is likely that some or all of these observed coincidences are false since :

(*a*) an approximate calculation of the effects of bremsstrahlung showed that even with the graphite counter, enough coincidences could exist to account wholly for the observed rate ;

(*b*) the formation of N^{13} on the target, due to the reaction $C^{12}(dn)N^{13}$ could have provided a source of coincident radiations comparable in strength with that observed.

A repetition of this experiment under better conditions (II.) has confirmed that the number of genuine gamma–gamma coincidences in the decay of F^{20} is very small.

§ 4. DISCUSSION.

(a) *The Decay Scheme of* F^{20}.

The small number of genuine gamma–gamma coincidences and the absence of a gamma-ray of energy 800 keV. in intensity comparable with that of the 1·64 MeV. radiation from F^{20} are incompatible with decay scheme I. (fig. 1). The results are, however, consistent with the decay scheme II., fig. 7, in which the 1·64 MeV. gamma radiation follows the beta particle emission. The fitting of the 2·45 MeV. gamma-radiation into this scheme requires a complex beta particle spectrum, and a slightly curved Kurie plot should have been found. The expected deviation from linearity (shown in fig. 4) is, however, small and would have escaped detection.

(b) *The mass of* F^{20}

Direction determinations of the mass of F^{20} in terms of that of F^{19} can be obtained from the energy release in the reactions F^{19} (dp) F^{20} and F^{19} $(n\gamma)$ F^{20}. A repetition of the observations of Bower and Burcham (1939) on the F^{19} (dp) reaction was made (see Appendix B), and a Q-value of 4·48±0·04 MeV. was obtained. Using the masses of the proton, deuteron and alpha particle given by Rosenfeld (1948), and for the mass of F^{19} the value 19·00449±0·00003 * (Tollestrup, Fowler and Lauritsen 1950) the mass of F^{20} is found to be 20·00626±0·00005. The observations of Kinsey, Bartholomew and Walker (1950) on the energy of the capture radiation in the F^{19} $(n\gamma)$ reaction lead to a mass for F^{20} of 20·00632±0·00006. The average of these two values is 20·00629±0·00005.

Fig. 7.

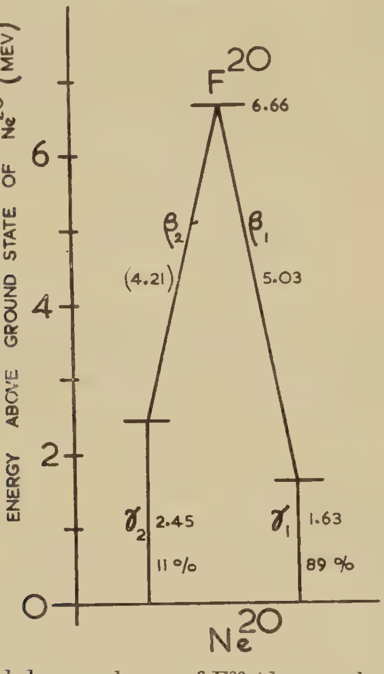

Proposed decay scheme of F^{20} (decay scheme II.).

---

* This recently published value has been adopted in preference to that used in the first report of these results (Jelley 1950).

The present results enable the mass of F^{20} to be found in terms of that of Ne^{20}, for which the value $19{\cdot}99890 \pm 0{\cdot}00006$ (Rosenfeld 1948) is assumed. Using the energy values $E_{\beta}=5{\cdot}03 \pm 0{\cdot}05$ MeV. and $E_{\gamma}=1{\cdot}63 \pm 0{\cdot}02$ MeV. the energy release in the decay of F^{20} is, according to decay scheme II. (fig. 7) $6{\cdot}66 \pm 0{\cdot}05$ MeV. and the mass of F^{20} becomes $20{\cdot}00606 \pm 0{\cdot}00008$, which is rather lower than the previous estimates. If this value is correct, an additional long-range proton group might be expected in the F^{19} (*dp*) reaction, but this could not be found. It seems possible, however, from the work reported in II. that the beta-particle energy may have been underestimated in the present experiments.

APPENDIX A.

Determination of the gamma-ray counter efficiencies and the evaluation of R *in the gamma-gamma coincidence experiment.*

Before evaluating the quantity R defined in §3 (e), it was necessary to determine the gamma-ray counter efficiencies at a number of gamma-ray energies. We will here denote these efficiencies by ϵ with two suffixes, the first indicating the energy of the radiation and the second to denote which counters are meant (*cf.* fig. 2(*d*)). The calibration was carried out by placing a $1{\cdot}4\,\mu$C Co^{60} source in the centre of the target area and finding the single and coincidence counting rates with the counters in their normal position. Assuming the mean energy of the gamma-radiation to be 1·2 MeV. and a zero angular correlation between the two components, the following absolute values for the overall efficiencies of the two counters were obtained

$$\epsilon_{1\cdot 2A}=7{\cdot}3\times 10^{-4} \text{ and } \epsilon_{1\cdot 2B}=2{\cdot}0\times 10^{-3}.$$

Use was then made of curves published recently by Maier-Leibnitz (1946) to obtain the relative values of the efficiencies at other energies; in this way the absolute efficiencies were determined for the following energies :

Counter	0·8	1·6	2·4	MeV.
A (graphite+Al)	4·8	9·4	13·0	$\times 10^{-4}$
B (brass+Al)	1·4	2·7	4·1	$\times 10^{-3}$

In this calculation it was assumed that counter A was made entirely of aluminium and counters B of brass ; the corresponding curves given by Maier-Leibnitz being employed. These assumptions are justified since (*a*) the aluminium walls of the counters proper were of a thickness small compared to the range of the secondary electrons, (*b*) graphite and aluminium have comparable values of density and atomic number, and (*c*) over the range of energies considered the form of the efficiency-vs.-energy curve is similar for aluminium and brass.

The ratio R, defined in § 3 (e) is a function of these efficiencies and the relative intensities of the radiations. The value of R for decay scheme I. assuming no angular correlation between the various gamma-ray components, is given by:

$$R_{\text{calc}} = \frac{f(\epsilon_{1\cdot 6B}\cdot\epsilon_{0\cdot 8A}+\epsilon_{0\cdot 8B}\cdot\epsilon_{1\cdot 6A})}{[f(\epsilon_{1\cdot 6B}+\epsilon_{0\cdot 8B})+(1-f)\epsilon_{2\cdot 4B}][f(\epsilon_{1\cdot 6A}+\epsilon_{0\cdot 8A})+(1-f)\epsilon_{2\cdot 4A}]}$$

where f and $(1-f)$ are the relative intensities of the (1·6 ; 0·8) and 2·4 MeV. transitions respectively. Inserting the absolute efficiencies obtained as described above and the value for f from § 3 (b) a value of 0·47 is obtained for R_{calc}. For decay scheme II $R_{\text{calc}}=0$.

APPENDIX B.

Determination of the Q-value of the Reaction F^{19} (*dp*) F^{20}.

In this experiment a thin BaF_2 target was bombarded by deuterons and the proton groups from the above reaction detected in a proportional counter. Calibrated mica absorbers were used to vary the residual range so that the various groups could be studied separately. Another proportional counter with a fixed amount of absorber was used for monitoring purposes. Direct resolution of the groups was found possible using a discriminator operating at high bias.

The protons of maximum energy were observed at three different angles with respect to the deuteron beam, 30°, 90° and 150° and their range was obtained by direct comparison with the range of the protons from the reactions C^{13}(*dp*) C^{14} and Be (*dp*) Be^{10} for which accurate Q-values are available. Throughout these experiments a deuteron energy of 930±15 keV. was used. The following Q-values were obtained:

Reference Reaction	Angle of Observation	Q MeV.
Be (*dp*) Be^{10}	30°	4·41
Be (*dp*) Be^{10}	90°	4·40
Be (*dp*) Be^{10}	150°	4·44
C^{13} (*dp*) C^{14}	30°	4·67
C^{13} (*dp*) C^{14}	90°	4·46
C^{13} (*dp*) C^{14}	150°	4·52

giving a mean value of 4·48±0·04 MeV.

ACKNOWLEDGMENTS.

The Author wishes to thank Dr. W. E. Burcham for his continual interest and advice through the work. Thanks are also due to R. M. Littauer for making available his spectrometer, to C. D. Curling and J. O. Newton who lent their apparatus for the (*dp*) experiment, and to W. Birtwhistle for maintenance and operation of the high-tension equipment.

The Author is indebted to the Department of Scientific and Industrial Research for financial assistance during the period of the work.

REFERENCES.

BLEULER, E., and ZUNTI, W., 1946, *Helv. Phys. Acta.*, **19**, 375.
BONNER, T. W., 1939, *Phys. Rev.*, **56**, 207.
BOTHE, W., and KOLHÖRSTER, W., 1929, *Z. f. Physik*, **56**, 751.
BOWER, J. C., and BURCHAM, W. E., 1939, *Proc. Roy. Soc.*, A, **173**, 379.
CURRAN, S. C., and STROTHERS, J. E., 1940, *Proc. Camb. Phil. Soc.*, **36**, 252.
DUNWORTH, J. V., 1940, *Rev. Sci. Instrum.*, **11**, 167.
HORNYAK, W. F., and LAURITSEN, T., 1948, *Rev. Mod. Phys.*, **20**, 191.
JELLEY, J. V., 1948, *Canad. J. Res.*, **26**A, 255; 1950, *Proc. Phys. Soc.*, A, **63**, 538.
JELLEY, J. V., and PAUL, E. B., 1948, *Proc. Camb. Phil. Soc.*, **44**, 133.
KINSEY, B. B., BARTHOLOMEW, G. A., and WALKER, W. H., 1950, *Phys. Rev.*, **78**, 481.
MAIER-LEIBUITZ, H., 1946, *Zeits. f. Naturforschung*, **1** (5), 243.
MARSHALL, J. S., and WARD, A. G., 1937, *Canad. J. Res.*, **15**A, 39.
MATTAUCH, J., and FLAMMERSFELD, A., 1949, *Isotopenbericht Zeits. f. Naturforschung.*
POWELL, C. F., 1940, *Nature, Lond.*, **145**, 155.
ROSENFELD, L., Nuclear Forces Fasc. II (Amsterdam: North Holland Publishing Co.).
SNOWDON, S. C., 1950, *Phys. Rev.*, **78**, 299.
TOLLESTRUP, A., FOWLER, W. A., and LAURITSEN, C. C., 1950, *Phys. Rev.*, **78**, 372.
WALKER, R. L., and MCDANIEL, B. D., 1948, *Phys. Rev.*, **74**, 315.
WIEDENBECK, M. L., 1947, *Phys. Rev.*, **72**, 429.

CVIII. *The Radioactivity of* F^{20}.—II.

By R. M. LITTAUER*,
Cavendish Laboratory, Cambridge †.

[Received August 23, 1950.]

SUMMARY.

Experiments on the radioactivity of F^{20} are described which give the following results: 3·5 per cent of the disintegrations go direct to the ground state of Ne^{20}, while the remainder leave Ne^{20} in an excited state of energy 1·63$\pm$0·02 MeV. The best present estimate of the F^{20} mass is 20·006 31$\pm$0·000 05, corresponding to a total energy release F^{20}—Ne^{20} of 6·87$\pm$0·07 MeV. A weak gamma ray of energy 1·0$\pm$0·1 MeV. is also observed, but its allocation to the decay of F^{20} is not established. Gamma–gamma coincidence experiments limit the fraction of disintegrations which produce *cascade* gamma rays to less than 2 per cent, unless one of the rays has a life-time longer than 10^{-6} sec.

§ 1. INTRODUCTION.

IN the preceding paper, hereafter referred to as I., J. V. Jelley has reported some experiments concerned with the short-lived beta emitter F^{20}. The main conclusion to be drawn from his work is the that dominant beta spectrum is linked with a single gamma ray. This result is borne out in the present investigation, which was undertaken with the object of clarifying some of the doubtful points raised in I. and of obtaining a more precise estimate for the mass-value of F^{20}.

§ 2. EXPERIMENTAL METHOD.

(a) *Production of* F^{20}.

F^{20} was produced throughout this work by intermittent bombardment of thin CaF$_2$ targets with 930 keV. deuterons, as described in I. The radiations were studied by spectrometer and coincidence counting methods. In the spectrometer experiments, the irradiation and counting periods were approximately equal in order to achieve maximum statistical accuracy. In the coincidence work, where the useful source strength is in any case limited, the bombarding periods were shortened and a greater fraction of the cycle was available for counting. The period of the switching operations was always short compared with the life-time of the decay.

---

* Communicated by Dr. W. E. Burcham.
† Now at Cornell University, Ithaca, N.Y.

(b) *The Beta Spectrometer.*

The spectrometer is a compact instrument of the 90° magnetic focusing type. This is a special case of the general group discussed by Stephens (1934): any homogeneous field extending over a wedge-shaped area gives simple refocusing of charged particles originating from a line source. It can easily be shown that the resolving power of such a spectrometer for a given transmission factor is independent of the angle of the wedge. The 90° instrument has the advantage over the more conventional 180° type that the source and detector lie outside the field gap, and that their separation is greater, which facilitates shielding. It has the disadvantage that the stray field at the edges of the pole-pieces modifies the trajectories of the particles.

This effect was not considered in the design of the instrument used for the work on the beta particle spectrum reported in I.; there was, moreover, some uncertainty in the calibration of this instrument, so that the values obtained with it must be regarded as only approximate.

For the design of the present spectrometer, the stray field was mapped with a spinning-coil fluxmeter, and a simple graphical method was used to plot the trajectories of electrons on this map. In this way it was easy to determine the position of source and detector for optimum focusing in the presence of the stray field.

Fig. 1 shows a cross-section in the median plane of the spectrometer (horizontal). For measurement of the beta spectra an internal target arrangement was used, as shown at (*a*). The active layer was deposited by evaporation *in vacuo* on a thin (0·5 mm.) copper backing (cooled at one side by water), which was mounted at 45° and had a projected width of 4 mm. The experimental resolving power with a source of this width is 1·8 per cent; the solid angle of acceptance of the spectrometer is 0·6 per cent of 4π.

For monitoring the activity of F^{20} produced on the target, the energetic beta rays emerged through the backing and the window W, and were counted in a pair of coincidence counters not shown in the diagram. The spectrometer counters were also operated in coincidence to reduce the background due to stray gamma radiation; the shielding from the target was completed by building up lead blocks outside the vacuum box.

For measuring gamma ray energies, the target arrangements shown in fig. 1 (*b*) were employed. To stop the energetic beta rays from entering the spectrometer, a sheet of copper (3·3 g/cm.^{2}) was interposed. This, and the thin aluminium wall of the spectrometer, acted as converter for Compton electrons; no localization of this converter was possible apart from the fact that the bombarding beam was relatively well focused and thus restricted the area of material which was effective. These conditions were of course reproduced during the calibration of the spectrometer for Compton distributions.

For an examination of photo-electrons, a thin (50 mg./cm.^{2}) lead radiator, 4 mm. wide, was mounted on the inside of the alumium cap.

The target activity was monitored by means of its gamma rays, which were recorded in an arrangement of coincidence counters. All readings were normalized to this monitor.

The spectrometer was calibrated by reference to the following well-known energies : the F line of Thorium B at 148 keV., the gamma rays of Co^{60} at 1·172 and 1·322 MeV. (Lind, Brown and DuMond 1949), and the ThC″ line at 2·62 MeV. Since the iron of the magnet is far from saturation and the main part of the reluctance of the magnetic circuit lies in the air gap, the field is very accurately proportional to the magnet current up to electron energies of 7 MeV. The fact that the calibration could be extrapolated to this region was verified by examining the gamma rays from $F^{19}(p\alpha', \gamma)O^{16}$ (at 6·13 and 6·98 MeV.; Walker and McDaniel 1948) with the spectrometer.

Fig. 1.

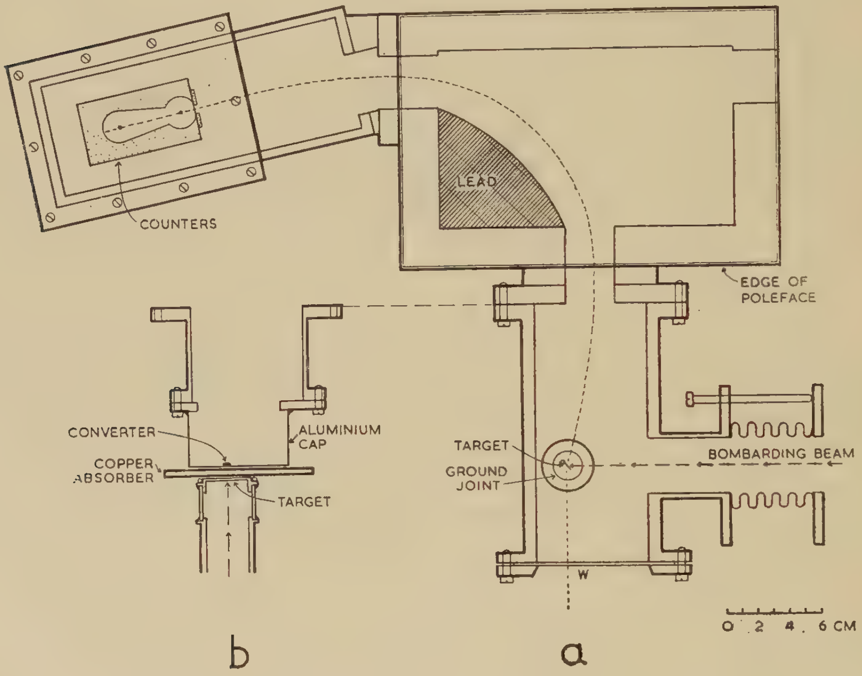

Cross-section of spectrometer.

The magnet current was stabilized by an electronic stabilizer using four valves of Mazda type 12E1 as control element. Relative values were read from a secondary standard meter, accurate to 0·2 per cent.

(c) *Coincidence Experiments.*

Fig. 2 shows the target arrangements used for the coincidence experiments. The target was deposited on a thin molybdenum backing supported by two wires in the aluminium can A. (This can was lined with very thin brass foil to avoid interaction of the bombarding deuterons with the aluminium.) The beam restricting aperture S was also of molybdenum, uncooled. Both the target and S reached dull red heat during a bombarding cycle ; this prevented the formation of carbon from decomposing pump vapours, and thus avoided the production of N^{13} by the reaction $C^{12}(d, n)$. The N^{13} provided a troublesome background of genuine gamma-gamma coincidences in the earlier parts of the work, as has now been verified by following the decay of these coincidences (half-life 10 mins.).

Fig. 2.

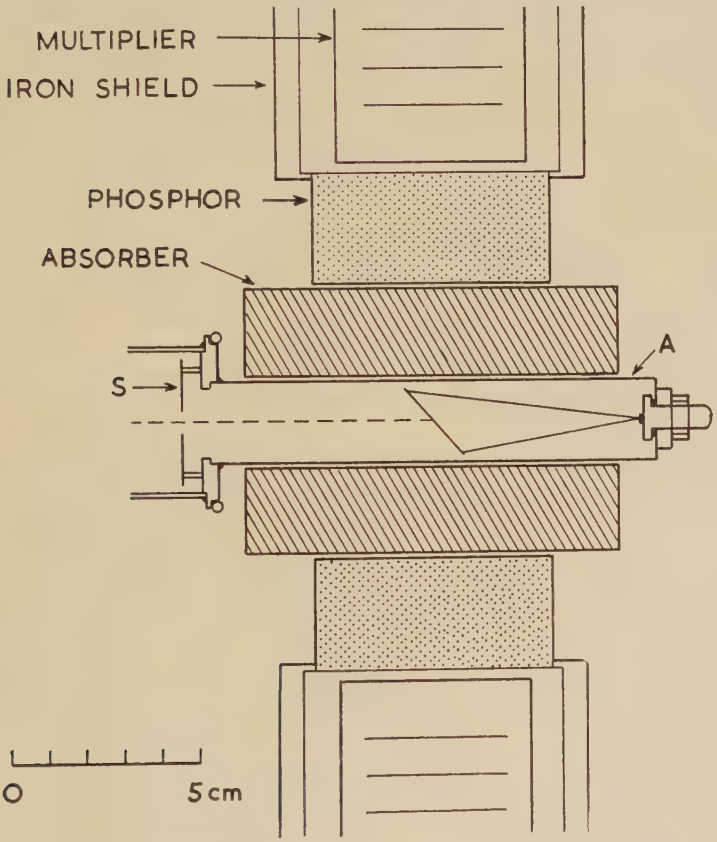

Target arrangements for coincidence experiments.

Scintillation counters were used to detect the gamma rays, as they are more efficient than the Geiger counters used in I., and permit higher counting rates to be used. These counters are shown in the 180° position in fig. 2 ; to allow for a possible strong angular correlation between the two quanta, duplicate experiments with the counters at right angles were also made, but yielded no different results. An additional improvement made in this work was the continuous recording of the chance coincidence rate by a method described elsewhere (Littauer 1950). This made it possible to use sources of such a strength that the chance rate exceeded the genuine rate, and also facilitated an immediate interpretation of the results. The coincidence resolving time was 10^{-6} sec.

§ 3. Results.

(a) *The Beta Particle Spectrum.*

Fig. 3 shows a Kurie plot, constructed in the usual way, of the observed spectrum from F^{20}. It is obvious that the spectrum is complex, with a main component of end-point 5·33±0·05 MeV., and a weaker one (3·5 per cent) of end-point 6·74±0·1 MeV.* There is no evidence of the presence of any internal conversion line in the region 0·15–7 MeV.

Fig. 3.

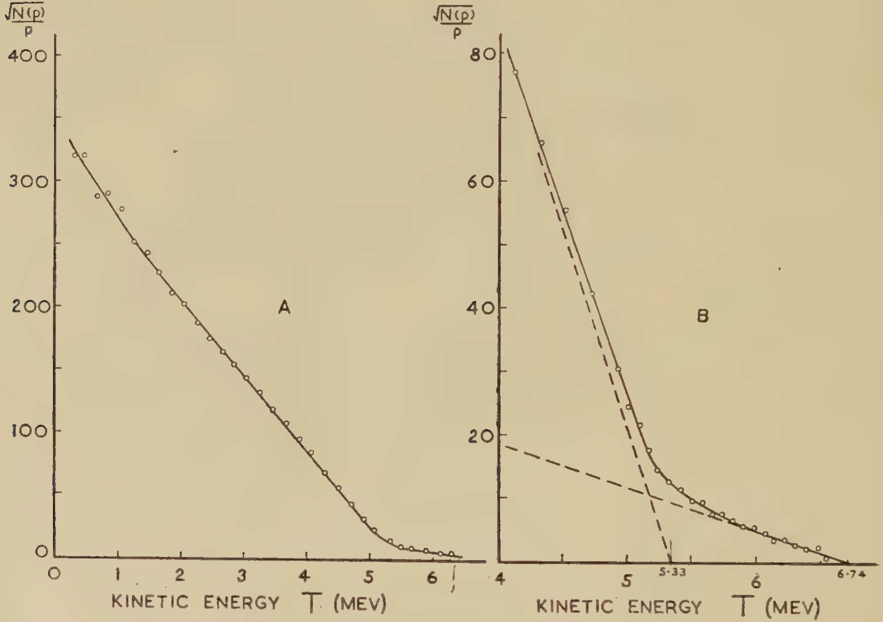

(A) Kurie plot from F^{20} beta ray spectrum.
(B) Detailed examination of high-energy region.

(b) *The Gamma Ray Spectrum.*

The results of an examination of the Compton recoil electrons are exhibited in fig. 4. The experimentally determined shape due to a monochromatic source is shown fitted to this plot, and it is clear that the points in the low energy region depart significantly from this shape.

---

* The energy of the main component differs appreciably from that obtained with the original, uncorrected spectrometer (*cf.* I.); the present work is regarded as more reliable. The earlier work did not reveal the higher energy component.

The observed differences are plotted on the same graph, and can be fitted reasonably well by another simple shape. It should be pointed out that the yields in this experiment were very low indeed and that the background, subtracted in Fig. 4, represented about 20 per cent of the maximum counting rate. The two gamma lines indicated have energies $1{\cdot}64 \pm 0{\cdot}03$ and $1{\cdot}0 \pm 0{\cdot}1$ MeV., and intensities roughly as 4 : 1. Other gamma lines in the region 0·7–3 MeV. would have been detected if their intensity had exceeded about 10 per cent of that of the main component.

An attempt to detect the photo-electrons from the main gamma component met with only fair success. The line appeared to be indicated but the intensity in this experiment was not sufficiently high to yield quite definite results. The gamma energy deduced from the position of the line is $1{\cdot}62 \pm 0{\cdot}02$ MeV., in good agreement with the value derived from the Compton distribution. The energy $1{\cdot}63 \pm 0{\cdot}02$ MeV. has been adopted as the best estimate.

Fig. 4.

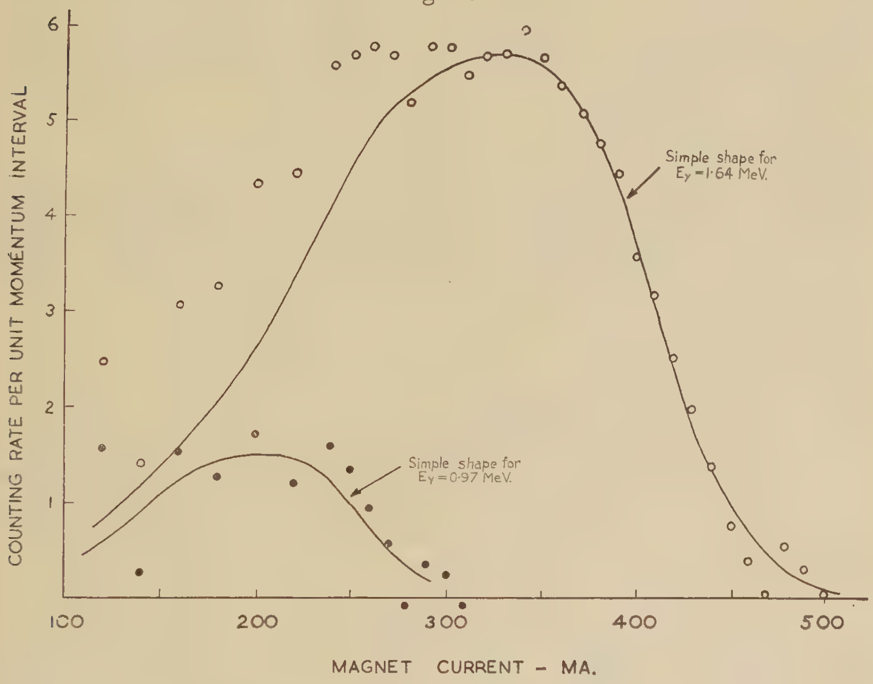

Compton electron distribution from the gamma rays of F^{20}.

The intensity obtainable with the spectrometer did not allow the high-energy gamma ray reported in I to be observed. Better efficiency for gamma ray detection can be achieved with an ionization chamber using liquid argon, in which the Compton secondaries give up all their energy. G. W. Hutchinson (1948) has developed such a "liquid argon spectrometer" in the Cavendish Laboratory; at the request of the author, a study of the F^{20} gamma ray spectrum was made with this instrument.

The intensity was sufficiently high to allow an examination of the lifetimes of the individual gamma components, whereas in the work reported in I. it was possible to check only that the average half-life of the gamma activity was consistent with its allocation to F^{20}.

This investigation * revealed the presence of two gamma ray lines of energy 1·64 and 1·0 MeV. and relative intensity 4 : 1 approximately, in agreement with the spectrometer work. A complex component of energy up to 4 MeV., not easily resolvable into separate lines, was also found. The decay periods of the 1 MeV. line and of the high-energy component were compared with that of the main line at 1·64 MeV., which is known to belong to the F^{20} decay (*cf.* I). The evidence concerning the 1 MeV. line was not conclusive, but did not contradict its allocation to the decay of F^{20}. The period of the higher energy component, however, was definitely longer ($\sim$1 min.), and it is therefore likely that this component, which may almost certainly be identified with the 2·45 MeV. radiation reported in I., does not in fact arise from the decay of F^{20}, but may be attributed to an unidentified contamination.

(c) *Gamma–gamma coincidences.*

In the analysis of the results of these experiments, we have assumed the efficiency of detection for gamma rays to be approximately independent of energy in the region 0·6–2·0 MeV., which introduces no error greater than about 30 per cent when the scintillation counters are used at low settings of discriminator bias.

If we put

α, β=efficiencies in the two gamma channels,
τ=coincidence resolving time,
$\bar{n}$=mean source strength,
p=fraction of disintegrations yielding two gamma rays in cascade,
T=time of counting,

we then have : the single counts recorded in channel A (after subtraction of the background)

$$S(A)=2p\bar{n}\alpha T+(1-p)\bar{n}\alpha T=(1+p)\bar{n}\alpha T.$$

Similarly $S(B)=(1+p)\bar{n}\beta T$.

The number of randon coincidences is

$$R=2(1+p)^2\alpha\beta\tau \,.\, \overline{n^2} \,.\, T,$$

and the genuine coincidences are given by

$$G=2p\bar{n}\alpha\beta T.$$

Hence

$$p/(1+p)=(\tau/2\alpha\beta T)^{\frac{1}{2}} \,.\, G/\sqrt{R}$$

$$=(1/S) \,.\, G/\sqrt{R},$$

where

$$S=(2\alpha\beta T/\tau)^{\frac{1}{2}}.$$

---

* The author is indebted to Mr. Hutchinson for permission to use these results before publication.

(We have assumed $\overline{n^2}=(\bar{n})^2$, which is approximately true for F^{20} under the conditions of the experiment.)

To measure S a source of known p (*e.g.* Co^{60} with $p=1$) was used, placed in the position of the target, with the same absorbers as in the corresponding F^{20} experiment.

Table I. gives the results of the experiments as a function of the absorbing material used to stop the hard beta rays.

TABLE I.

Apparent values of p with various absorbing materials. (p is the fraction of disintegrations which yield cascade gamma rays).

Absorber	G/5 min.	R/5 min.	S	p (%)
Graphite	5±10	230	42	0·8±1·6
Aluminium	50±20	450	70	3·4±1·4
Copper	170±40	660	120	5·8±1·3
Lead	145±40	850	31	19±5

It is evident that the apparent value of p rises with the atomic number of the absorber, and that the true value must be well below 2 per cent. This demonstrates the effect of bremsstrahlung from the hard beta rays, and also shows that there cannot be a cascade of gamma rays (of life-time less than 10^{-6} sec.) in the decay of F^{20} with fractional intensity above 2 per cent.

Rough experiments were also made on beta-gamma coincidences from F^{20}. These established that there is no beta–gamma angular correlation greater than 7 per cent, and that there are 1·06±0·1 gamma quanta per beta particle. It has not been possible to separate the high-energy beta component for this measurement on accouut of the low intensity near the end-point of the spectrum.

§ 4. DISCUSSION.

(*a*) *The Mass of* F^{20}.

An estimate of the mass difference F^{20}—Ne^{20} can be obtained (as in I.) by adding the energies of the prominent gamma line and of the main beta spectrum, for there can be no doubt that these must occur in cascade. Thus the total energy released in the decay is 6·96±0·06 MeV., which corresponds to a mass difference of 7·47±0·06 mMU. On the basis of a Ne^{20} mass of 19·998 90±0·000 06 (Rosenfeld 1948), this gives a F^{20} mass of 20·006 37±0·000 08.

Another estimate of the F^{20} mass can be obtained from the mass of F^{19} and the Q of either of the reactions $F^{19}(d, p)$ or $F^{19}(n, \gamma)$. These reactions give a mean mass difference $F^{20}-F^{19}$ of 1·001 80±0·000 04 (*cf.* I.) ; if we take the F^{19} mass to be 19·004 49±0·000 03 (Tollestrup, Fowler and Lauritsen 1950), then the F^{20} mass becomes 20·006 29± 0·000 05.

The two estimates of the F^{20} mass differ by 0·08±0·10 mMU, which indicates a satisfactory agreement. The most likely present estimate of the mass of F^{20} is

$$20{\cdot}006\ 31 \pm 0{\cdot}000\ 05.$$

(b) *The Decay Scheme of* F^{20}.

If the high-energy beta component corresponds to a decay of F^{20} direct to the ground state of Ne^{20}, its maximum energy, on the basis of the present spectrometer measurements, should be 6·96±0·06 MeV. The experimental upper limit of the distribution is 6·74±0·1 MeV., which differs from the expected value by 0·22±0·12 MeV. Despite this small discrepancy, however, it is assumed that the transition does indeed go to the ground state ; there is no evidence to support an alternative hypothesis.

Table II. gives the ft. values (*cf.* Konopinski 1943) of the two partial beta components ; these values are not inconsistent with the assumption that the transitions to the excited state and ground state of Ne^{20} are respectively allowed (unfavoured) and second forbidden, as required by the nuclear shell model (Feenberg and Hammack 1949). On this assumption, and taking the excited state of Ne^{20} concerned to be a (2, +) state the ground state of F^{20} should be of even parity and spin 2 or 3.

TABLE II.

ft. values for the two partial beta ray spectra.

E_{max}	*t*	*f*(E)	*ft*
11·4 mc^2	12 secs.	$6{\cdot}5\times10^3$	$0{\cdot}8\times10^5$
14·2	350	2×10^4	$0{\cdot}7\times10^7$

Fig. 5 shows a number of decay schemes that might be postulated on the basis of these results. Scheme I, which contains only definitely established transitions, is incomplete in so far as it does not account for the presence of the 1 MeV. gamma radiation ; it must be remembered, however, that the allocation of this to F^{20} is still open to question. (The 2·45 MeV. component reported in I. has been omitted on the basis of the present results.)

Decay shemes II. and III. are more speculative and would require further evidence to establish them. Scheme II. postulates a beta component of energy about 6·0 MeV., linked with the 1 MeV. gamma ray. We have attempted to analyse the experimental Kurie plot into three components, as shown in fig. 6. The maximum intensity of the 6 MeV. component that can be accommodated is about 5 per cent, which is insufficient for the requirements of scheme II. The broken curve in fig. 6 shows the Kurie plot* that would be expected if scheme II. were indeed correct. It is seen that little evidence to support this scheme can be adduced.

---

* In the construction and analysis of the Kurie plots the effect of the finite spectrometer resolution has been neglected, as this is small compared with the other experimental uncertainties.

Scheme III. (A or B) is consistent with the data from the coincidence experiments only if the lower of the cascade gamma transitions has a life-time longer than 10^{-6} sec., so that the quanta should not be recorded as coincident. If the level arrangement B is correct, so that the gamma transition has only 600 keV. of energy available, a spin $\geqslant 3$ for the postulated level would suffice for this requirement. This possibility might repay further study. (A total internal conversion of the second quantum is ruled out by the results of both I. and the present work.)

Fig. 5.

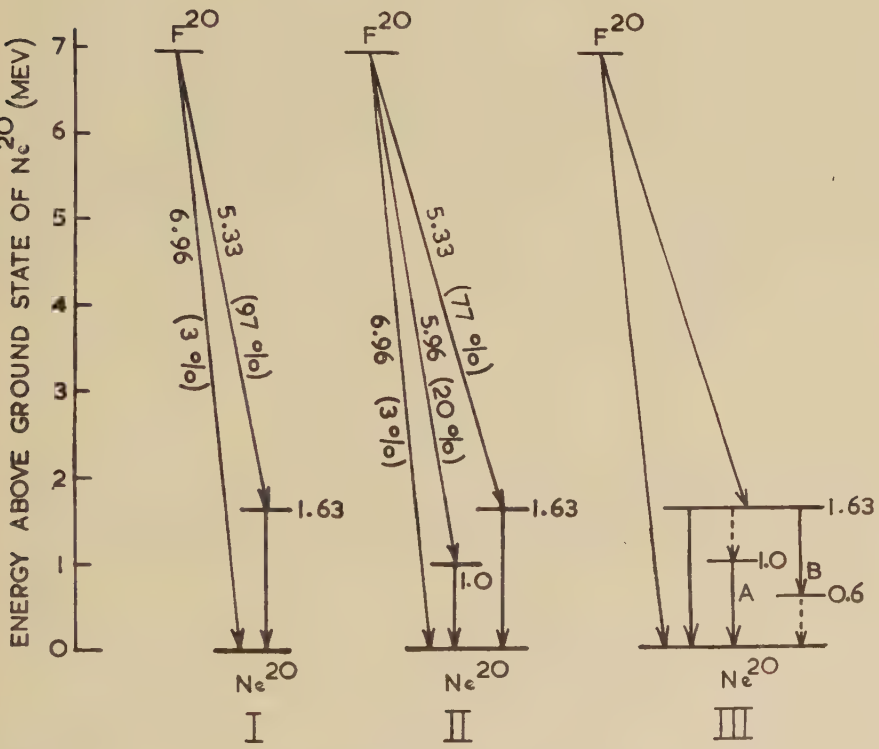

F^{20} decay schemes.
Scheme I., though possibly incomplete, is the only firmly established one. The energies given represent the best present estimates.

Acknowledgments.

The author wishes to thank Dr. J. V. Jelley for his co-operation in the early experiments, Mr. E. S. Shire for the design of the original spectrometer and Mr. W. Birtwhistle for operation of the high tension equipment. He is indebted to the Department of Scientific and Industrial Research for a grant during the period of this work.

Fig. 6.

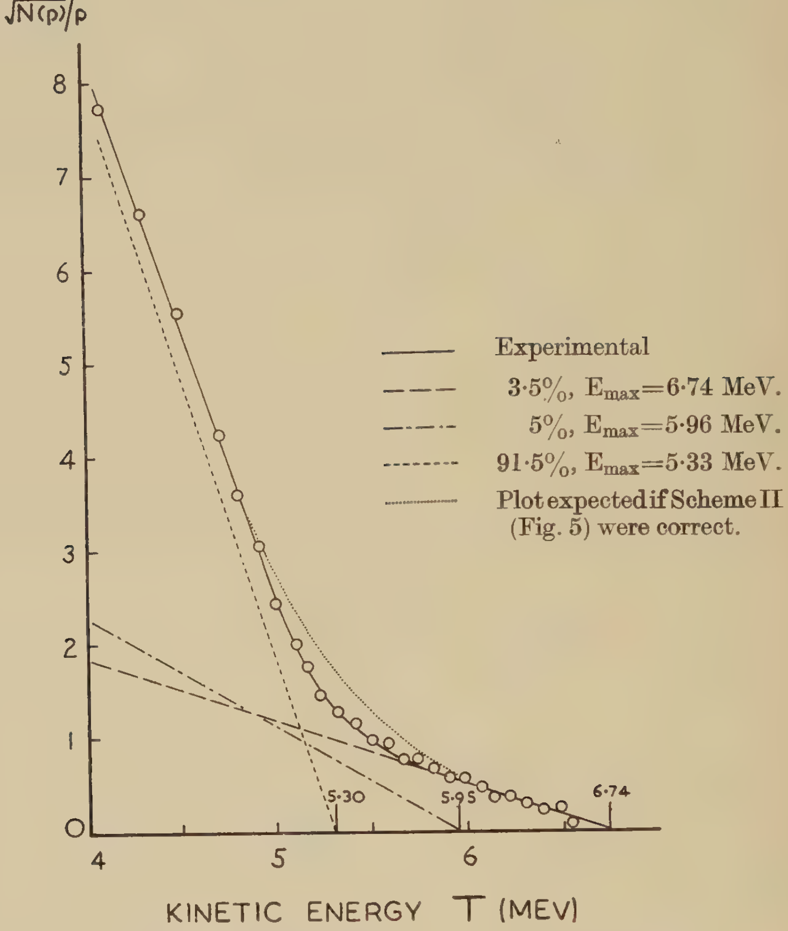

Constructed Kurie plots for the F^{20} beta ray spectrum.

References.

Feenberg, E., and Hammack, K. C., 1949, *Phys. Rev.*, **75,** 1877.
Hutchinson, G. W., 1948, *Nature, Lond.*, **162,** 610.
Konopinski, E. J., 1943, *Rev. Mod. Phys.*, **15,** 209.
Lind, D. A., Brown, J. R., and DuMond, J. W. M., 1949, *Phys. Rev.*, **76,** 1838.
Littauer, R. M., 1950, *Rev. Sci. Instrum.*, **21,** [8], 750.
Rosenfeld, L., 1948, *Nuclear Forces* (Elsivier : North Holland Publishing Co.).
Snowdon, S. C., 1950, *Phys. Rev.*, **78,** 299.
Stephens, W. E., 1934, *Phys. Rev.*, **45,** 514.
Tollestrup, A., Fowler, W. A., and Lauritsen, C. C., 1950, *Phys. Rev.*, **78,** 372.
Walker, R. L., and McDaniel, B. D., 1948, *Phys. Rev.*, **74,** 315.

CIX. *The Emission of Short Range Alpha Particles from Light Elements under Proton Bombardment.—IV. The Reaction* $^{19}F(p\alpha)^{16}O$ [*].

By Joan M. Freeman,
Cavendish Laboratory, Cambridge[†].

[Received August 23, 1950.]

Summary.

The short range alpha particles emitted in the proton bombardment of fluorine have been examined with a magnetic analyser for proton energies from 300 to 950 keV. In the $^{19}F(p\alpha, \gamma)^{16}O$ reaction three alpha particle groups have been measured, the average values of the energy releases being $Q_1=1{\cdot}979\pm0{\cdot}009$, $Q_2=1{\cdot}200\pm0{\cdot}010$ and $Q_3=0{\cdot}996\pm0{\cdot}010$ MeV.; the resonances for all three groups appear to be the same. The relative intensities of the groups at six resonances have been calculated. Angular distribution measurements indicate that there are no large departures from isotropy in the cases examined. Energy measurements of the alpha particles associated with pair emission in the $^{19}F(p\alpha, \pi)^{16}O$ reaction give a value for the energy release of $2{\cdot}056\pm0{\cdot}012$ MeV.

§1. Introduction.

It is well known that the proton bombardment of fluorine can lead to the emission of short range alpha particles (subsequently designated α_1-particles) followed by gamma radiation of about 6 MeV. energy, according to the scheme :

$$\left.\begin{array}{c} ^{19}F+{}^1H\rightarrow{}^{20}Ne^*\rightarrow{}^{16}O^*+{}^4He+Q_1, \\ ^{16}O^*\rightarrow{}^{16}O+\gamma_1. \end{array}\right\} \qquad (1)$$

Accurate measurements of the energy of the gamma rays by Walker and McDaniel (1948) have shown that in addition to radiation of 6·13 MeV. energy a component of 6·98 MeV. radiation is also present, being directly associated with the lower energy radiation, although the ratio of the intensities of the two components varies from one resonance to another. It seemed probable that the 7 MeV. radiation was produced in a competing reaction similar to (1) in which a higher excited state of oxygen-16 was involved :

$$\left.\begin{array}{c} ^{19}F+{}^1H\rightarrow{}^{20}Ne^*\rightarrow{}^{16}O^{**}+{}^4He+Q_2, \\ ^{16}O^{**}\rightarrow{}^{16}O+\gamma_2. \end{array}\right\} \qquad (2)$$

[†] Communicated by Dr. W. E. Burcham.

and this was proved by observations of alpha particles of shorter range than those designated α_1 above (Burcham and Freeman 1949 a). The excitation function for these shorter range particles showed resonances in the region of proton bombarding energies from 300 to 950 keV. coinciding with resonances for the production of the α_1-particles, the intensity ratios varying considerably from one resonance to another. It was also found that the energy release Q_2 for the shorter range alpha particles was greater at the 873 keV. resonance than at the other resonances investigated. This evidence suggested the existence in the oxygen nucleus of excited levels at 7·15 and 6·94 MeV. above the ground state as well as the 6·13 MeV. level, and the pair-emitting level at about 6·00 MeV.

By improvement in the resolution of the magnetic analyser used for these investigations it has now been possible to measure the energies and intensities of the alpha particle groups more accurately and to show that at most of the resonances the shorter range alpha particles consist of two groups (designated α_2 and α_3). At the 873 keV. resonance the α_2-group, emitted in accordance with reaction (2), is the more intense, and at the other resonances studied the lower energy α_3-group, coming from

$$\left.\begin{array}{c} {}^{19}\mathrm{F}+{}^{1}\mathrm{H}\rightarrow{}^{20}\mathrm{Ne}^{*}\rightarrow{}^{16}\mathrm{O}^{***}+{}^{4}\mathrm{He}+Q_3, \\ {}^{16}\mathrm{O}^{***}\rightarrow{}^{16}\mathrm{O}+\gamma_3. \end{array}\right\} \quad . \; . \; . \; . \quad (3)$$

predominates. These groups have also been studied by Chao, Tollestrup, Fowler and Lauritsen (1950), whose results are in substantial agreement with those presented in the present paper in the cases where they overlap†. The energy of the gamma radiation (γ_2 and γ_3) associated with the α_2- and α_3-particle emission was measured carefully by Rasmussen, Hornyak, Lauritsen and Lauritsen (1950), and although the two lines were not resolved the predominant energy was shown to be less (6·99±·05 MeV.) at the 873 keV. resonance than at 939 keV. where an energy of 7·09±0·06 MeV. was found.

In the work described in subsequent sections the energies of the α_1-, α_2- and α_3-particles have been measured at a number of resonances and the corresponding Q-values deduced ; excitation functions have been obtained and the relative intensities of the groups at most of the resonances from 340 to 939 keV. have been determined. Some observations on the angular distributions of the alpha particles are also presented.

It is known that the proton bombardment of fluorine can also lead to resonance reactions in which either a long range alpha particle is emitted or a transition may occur to the lowest excited state of ^{16}O with the emission of a short range alpha particle (designated α_π) followed by an electron–position pair (see for example Rassmussen *et al.* 1950, Chao *et al.* 1950, and references included therein)

---

† We are grateful to Professor Lauritsen for communicating these results to us prior to publication.

$$\left.\begin{array}{l} {}^{19}\mathrm{F}+{}^{1}\mathrm{H}\rightarrow{}^{20}\mathrm{Ne}^{*(\pi)}+{}^{16}\mathrm{O}^{*(\pi)}+{}^{4}\mathrm{He}+\mathrm{Q}_\pi, \\ {}^{16}\mathrm{O}^{*(\pi)}\rightarrow{}^{16}\mathrm{O}+e^{+}+e^{-}. \end{array}\right\} \quad . \quad . \quad . \quad . \quad (4)$$

Some measurements on the α_π-particles are described in section 3(*e*).

§ 2. EXPERIMENTAL METHOD.

The 90° magnetic analyser used for the study of the short range alpha particle groups has already been described (Burcham and Freeman 1949b, 1950a, 1950b, subsequently referred to as I., II. and III.). In much of the work the magnet was used on its side so that observations could be made in a horizontal plane ; the proton beam which reached the target could be restricted to a diameter of 5 mm. and the zinc sulphide scintillation screen used with an EMI type 4588 photo-multiplier for detecting the analysed particles was then made 5 mm. wide in the focusing plane. Under these conditions the effective resolution of the system (ΔE/E) was 4 per cent in energy. The analyser was calibrated by observations on the peaks of proton and deuteron groups of known energy scattered from a thin gold film, and of deuteron and alpha particle groups from the proton bombardment of beryllium (*cf.* I.; the Q values used for the ${}^{9}\mathrm{Be}(pd){}^{8}\mathrm{Be}$ and ${}^{9}\mathrm{Be}(p\alpha){}^{6}\mathrm{Li}$ reactions were 0·558 and 2·121 MeV. respectively (Tollestrup, Fowler and Lauritsen 1949)).

The voltage scale of the 1 MV. accelerating equipment set used for the experiments was calibrated by reference to the gamma ray excitation function for the fluorine reaction (1), observations being made with a thick sodium fluoride target, using a Geiger counter. The relative positions of the gamma ray resonances have been determined by the work of Bennett *et al.* (1946) and Bonner and Evans (1948), and the absolute values were estimated by correcting their value of 862 keV. for the most prominent resonance in the region explored to the figure of 873·5 keV. found by Herb, Snowdon and Sala (1949), and multiplying their figures for the other resonances by the same factor.

The fluorine targets used for the alpha particle work were prepared by evaporating thin layers of calcium fluoride on copper buttons in vacuo ; the surface densities of the layers were estimated by weighing pieces of mica placed close to the buttons during the evaporation process. Target thickness effects were calculated on the assumption that the stopping power of calcium fluoride for protons of 500 keV. energy was 260 keV./mgm./cm.^{2} and that for alpha particles of 1 and 2 MeV. energy it was 1600 and 1100 keV./mgm./cm.^{2} respectively. In most cases targets of thickness 0·02 mgm./cm.^{2} or less were used.

In the experiments on the alpha particles associated with gamma ray emission the yield was monitored by means of a Geiger counter, mounted vertically below the target ; simultaneous measurements of alpha particle and gamma-ray intensities were made, the background of the Geiger counter being first determined by observations with a blank target. Counts were usually made for a standard number of microcoulombs collected by the target, as indicated by a current integrator.

Fig. 1.

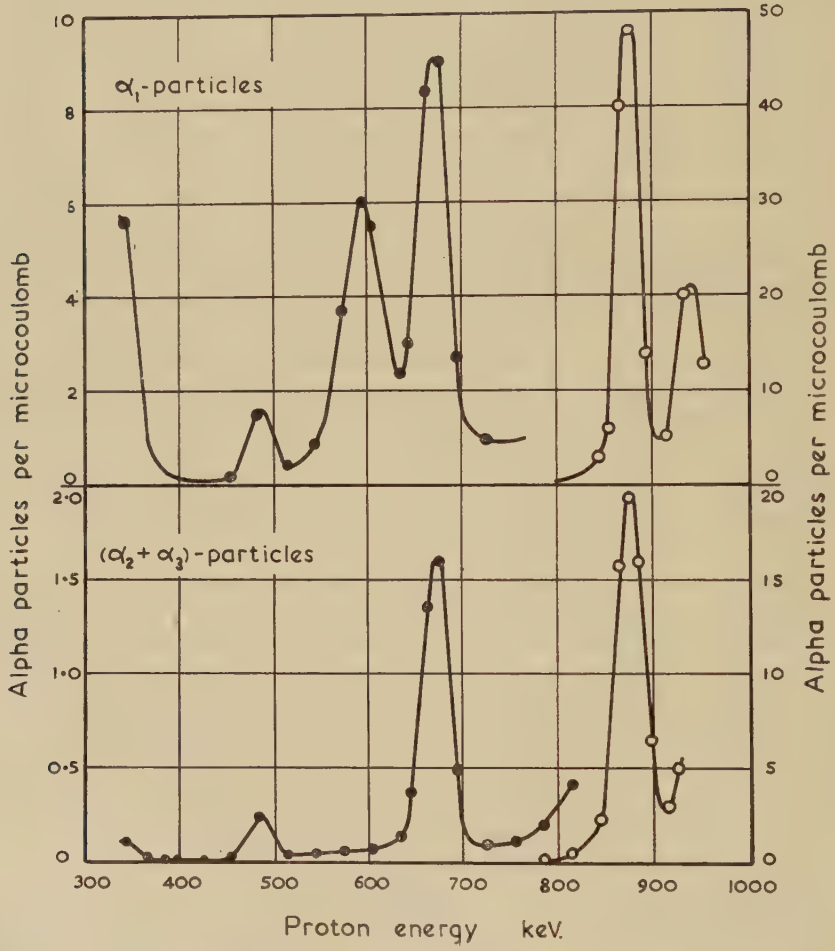

Excitation functions for the α_1-particles and the unresolved $(\alpha_2+\alpha_3)$-particles from the $^{19}F(p\alpha, \gamma)^{16}O$ reaction. Left-hand ordinates refer to the region below 800 keV. proton bombarding energy, and right-hand ordinates to that above 800 keV.

§ 3. EXPERIMENTAL RESULTS.

(a) *Alpha particles associated with gamma radiation.*

In the first experiments (Burcham and Freeman 1949 a), in which an analyser resolution of 10 per cent in energy was used, the lower energy (α_2- and α_3-) particles appeared as a single group. The excitation functions for these and for the α_1-particles were observed at the same time by measuring the intensity at the peak of each group as a function of proton bombarding energy from 330 to 950 keV. Observations were made at an angle of 83° with the proton beam. The curves are reproduced in fig. 1, in which the proton energy scale has been adjusted to place the most prominent resonance in the α_1-particle curve at the value 873·5 keV. The widths of the resonances are about 30 keV., which is equal to the estimated spread in energy of the bombarding proton beam, except in the case of the 598 keV. resonance in the α_1-particle curve which is slightly broader, as expected from the observations of Burcham and Devons (1939), and Bonner and Evans (1948). All the resonances observed for the lower energy alpha particles appear to coincide exactly with the positions of α_1-particle resonances and it may be concluded that the same excited levels of the compound $^{20}Ne^*$ nucleus are involved in each case, although the branching ratios vary with proton energy. There is no resonance in the curve for α_2- and α_3-particles corresponding to the 598 keV. resonance for α_1-particles.

For more accurate energy measurements an analyser resolution of 4 per cent in energy was used, and the alpha particles were observed at an angle of 135° with the proton beam. Fig. 2(*a*–*f*) shows the alpha particle spectra obtained with targets of thickness $\sim$0·02 mgm./cm.^{2} at the 939, 873, 669, 598, 486 and 340 keV. resonances. Excepting the case of the 598 keV. resonance, where only the α_1-particles appear, there is evidence for both α_2- and α_3-particle groups at each resonance, although for the lower resonances the position and intensity of the weakest (α_2) group cannot be fixed very accurately. During the course of the experiments in which these spectra were obtained a film of carbon contamination formed on the target surface. The development of this contamination was traced by observations from time to time on the position of the peak of the α_1-particle group at the 873 keV. resonance and the corrections to be applied to the observed alpha particle energies were so obtained. The spectra shown in fig. 2 have been corrected in this way. Targets were frequently changed in order to avoid the necessity for large corrections for the carbon deposit. The effective target thicknesses were estimated to be equivalent to about 22 keV. for 2 MeV. alpha particles or 32 keV. for 1 MeV. alpha particles, so that corrections for target thickness were small. This was verified by observations of the extrapolations of the high energy sides of the spectra as described in II. and III.

From the corrected energies of the three sets of alpha particle groups the corresponding Q-values for reactions (1), (2) and (3) were obtained, and these are given in Table I. The probable erros are calculated from the estimated uncertainties in the energy calibration of the analyser and in the target thickness and carbon contamination corrections. The mean values for Q_1, Q_2 and Q_3 were estimated by weighting the figures for each resonance according to the inverse squares of the probable errors

Fig. 2 (*a–c*).

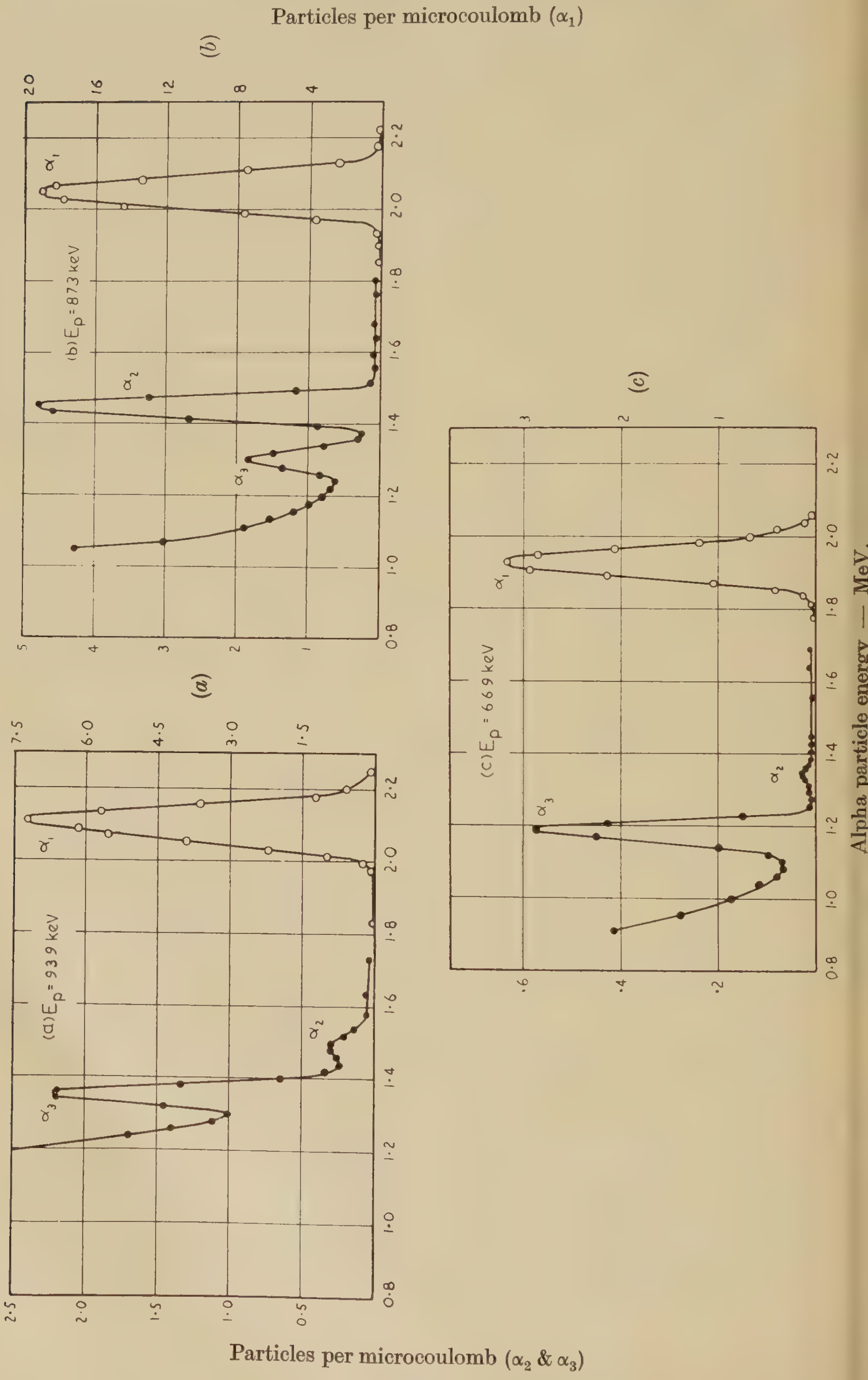
Particles per microcoulomb (α_1)
(b)
20
16
12
8
4
5
4
3
2
1
(b) E_p = 873 keV
α_1
α_2
α_3
0·8
1·0
1·2
1·4
1·6
1·8
2·0
2·2
(a)
7·5
6·0
4·5
3·0
1·5
2·5
2·0
1·5
1·0
0·5
(a) E_p = 939 keV
α_1
α_2
α_3
(c)
3
2
1
·6
·4
·2
(c) E_p = 669 keV
α_1
α_2
α_3
Alpha particle energy — MeV.
Particles per microcoulomb (α_2 & α_3)

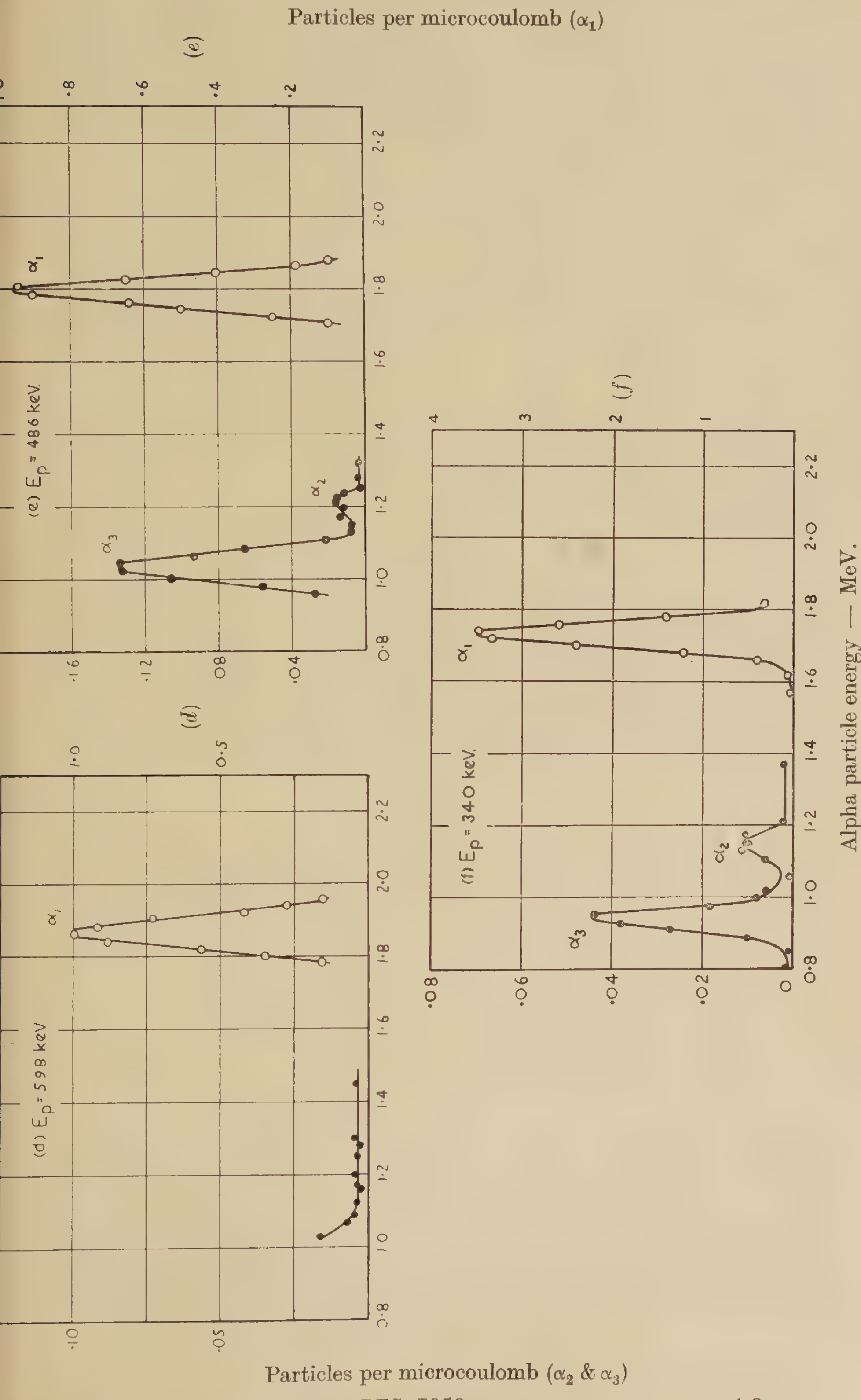

Alpha particle spectra from the ^{19}F($p\alpha, \gamma$)^{16}O reaction at proton energies of (*a*) 939, (*b*) 873, (*c*) 669, (*d*) 598, (*e*) 486 and (*f*) 340 keV. Right-hand ordinates give yields of α_1-particles per microcoulomb of protons and left-hand ordinates give the α_2- and α_3-particle yields in the same units. Abscissæ give alpha particle energies in MeV.

quoted. The values obtained ($Q_1=1{\cdot}979\pm0{\cdot}009$, $Q_2=1{\cdot}200\pm0{\cdot}010$, $Q_3=0{\cdot}996\pm0{\cdot}010$ MeV.) are in very good agreement with the figures deduced by Chao *et al.* (1950) from measurements at the 873 and 1353 keV. resonances ($Q_1=1{\cdot}977\pm0{\cdot}008$, $Q_2=1{\cdot}204\pm0{\cdot}008$ and $Q_3=1{\cdot}002\pm0{\cdot}008$ MeV.) and with the value $Q_1=1{\cdot}969$ MeV. given by Strait, Van Patter and Buechner (1950).

TABLE I.

E_p (keV.)	Q_1 (keV.)	Probable error (keV.)	Q_2 (keV.)	Probable error (keV.)	Q_3 (keV.)	Probable error (keV.)
939	1991	20	1199	20	999	20
873	1980	14	1195	14	996	14
669	1984	20	1219	25	1017	20
598	1959	25	—	—	—	—
486	1962	35	1191	35	973	35
340	1979	20	1207	25	971	25
Weighted mean	1979	9	1200	10	996	10

The relative yields at 135° of α_1-, α_2- and α_3-particles, at each of the resonances studied, were obtained from the spectra shown in fig. 2 by calculating for each group the integral $\int N(E)dE/E$, where $N(E)$ is the number of alpha particles counted at a given setting of the field current of the magnetic analyser, corresponding to the energy E. A correction for the number of singly-charged alpha particles expected to be associated with each of the observed doubly-charged groups was made using the data given by Briggs (1927) and Knipp and Teller (1941). The values thus obtained for the ratios α_1/α_2, α_1/α_3 and $\alpha_1/(\alpha_2+\alpha_3)$ at each resonance are set out in Table II. In the cases where the ratios are large the figures must be regarded as rough approximations only. An allowance for scattered protons had to be made in estimating the yield of the α_3-group at the 939 keV. resonance. In the region where the

TABLE II.

E_p (keV.)	$\dfrac{\alpha_1}{\alpha_2}$	$\dfrac{\alpha_1}{\alpha_3}$	$\dfrac{\alpha_1}{(\alpha_2+\alpha_3)}$
939	26	3·3	2·9
873	3·8	8·6	2·6
669	250	4·7	4·6
598	>400	>400	200
486	65	4·0	3·8
340	250	50	40

results in Table II. overlap the observations of Chao *et al.* (1950), for an angle of 138°, a comparison shows general but not complete agreement.

(b) *Angular distributions.*

The angular distributions of the alpha particles associated with gamma-ray emission have been examined at several resonances, over a limited range of angles. The experimental arrangement, which has already been described (1, § 2 (*d*)), permitted observations to be made at angles between 60° and 135°. Thin targets were used and the variation in the effective target thickness as the target was rotated for each angular position was taken into account by the use of the gamma ray monitoring counter mounted vertically below the target. Observations were made of the ratio of the alpha particle counting rate at the peak of the spectrum under examination to the simultaneous gamma ray counting rate (corrected for background). The distributions of α_1-particles from the 939, 873, 669, 598 and 340 keV. resonances were observed, and for the energy of 669 keV. the α_3-particle distribution was also studied. When corrected to the centre of mass system the readings at all resonances showed deviations from isotropy slightly outside the statistical accuracy, which was about 10 per cent. Now the distribution of α_1-particles emitted at the 340 keV. resonance has been examined by Van Allen and Smith (1941), and shown to be spherically symmetrical to within 2 per cent. It was therefore assumed that the distribution obtained in the present experiment at this resonance actually corresponded to an isotropic distribution and that apparent variations in yield with angle were due to systematic errors which would affect the observations at all resonances in the same way. The 340 keV. results were therefore used to correct the observations made at the other resonances ; for each case the yield observed at a given angle θ was divided by the yield of α_1-particles obtained from the 340 keV. resonance at the same angle θ. The distributions derived in this way are shown in fig. 3 ; suitable normalizing factors have been applied to make the average value of the ratio $I_\theta(E)/I_\theta(340 \text{ keV.})$ approximately unity in each case. It can be seen that, within the experimental accuracy (about 10 per cent) and over the limited range of angles which it was possible to cover, no significant departures from isotropy are apparent in any of the cases examined. This result is in agreement with conclusions of Chao *et al.* (1950) derived on a different basis : they measured, for a number of resonances, the yields of α_{-1}-, α_2- and α_3-particles from a given target at a particular angle (138°) ; the total yields over 4π steradians were then calculated on the assumption of isotropic distributions of all the particles, and these figures were found to agree to within 10 per cent with total yields of gamma radiation measured simultaneously.

(c) *Alpha particles associated with pair emission.*

The α_π-particles emitted according to the reaction (4), § 1, involving the lowest excited state of ^{16}O, were studied in the neighbourhood of the resonance at 843 keV., which is known from measurements of the electron–positron pairs (Bennett *et al.* 1946). The alpha particle spectrum obtained at an angle of observation of 135° and a bombarding energy

Fig. 3.

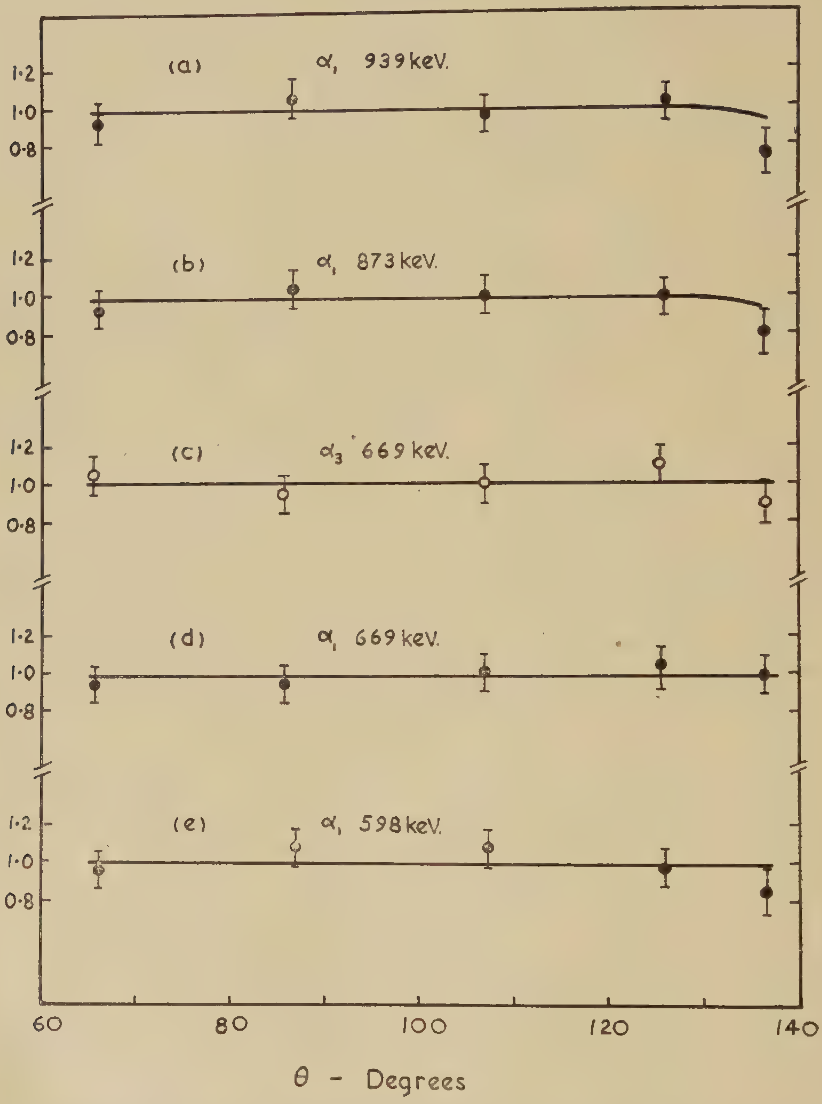

Angular distributions of the alpha particles from the $^{19}F(p\alpha, \gamma)^{16}O$ reaction : α_1-patricles at proton energies of (*a*) 939, (*b*) 873, (*d*) 669, (*e*) 598 keV. ; curve (*c*) is for α_3-particles at 669 keV.

of 830 keV. is shown in fig. 4. The target was 0·02 mgm./cm.^{2} thick and the analyser resolution 4 per cent. The presence of two groups is evident although complete resolution was not obtained. The lower energy group shown in the figure has an energy which would correspond to α_1-particles from the " tail " of the 873 keV. resonance studied above. The higher energy group (2·08 MeV.) is attributed to the α_π-particles preceding pair emission according to (4). A similar spectrum was obtained at proton energy of 820 keV., and from the two measurements a mean Q-value for reaction (4) was deduced as $Q_\pi = 2{\cdot}056 \pm 0{\cdot}012$ MeV. This result is in agreement with the value of 2·061±0·010 MeV. found by Chao *et al.* (1950).

Fig. 4.

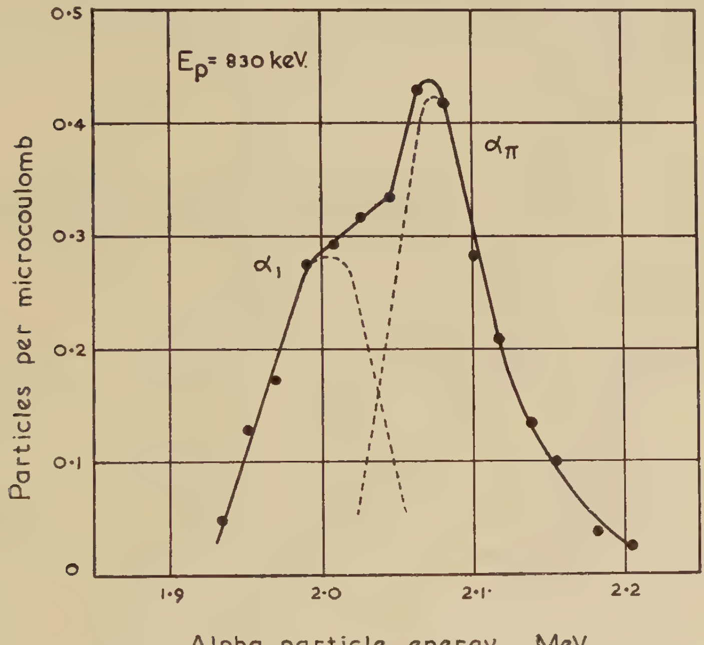

Alpha particles from the reactions $^{19}F(p\alpha, \gamma)^{16}O$ and $^{19}F(p\alpha, \pi)^{16}O$ at a proton bombarding energy of 830 keV.

§ 4. DISCUSSION.

From the present state of knowledge concerning reactions produced by the proton bombardment of fluorine one can draw up a generalized disintegration scheme as shown in fig. 5. The excited states formed in ^{20}Ne appear to fall into two classes : (i) levels from which transitions may occur either to the ground state of ^{16}O with long range alpha particle (α_0) emission or to the lowest excited state of ^{16}O with short range alpha particle (α_π) emission followed by the emission of an electron–positron pair (π) ; (ii) levels from which transitions may occur to any one of the next three excited levels of ^{16}O with emission of short range alpha particles (α_1, α_2 or α_3) followed by gamma radiation (γ_1, γ_2 or γ_3). In the latter case the relative probabilities of the transitions to the three ^{16}O levels vary considerably from one resonance to another as is shown by the intensity ratios listed in Table II. An attempt was made to determine the way in which these relative probabilities might be governed by the penetrability factors for the emitted alpha particles, whose energies are well below the barrier of the residual ^{16}O nucleus. The penetrability factors were calculated from the formulæ given by Bethe (1937), assuming a constant value for the radius of the ^{16}O nucleus derived from the data of Amaldi and Cacciapuoti (1947). The factors appropriate to alpha particles emitted with angular momenta of all values up to $l=4$ were calculated and an attempt was made to select consistent sets of the ratios of these factors which would fit the observed α_1/α_2 and α_1/α_3 ratios at the various resonances, and give some information about the angular momenta of the emitted particles and the spins of the $^{16}O^*$ levels. No such self-consistent sets could however be found. One is tempted to conclude, in a general way, that in the cases where the ratios α_1/α_2 or α_1/α_3 are fairly small the angular momenta of the α_1-particles are greater than those of the lower energy particles, so that the emission probabilities of the latter are raised to comparable values. On the other hand, in the case of the 598 keV. resonance the high relative probability of α_1-particle emission could be accounted for if these particles were assumed to be emitted with small or zero angular momentum while the lower energy

Fig. 5.

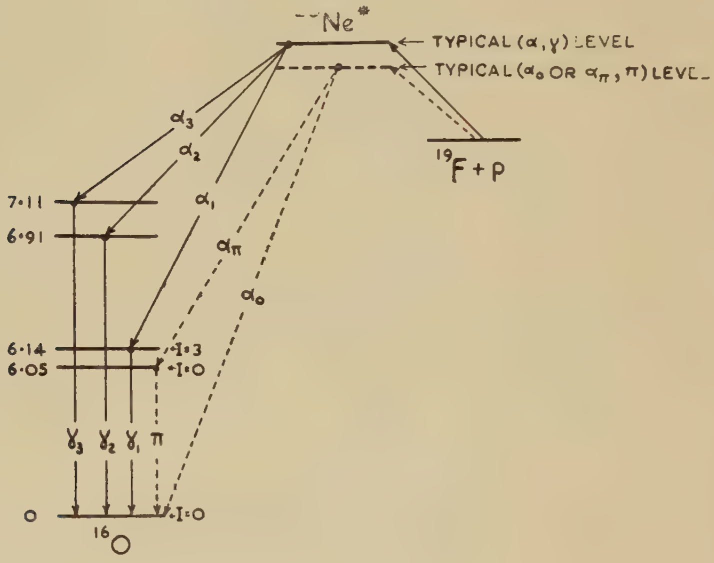

Disintegration modes in the proton bombardment of fluorine. The values (in MeV.) assigned to the ^{16}O levels are derived form the value $Q_0=8{\cdot}11$ MeV. given by Chao *et al.* (1950).

particles encountered an appreciable angular momentum barrier. Such an assumption would also account for the greater width of the 598 keV. resonance compared with the other resonances (*cf.* Devons and Hine 1949).

The recent angular correlation measurements made in this laboratory for the α_1-particles and γ_1-radiation from the 340 keV. resonance (Barnes, French and Devons 1950) indicate a useful method of obtaining data on the angular momenta of the α-particles from the various $^{20}Ne^*$ levels, and the spins of these and the $^{16}O^*$ levels. When such data have been obtained, further deductions may then be possible from the observed intensity ratios discussed above. It may appear, for example, that the radius of the $^{16}O^*$ nucleus is not the same for the three levels of excitation involved.

Acknowledgments.

I should like to express my thanks to Dr. W. E. Burcham for much advice and assistance in this work. I also wish to thank Messrs. W. Birtwhistle and D. D. Stewart for much technical assistance.

References.

Amaldi, E., and Cacciapuoti, B. N., 1947, *Phys. Rev.*, **71**, 739.

Barnes, C. A., French, A. P., and Devons, S., 1950, *Nature, Lond.*, **166**, 145.

Bennett, W. E., Bonner, T. W., Mandeville, C. E., and Watt, B. E., 1946, *Phys. Rev.*, **70**, 882.

Bethe, H. A., 1937, *Rev. Mod. Phys.*, **9**, 166, 178.

Bonner, T. W., and Evans, J. E., 1948, *Phys. Rev.*, **73**, 666.

Briggs, G. H., 1927, *Proc. Roy. Soc.* A, **114**, 341.

Burcham, W. E., and Devons, S., 1939, *Proc. Roy. Soc.* A, **173**, 555.

Burcham, W. E., and Freeman, J. M., 1949 a, *Phys. Rev.*, **75**, 1756; 1949 b, *Phil. Mag.*, **40**, 807 ; 1950 a, *Ibid.*, **41**, 337 ; 1950 b, *Ibid.*, **41**, 921.

Chao, C. Y., Tollestrup, A. V., Fowler, W. A., and Lauritsen, C. C., 1950, *Phys. Rev.*, **79**, 108.

Devons, S., and Hine, M. G. N., 1949, *Proc. Roy. Soc.* A, **199**, 56.

Herb, R. G., Snowdon, S. C., and Sala, O., 1949, *Phys. Rev.*, **75**, 246.

Knipp, J., and Teller, E., 1941, *Phys. Rev.*, **59**, 659.

Rasmussen, V. K., Hornyak, W. F., Lauritsen, C. C., and Lauritsen, T., 1950, *Phys. Rev.*, **77**, 617.

Strait, E. N., Van Patter, D. M., and Buechner, W. W., 1950, *Bull. Amer. Phys. Soc.*, **2255**, No. 1, 33.

Tollestrup, A. V., Fowler, W. A., and Lauritsen, C. C., 1949, *Phys. Rev.*, **76**, 428.

Van Allan, J. A., and Smith, N. M., 1941, *Phys. Rev.*, **59**, 501.

Walker, R. L., and McDaniel, B. D., 1948, *Phys. Rev.*, **74**, 315.

CX. *An Interferometric Study of some Optical Properties of Evaporated Silver Films.*

By R. C. Faust, Ph.D.*,
Royal Holloway College †.

[Received August 23, 1950.]

[Plates XXXVI. & XXXVII.]

Abstract.

Thermally evaporated silver films have been studied in the reflectivity range of 4 to 95 per cent. The air–silver and glass–silver reflection and transmission coefficients, the corresponding reflection phase changes and the apparent film thickness have been measured and compared with those of sputtered silver films. For very thin films, in a region where the light absorption is high, the glass-silver reflection coefficient passes through a minimum, and in the yellow and the green, but not in the blue, the glass–silver reflection phase change suddenly alters from an advance to a retardation. This transition in the phase change is intimately associated with the reflected fringe asymmetry.

§ 1. Introduction.

The presence of metallic coatings on the plates of an interferometer modifies the fringe patterns, the reflected system being affected differently from the transmitted one. In fig. 1 are seen three isotropic dielectric media 1, 2, 3, separated by the two parallel planes XX′ and YY′ which may or may not be coated with metallic films. The central medium has a refractive index μ and a geometrical thickness t. Monochromatic radiation which is incident upon XX′ enters medium 2 at an angle θ with the normal, and gives rise to a transmitted series of parallel wave trains $a, b, c, \ldots$, and a reflected series A, B, C, ... The optical properties of the boundary XX′ for light incident from medium 1 are an amplitude reflection coefficient r_1, an amplitude transmission coefficient t_1, a reflection phase change α_1 and a transmission phase change β_1; if the light is incident upon XX′ from medium 2 the same symbols are used with the suffix 2. If the light falls upon YY′ from medium 2 the reflection and transmission coefficients are ρ and τ, whilst the reflection phase change is γ. These optical values, which apply to light of vacuum wavelength λ incident upon the interferometer at one particular angle, are in general dependent upon the state of polarization.

---

* Communicated by Professor S. Tolansky.

† Now at the British Rayon Research Association, Urmston.

The resultant intensity of the transmitted light is a periodic and symmetrical function of the phase quantity

$$\delta=4\pi/\lambda \,.\, \mu t \cos\theta+\alpha_2+\gamma \quad . \; . \; . \; . \; . \; . \; . \; . \quad (1)$$

the greatest and least intensities occurring at $\delta=2n\pi$ and $(2n+1)\pi$ respectively. It has, however, been shown by Hamy (1906) that the reflected intensity is a periodic but generally asymmetrical function of δ. A given reflection minimum is therefore not necessarily equidistant (in terms of δ) from the two neighbouring reflection maxima, nor does the condition for a reflection minimum generally correspond to that leading to a transmission maximum. It is to be noted, however, that whenever XX′ is an uncoated dielectric interface the reflected fringe pattern is symmetrical, the reflected intensity minima coinciding with the transmitted maxima.

Fig. 1.

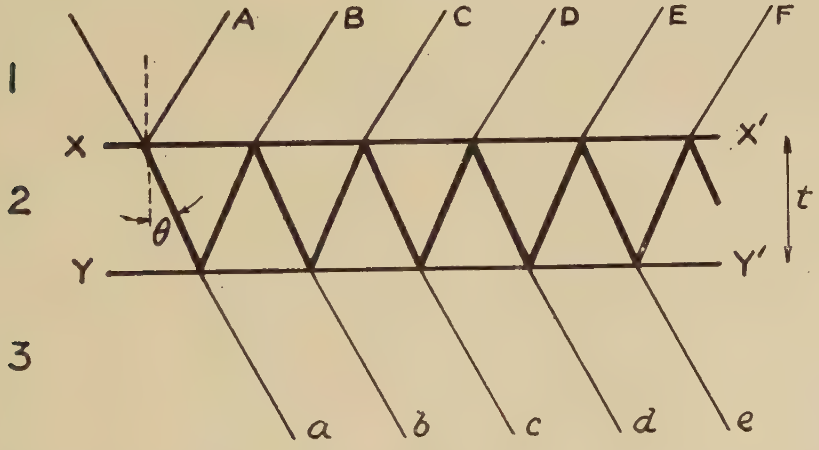

Hamy confirmed his theoretical predictions by observing the reflected fringe system produced by interferometers whose plates had been coated with chemically deposited silver films. More recently silver films evaporated on to glass have been similarly studied by Holden (1949), who, having compared his findings with the optical properties of sputtered films as determined by Rouard (1937), suggested that certain features of the reflection fringe asymmetry are closely associated with the glass–silver reflection phase change. In order to test this idea the properties of evaporated silver films have been examined at normal incidence and compared with those of sputtered films. The apparent film thickness, the reflection and transmission coefficients and the reflection phase changes at both the air–silver and glass–silver interfaces were measured and the results related to the observed reflection fringe asymmetry.

The silver, evaporated from molybdenum strip filaments at a pressure of about 5×10^{-5} mm. Hg, was deposited on to two glass optical flats and a thin glass coverslip. The variation in the mass deposited upon unit surface area was so slight that the three silverings could be regarded as identical. The two flats formed an air-gap interferometer, whilst the coverslip was employed for the determination of the glass–silver reflection phase change. All the measurements were made in the space of a few hours during which time no significant changes in the films' properties or appearance were detected.

The electron microscope has revealed a discontinuous structure in semi-transparent metal films, and thus one may not strictly speak of the thickness of a film. The interferometric method [Khamsavi and Donaldson (1947), Avery (1949)] which was employed yields an apparent thickness D, which is that the film would have if it were uniformly distributed and of the same density as the bulk metal. A strip of the evaporated film was gently removed with a razor blade and an opaque silver film deposited over the whole surface. the height of the well-defined step being determined from reflected Fizeau fringes. The probable error in the mean step height did not exceed ±15 A. for apparent film thicknesses in excess of 100 A. and ±25 A. for thinner films.

Fig. 2 (*a*).

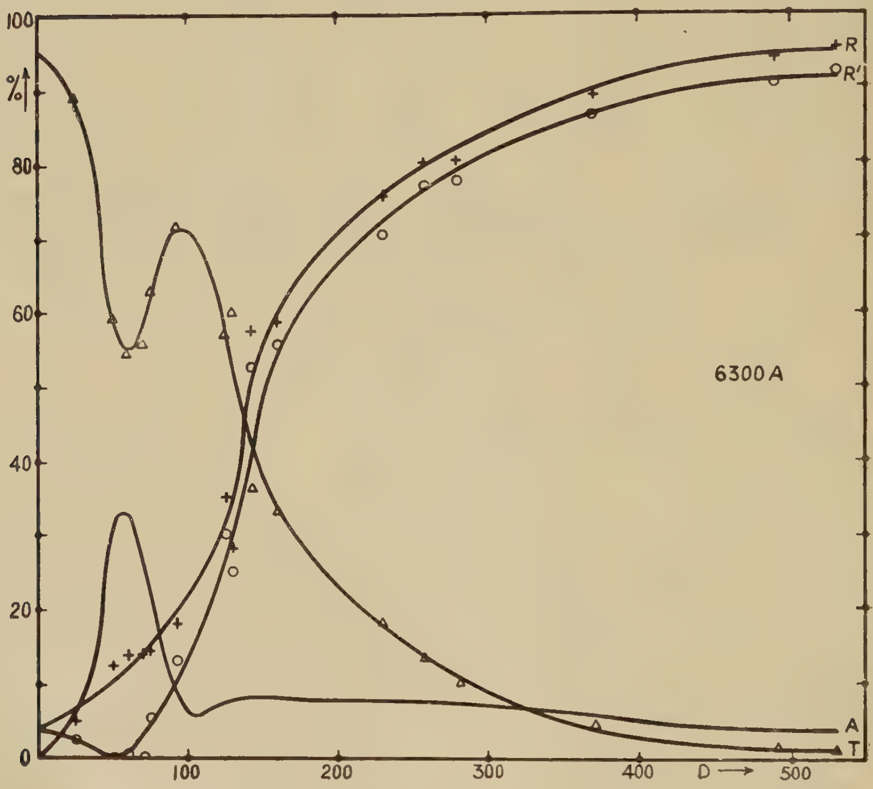

§ 2. THE REFLECTION AND TRANSMISSION COEFFICIENTS.

An electron multiplier cell was used to compare the incident light intensity with the intensities of the beams reflected and transmitted by the silver films, the angle of incidence being only 4°. After the introduction of correction terms necessitated by the presence of the glass substitute, the desired air–silver and glass–silver reflection and transmission coefficients were calculated. Three wavelength bands were selected by filters ; 6700 A. to 5900 A. with a peak at 6300 A., 5500 A. to 5200 A. with a peak at 5400 A., and 4650 A. to 4350 A. with a peak at 4500 A.

Fig. 2 (*b*).

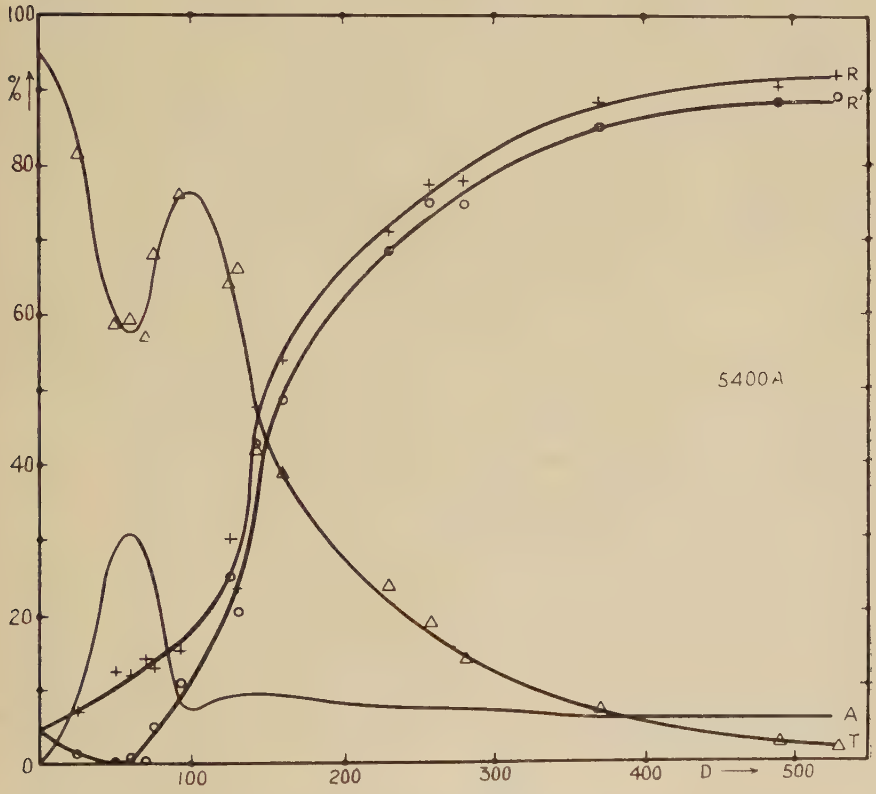

The results are presented graphically in fig. 2. As the air–silver and glass–silver transmission coefficients agreed to within the estimated error (±0·02 T), a mean value T has been taken. The error in the air-silver reflection coefficient R is about ±0·01 R for high reflectivities, but increases to ±0·04 R when the reflectivity is below 10 per cent. The inaccuracies in the glass–silver reflection coefficient R′ are greater, rising from ±0·02 R′ to as much as ±0·5 R′ at the reflectivity minimum.

The absorption for light incident from the air side A and from the glass side A′ have been calculated from the measured quantities, the presence of any light scattering being neglected. Being difference terms their errors are relatively high and small fluctuations in the calculated absorptions are not necessarily significant.

These results have been compared with those obtained by Goos (1936) and Rouard (1937) for sputtered films, and by Krautkrämer (1938), Strong and Dibble (1940), and Sennett and Scott (1950) for evaporated silver films. The following apparent general conclusions may be drawn :—

Fig. 2 (*c*).

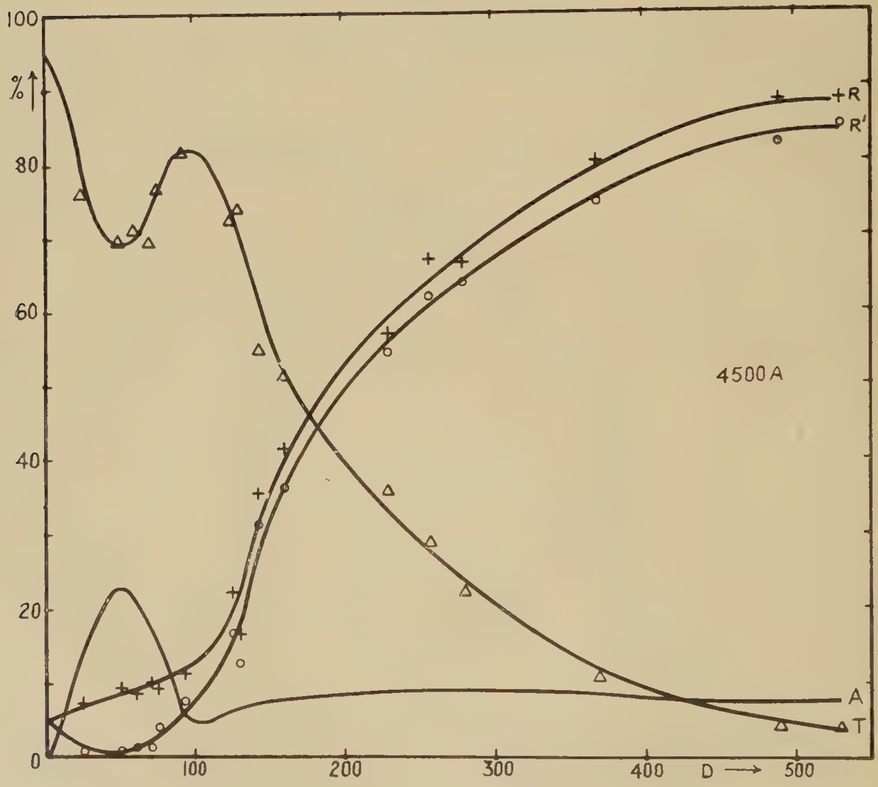

(1) At a given wavelength the air–silver reflection coefficient R decreases with diminishing film thickness until the value appropriate to the substrate alone is reached.

(2) The wavelength variation of R depends upon the film thickness. Normally R increases with increasing wavelength, but with very thin films the opposite behaviour has been found by Goos, Sennett and Scott, and the writer, whose 25 A. thick film had the coefficients 5·0 per cent. (6500 A.), 6·9 per cent. (5400 A.) and 7·4 per cent (4500 A.).

(3) At a given wavelength the substrate-silver reflection coefficient R′ decreases with diminishing film thickness until a low minimum value is reached ; it then increases finally attaining the value appropriate to the uncoated substrate. R′ is apparently always less than R.

(4) For thick films R′ rises with increasing wavelength, but for thin films in the neighbourhood of the R′ minimum the reverse may occur, this behaviour being responsible for the beautiful reflection colours observable in thin films. The 50 A. film, for example, was blue-mauve in reflection from the glass side, R′ being greater in the blue than in the red. The 25 A. film appeared rose-pink, R′ now being weaker in the blue ; the reflection colour from the air side of this film was a brilliant torquoise because R possessed the relatively uncommon property of being strongest in the blue.

(5) The transmission measurements made by the different workers show little agreement, the major differences occurring in the neighbourhood of the substrate-silver reflectivity minimum. In this region the writer has found that the general increase in transmission with diminishing film thickness is interrupted by a marked local minimum. This was not observed by Goos or by Strong and Dibble. (Rouard and Krautkrämer did not take transmission measurements in this region.) The recent work of Sennett and Scott is very illuminating ; they found a minimum with high but not low rates of evaporation, the relevant factor being the film structure.

(6) Whether there is a minimum in the transmission curve or not, the absorption terms A and A′ have peak values for all wavelengths in the neighbourhood of the substrate-silver reflectivity minimum. The peak absorption for both A and A′ decreases with shortening wavelength, but for the purpose of clarity A′, which is everywhere greater than A, has not been plotted. According to Sennett and Scott the slower the rate of absorption, the greater the film thickness for which the peak occurs, the onset of this high absorption being closely related to the state of aggregation of the film. For evaporation times of less than a minute the maximum absorption was found for an approximate film thickness of 100 A. ; the figure obtained by the writer using high evaporation rates was 60 A. (The slight dip near the peak of the absorption curve lies within the experimental errors.)

It is thus evident that the exact mode of film preparation plays a very important role in determining the film properties, and quantitative comparisons between sets of films made under different conditions are unsatisfactory. The general qualitative behaviour described above is, however, apparently common to all sets of silver films, evaporated or sputtered.

§ 3. OBSERVATION OF THE FRINGE PATTERNS.

The theory of reflection fringe asymmetry was originally developed for a plane-parallel sheet interferometer, but both v. d. Pahlen (1912) and Brossel (1947) have shown that provided the gap thickness and the slope of a wedge interferometer are small, the fringe intensity distribution on a Feussner surface differs negligibly from that produced by a sheet interferometer. A wedge can therefore be utilized to study the fringe patterns produced by metal-coated interferometer plates, any asymmetry due to the wedge slope being insignificant. There are two zero order Feussner surfaces on which the fringes lie, one in transmission, the other in reflection, but they do not exactly coincide even when the light falls upon the interferometer at normal incidence. In order therefore that both surfaces could be focused simultaneously a well-collimated normally incident beam, an interferometer of small gap and slope, and a 2-inch (N.A. 0·17) objective were used.

Fizeau fringes and fringes of equal chromatic order (Tolansky 1945) were studied in both transmission and reflection. The observation of the fringes of equal chromatic order was carried out, using a specially constructed plane grating spectrograph (14,200 lines/inch, inverse dispersion 50 A./mm.). The spectrum was normal, wavelength differences being proportional to the linear displacements on the photographic plate.

§ 4. THE AIR-SILVER REFLECTION PHASE CHANGE.

Consider an air-gap interferometer with an unsilvered front surface XX′ and a rear surface YY′, of which one half is silvered. The reflection Fizeau fringes, the minima of which coincide with the transmission maxima, run from the glass/glass to the glass/silver region and at the junction a fringe displacement is observed (figs. 11, 13, Pl. XXXVI.). At normal incidence the positions of the reflection minima in the two regions are determined by the equation

$$n\lambda=2t+\Omega\lambda=2t'+\Omega'\lambda, \quad . \quad . \quad . \quad . \quad . \quad . \quad . \quad . \quad (2)$$

in which the dash notation applies to the unsilvered region. This is derived from equation (1), t and t' being the two gap thicknesses at which a fringe of given order n occurs. Ω and Ω', representing the phase terms, are related by $(\Omega-\Omega')=1/2\pi\,.\,(\gamma-\gamma')$, where γ and γ' are the phase changes (in radians) at the air silver and the air–glass surfaces respectively.

If $dq\lambda$ represents twice the silver film thickness and dp the observed fractional order shift of the two fringe systems, then one obtains

$$2(t'-t)=(dq+dp)\lambda=\lambda/2\pi\,.\,(\gamma-\gamma'), \quad . \quad . \quad . \quad . \quad . \quad (3)$$

in which dp is positive when the fringes in the silvered region are on the side of decreasing gap thickness relative to those in the unsilvered region. It is known from the Fresnel coefficients that the reflection phase change γ' at an air-dielectric interface is $\pm\pi$, the sign being in doubt. Following Rouard (1937) the negative sign is here accepted, the phase change being interpreted as an advance, *i.e.* the optical gap is smaller than the geometrical one.

If a film is of high reflectivity the reflection fringes are barely visible in the region where the silver film covers the rear surface. Transmission fringes can be used instead, the fringe contrast and sharpness being enhanced by coating the front surface with a highly reflecting, semi-transparent film. Equation (3) also holds for these transmission fringes which are unfortunately very diffuse (*cf.* fig. 3, Pl. XXXVI.).

Such measurements were made for the three mercury radiations 5780, 5461 and 4358 A. The phase changes, all of which are advances, are shown graphically in fig. 4 as fractions of π. For film thicknesses above 100 A. the error is $\pm 0{\cdot}02$, whilst for thinner films it reaches $\pm 0{\cdot}03$. With a given film the relative values for different wavelengths are more accurate ($\pm 0{\cdot}01$), since they are uninfluenced by uncertainties in the film thickness.

Fig. 4.

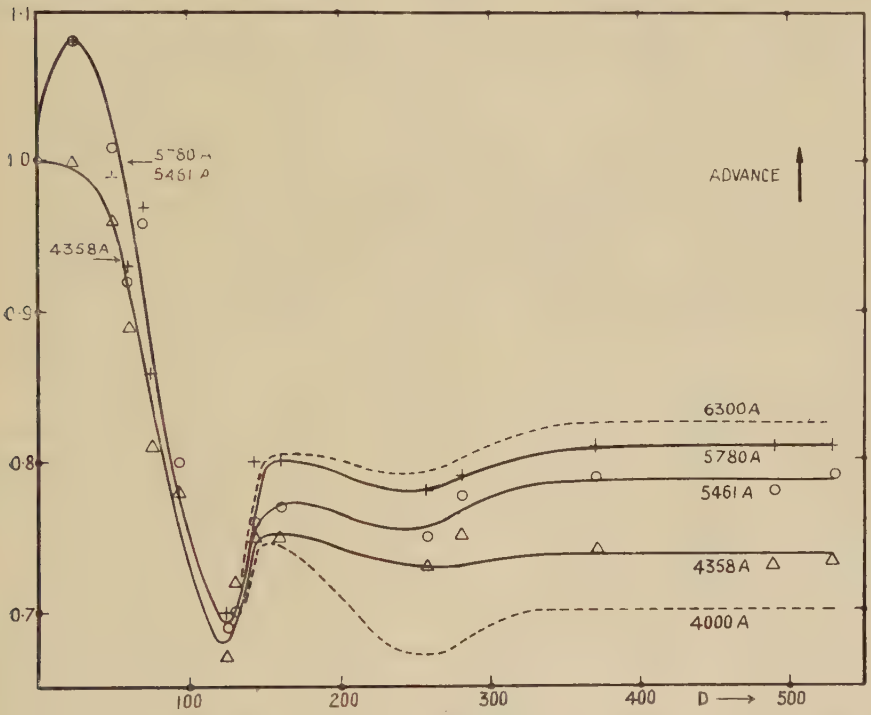

An alternative method of determining the air-silver phase change is to study the transmission fringes of equal chromatic order arising within an air-gap interferometer formed from two identically silvered optical flats Such a fringe pattern is shown in fig. 5 (Pl. XXXVI.) for 529A thick films, the mercury spectrum being superimposed upon one half of the field of view. The wave-number difference between any two transmitted fringes of order n and $(n+1)$ is

$$\Delta\nu=\nu_{n+1}-\nu_n=\frac{\lambda_n-\lambda_{n+1}}{\lambda_n\lambda_{n+1}}=\frac{1}{2t}[1-(\Omega_{n+1}-\Omega_n)] \quad . \quad . \quad . \quad (4)$$

the order increasing with decreasing wavelength. As the variation of Ω from order to order (*i. e.* with wavelength) is slight, the wave-number difference closely approaches the constant value $\frac{1}{2}t$. The wavelength difference $(\lambda_n-\lambda_{n+1})$ must therefore decrease rapidly as the wavelength shortens. The effective order of interference may be found from the equation

$$n-\Omega=2t/\lambda_n=\frac{\lambda_{n+1}}{\lambda_n-\lambda_{n+1}} \quad . \quad . \quad . \quad . \quad . \quad . \quad . \quad (5)$$

in which, as N. Barakat has remarked, the fractional part represents Ω, n being of necessity integral. Here $\Omega=\gamma/\pi$ where γ is the desired air-silver reflection phase change.

The fringe pattern of fig. 5 (Pl. XXXVI.) is analysed in Table I. The

TABLE I.

Wave-length (A.U.)	Wave-number (cm.$^{-1}$)	Wave-length differences	Wave-number differences	$6\,.\,\Delta\nu$	$n-\Omega$	Ω (Fizeau)
6457	15487	270	676	—	22·83	—
6187	16163	247	672	4037	23·82	—
5940	16835	229	675	—	24·82	—
5711	17510	211	672	4035	25·81	—0·81
5500	18182	196	672	—	26·80	—0·79
5304	18854	181	670	4033	27·79	—
5123	19524	171	674	—	28·77	—
4952	20198	160	670	4028	29·77	—
4792	20868	149	670	—	30·76	—
4643	21538	139	664	4020	31·75	—
4504	22202	132	671	—	32·72	—
4372	22873	125	673	4019	33·71	—0·72
4247	23546	—	—	—	34·71	—

wave-number differences are almost constant but, as seen from the fifth column, there is a gradual diminution due to the slowly varying phase change. The geometrical gap thickness can only be found from the approximate equation $\Delta\nu=\frac{1}{2}t$, and as a small error in t leads to a large percentage error in Ω, another procedure had to be adopted. The value chosen for t was such that the phase changes calculated from the fringes of equal chromatic order agreed as closely as possible with those determined from the Fizeau fringes. In this particular example the chosen value was $2t=1{\cdot}474\times10^{-3}$ cm. ($\Delta\nu=678$ cm.$^{-1}$), the calculated effective order being given in the sixth column. In the final column is the value of Ω obtained from Fizeau fringes. To ascribe a unique value to the geometrical gap implies an abrupt interface between the silver film and the air, and is therefore equivalent to defining the film thickness. In this way the phase changes at the two wavelengths 6300 A. and 4000 A. were found for films thicker than 125 A. These are represented by the dotted curves in fig. 4.

An opaque film, whose phase change was required, was matched against a semi-transparent 370 A. film and the reflection fringes of equal chromatic order were studied (fig. 6, Pl. XXXVI.). It was known that the reflection minima coincided with the theoretical positions of the transmission maxima (*cf.* § 6), and the phase change could therefore be calculated from equations (4) and (5) in which it was possible to introduce an approximate value for the correction term $(\Omega_{n+1}-\Omega_n)$. Here, however, $\Omega=1/2\pi\,.\,(\alpha_2+\gamma)$ where α_2 is the already-determined phase change at the transparent film and γ is the desired phase change at the opaque film. The values obtained are close to those found for relatively thick semi-transparent films.

Wavelength (A.)	6300	5780	5460	4360	4000
γ (in terms of π)	0·84	0·82	0·80	0·73	0·70

Several conclusions may now be drawn from fig. 4.

(1) For thick films the air–silver reflection phase change increasingly departs from π with shortening wavelength, the difference in the phase change between 6300 A. and 5461 A. being almost the same as that existing between 4358 and 4000 A. These effects, corresponding to the more rapid falling off of the reflectivity as the wavelength is lowered, were also detected by Meggers (1921) for cathodically sputtered, thick silver films.

(2) As the film thickness is reduced the phase change oscillates, a well-marked drop occurring at about 125 A., *i. e.* for a reflectivity in green of about 25 per cent. Such a minimum was also noted by Rouard for a film thickness of 90 A. and a reflectivity of about 20 per cent. In this region the wavelength sensitivity of the phase change is very slight.

(3) For very thin films the phase change is close to π and even becomes greater than this quantity, thus being observed as an advance relative to that at a dielectric face. Such advances were also measured by Rouard for films below 32 A. thickness. With such thin films the phase change deviates least from π in the blue in accordance with the unusual behaviour of the air-silver reflection coefficient. Further reductions in the film thickness cause the phase change to attain the value π appropriate to the substrate alone.

§ 5. THE GLASS–SILVER REFLECTION PHASE CHANGE.

The glass-silver reflection phase change was measured by viewing reflection Fizeau fringes within a thin glass cover slip, the rear face of which was half-covered by the silver film. The phase change at the glass–air face, which according to theory is zero, was accepted as a standard. A knowledge of the film thickness was not required in order to calculate the glass–silver phase change which is provided by $2\pi\,.\,dp$, where dp is the observed fringe displacement at the boundary of the two halves of the interferometer (*cf.* equation (3)). When the film reflectivity was too great to yield satisfactory reflection fringes the front surface of the cover slip was coated with a highly reflecting, semi-transparent film and the transmission fringes were then studied. The lack of planeness of the faces of the glass slip often produced an irregular fringe spacing, and the very low glass–silver reflectivity of thin films resulted in a poor fringe visibility. For these reasons an accuracy better than ±0·04 cannot be claimed for the phase change measurements shown in fig. 7 as fractions of π.

For thick films the phase change is an advance which more closely approaches π the longer the wavelength. In the yellow and green a decrease in film thickness causes this advance to become a marked retardation, the transition, which covers a very narrow thickness range, occurring at that thickness (60 A.) for which the glass–silver reflection coefficient is at its minimum value. This retardation then diminishes, presumably reaching zero, the value appropriate to the uncoated dielectric. In the blue, on the other hand, the initial phase advance decreases and might become a very slight retardation before it finally vanishes. Similar results were found with the sputtered films studied by Rouard, the conversion of an advance into a retardation occurring in the neighbourhood of the glass–silver reflectivity minimum for wavelengths greater than 4358 A.

Fig. 7.

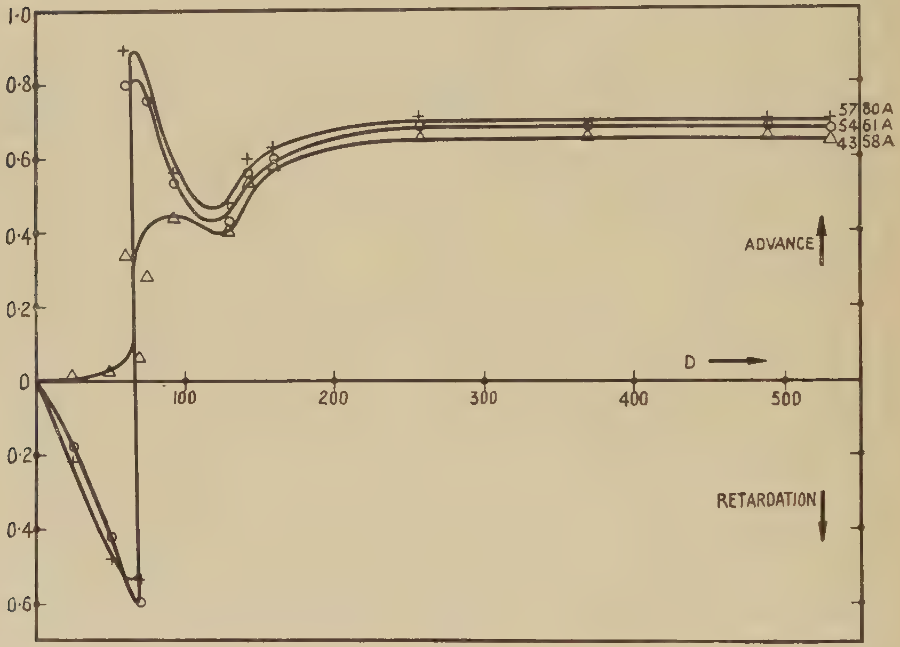

The reflection fringes obtained with the 61 A. film at the wavelength 5461 A. are shown in fig. 8 (Pl. XXXVI.), the fringes in the silvered part (the lower region of poorer contrast) being on the side of increasing gap thickness relative to those in the unsilvered part. The glass-silver phase change is therefore an advance. The film edge is not abrupt, and as the deposit becomes thinner this advance rapidly diminishes and even becomes a retardation, the fringes moving to the side of decreasing gap. This demonstrates the high sensitivity of the phase change to alterations in the thickness of such low reflectivity films.

The glass-silver phase change apparently deviates from π to a greater extent than the air silver phase change for all wavelengths and film thicknesses, this behaviour probably corresponding to the relatively low reflectivity on the substrate side of the film.

§ 6. REFLECTION FRINGE ASYMMETRY.

The phase quantity χ, which is determined solely by the optical properties of the upper interferometer surface XX′ according to the expression

$$\chi=\beta_1+\beta_2-\alpha_1-\alpha_2 \quad . \quad . \quad . \quad . \quad . \quad . \quad . \quad . \quad . \quad (6)$$

decides whether or not the reflection fringes shall be asymmetrical. It is, however, the combined properties of both interferometer plates which shapes the reflection fringe pattern and determines at what value of δ the reflection minima will occur. The theoretically predicted fringe behaviour is summarized in the following Table, in which it is to be noted that $\delta=2n\pi$ always corresponds to the transmission maxima and that $l=2t_1t_2\rho[\rho^2r_2(r_1r_2+t_1t_2)-r_1]$.

TABLE II.

χ	Condition	Reflection fringe pattern	Reflection minima in terms of δ
$(2N+1)\pi$	$l<0$	Symmetrical	$2n\pi$
$(2N+1)\pi$	$l=0$	Uniform field	—
$(2N+1)\pi$	$l>0$	Symmetrical	$(2n+1)$
$2N\pi$		Symmetrical	$(2n+1)\pi$
Between $(2N+1)\pi$ and $2N\pi$		Asymmetrical, minima closer to maxima of lower order	Between $2n\pi$ and $(2n+1)\pi$
Between $(2N+1)\pi$ and $(2N+2)\pi$		Asymmetrical, minima closer to maxima of higher order	Between $2n\pi$ and $(2n-1)\pi$

For relatively thick films the form of the reflection fringes was studied by simultaneously viewing the reflected and transmitted fringe systems. In this way the Fizeau fringes of fig. 9 (Pl. XXXVI.) were obtained with the 529 A. thick films at the wavelength 5461 A., faint secondary fringes arising from the 45° reflector being visible across the reflected pattern. The reflection minima agreed in position with the transmission maxima to within 0·02 of an order, a difference attributable to collimation and focusing uncertainties. Fringes of equal chromatic order were also observed with the same interferometer, the close agreement of the fringe positions throughout the visible spectrum being seen from fig. 10 (Pl. XXXVI.). This coincidence of the reflection minima with the transmission maxima was also discovered for all film thicknesses in excess of 142 A. (47 per cent reflectivity in the green), nor was any asymmetry perceptible. The phase term χ must, therefore, be close to an odd multiple of π for all wavelengths.

Because of the diffuseness of transmission fringes at low reflectivities a different method was adopted for thinner films. Only a half of each of the two glass interferometer plates was silvered and the interferometer was divided into four regions by the intersection of the two straight line edges of the films. In fig. 11 (Pl. XXXVII.) are seen the four separate Fizeau fringe systems observed in reflection (5461 A.) with the 93 A. films. Quoting the upper interferometer face first the four regions are glass/glass, glass/silver, silver/glass and silver/silver; the reflection minima in the two first-named regions coincide with the transmission maxima at $\delta=2n\pi$ and thus form reference marks. The fringe displacements for the 93 A. films are given below as fractions of an order, the fringes in the second region being on the side of decreasing gap thickness, *i.e.* decreasing δ.

A.	glass/glass–glass/silver	0·067
B.	glass/glass–silver/glass	0·147
C.	silver/glass–silver/silver	0·067
D.	glass/silver–silver/silver	0·152
E.	glass/silver–silver/glass	0·080, 0·085.

The origin of the displacement A as the combined effect of the film thickness and the air-silver reflection phase change has already been described in § 3. The inequality of the displacements A and B shows that the addition of a silver film to the upper plate XX′ is not equivalent to adding one to the lower plate YY′, the difference E representing the influence of χ. A value for E can also be obtained from displacements C and D. As, however, the positions of the reflection minima are dependent upon the reflectivity of the lower interferometer face whenever χ deviates from a multiple of π, the displacement A might differ from C and displacement B from D; the two calculated values of E should, however, be identical. No conclusive evidence was found for such differences, this probably being due to the small alteration in the rear surface reflectivity (4 to 14 per cent) from one region to another.

In fig. 12 are seen the differences E expressed as fractions of an order, positive values signifying that χ is larger than $(2N+1)\pi$ and negative ones that it is below $(2N+1)\pi$. When E is $\pm 0{\cdot}5$, χ is an even multiple of π; this condition is closely approached with the 50 A. films in the green, the reflection fringes in the silver/glass and silver/silver regions then possessing the transmission-like appearance illustrated in fig 13 (Pl. XXXVII.). When χ is no longer an integral value of π the reflected fringe pattern is asymmetrical in the sense indicated in Table II.

The 61 A. thick film is of interest In the yellow and the green the Fizeau fringe asymmetry is such that the minima are closer to the maxima of higher order. The displacement E, however, is apparently negative, not positive, since the minima in the silver/glass region appear to be on the side of greater order relative to those in the glass/silver region. Two explanations are possible for this behaviour : χ lies between $(2N+1)\pi$ and $(2N+2)\pi$ and some spurious edge effect gives the impression of a fringe movement towards larger orders instead of smaller ones, or χ is between $2N\pi$ and $(2N-1)\pi$, in which instance the displacements E in the yellow and green should read $-0{\cdot}58$ and $-0{\cdot}69$ instead of 0·42 and 0·31 The first explanation is favoured, the spurious influence being provided by the rapid variations in the glass-silver phase change which take place at the film edge (*cf.* fig. 8, Pl. XXXVI.), these variations bringing about marked changes in the value of χ in accordance with the arguments of the following section. In the blue, where the glass–silver phase change suffers only mild alterations and does not change sign, no edge effects are noticeable, and E is undoubtedly positive. This strong wavelength sensitivity of the film properties is illustrated in fig. 14 (Pl. XXXVII.), which shows fringes of equal chromatic order taken across the boundary

Fig. 12.

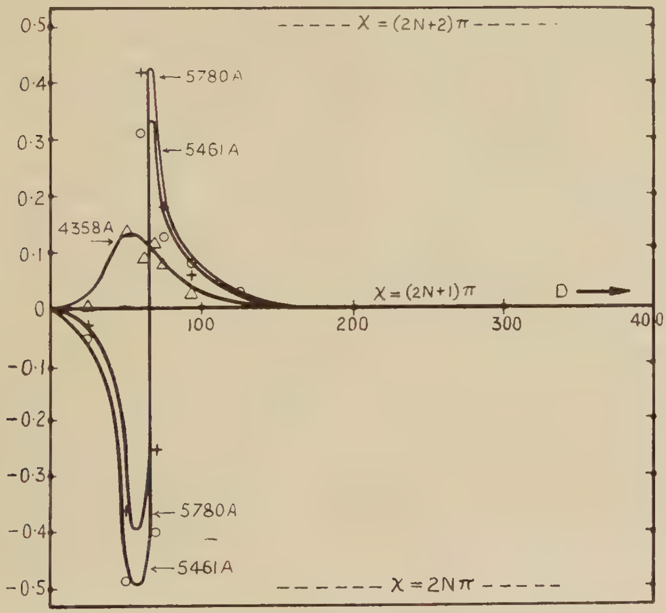

between the silver/silver and the glass/silver regions of an air-gap interferometer formed with the 61 A. films. In the blue the silver/silver minima are close to but on the low order (long wavelength) side of the glass/silver ones. As the wavelength increases the silver/silver minima become more displaced relative to those in the other region, but despite appearances this fringe displacement is towards longer and not shorter wavelengths, the strong slope of the silver/silver fringes at long wavelengths representing marked changes in the optical properties as the film thickness alters slightly.

§ 7. Discussion.

If the film thickness is greater than about 150 A. the phase term χ is close to $(2N+1)\pi$ for all wavelengths, this being the value appropriate to the dielectric substrate. At the wavelength 4358 A. further reductions in film thickness cause a small initial increase in χ which is then followed by a decline, $(2N+1)\pi$ again being reached for the thinnest films. The behaviour at the two longer wavelengths is, however, different. At first χ increases rapidly, closely approaching $(2N+2)\pi$ in the yellow and possibly also in the green. Then at an approximate thickness of 60 A. it abruptly drops to about $2N\pi$; this rapid decline is followed by an increase, $(2N+1)\pi$ being reached from the lower side and not the upper one as in the blue. Holden (1949) who has utilized microphotometer traces to study the reflection fringe asymmetry in the green, discovered that the magnitude of χ rapidly diminishes from about $(2N+2)\pi$ to $2N\pi$ at an approximate air-silver reflectivity of 15 per cent, this being in agreement with the present work where the transition occurs at a reflectivity in the green of 12 per cent.

In equation (6) the quantity χ was defined as the sum of the air silver and glass-silver transmission phase changes minus the sum of the air–silver and glass–silver reflection phase changes. The two transmission phase changes are unknown and their contribution cannot be assessed. It is reasonable to assume that they suffer no rapid alteration in magnitude within the thickness range 50 to 70 A. In the same region the air–silver reflection phase change undergoes relatively mild oscillations, and the glass–silver reflection phase change must therefore exert the greatest influence. For example, at 60 A. this phase change abruptly increases by about $1{\cdot}4\pi$ in both the yellow and the green (phase advances are negative in sign). At the same thickness the fringe displacement E decreases by about 0·75 of an order, thereby indicating that χ has been reduced by an amount between π and 2π. In the blue, however, both the phase change and χ show only gentle variations and neither reverses sign. The general similarity between the curves in figs. 7 and 12 in the thickness range 0 to 100 A. is indeed striking, the two series of measurements being in harmony. Holden's suggestion that the reflection fringe asymmetry and the glass–silver reflection phase change are intimately related therefore receives experimental confirmation.

The experimental results may now be summarized and compared with the predictions of Table II.

(1) For thick and very thin silver films the phase term χ is close to an odd multiple of π, the light absorption is small and the ratio R/R' nearly unity. In an interferometer constructed of such films the reflection minima and transmission maxima are almost in perfect coincidence.

(2) In the immediate neighbourhood of the minimum in the glass-silver reflectivity curve the absorption and the ratio R/R' are large and χ deviates from $(2N+1)\pi$. The reflection fringes are then usually asymmetrical. In the blue, where the maximum absorption is relatively small, the deviation is less pronounced than in the green and yellow for which wavelengths χ closely approaches both $2N\pi$ and $(2N+2)\pi$ thereby producing nearly symmetrical reflection fringes, the minima of which coincide with the transmission maxima.

(3) In this same transition range χ should pass through the value $(2N-1)\pi$ in both the green and the yellow. As the ratio R/R' will then be very high, the reflection and transmission minima might coincide in an air-gap interferometer using such a film for the upper plate XX′; this is particularly likely when the reflectivity of the rear surface YY′ is high.

The optical properties of sputtered and evaporated silver films have been shown to possess similar characteristics. Gold films, whether they are sputtered, Rouard (1937) and Goos (1937), or evaporated, Sennett and Scott (1950), display the same general features as those of silver, and it is probable that these films will also produce reflection fringe asymmetry. Furthermore, the writer has observed asymmetrical reflection fringes using evaporated aluminium films, which Sennett and Scott have also shown to possess a peak absorption at a certain film thickness. The conclusions reached in this paper are therefore possibly typical of a number of metallic films.

Metal films have been regarded by Rouard and others as homogeneous layers of definable thickness and the principles of optical interference have therefore been applied to them. From the oscillating nature of the optical properties of the films it is then concluded that the optical constants vary with film thickness. A more satisfactory approach appears to be to adopt the ideas of Maxwell Garnett (1904, 1905), who regards the film as consisting of many regularly scattered globules, the optical constants of which are the same as those of the bulk metal. The sphere diameters, which are small relative to the wavelength of light, are not necessarily uniform, the characteristic of each film being the volume of metal spheres in unit volume of the film. Krautkrämer and Sennett and Scott have demonstrated that this theory provides a qualitative behaviour for many of the properties of metallic films, but that a number of features still remain unexplained. The theory might be improved by considering the non-spherical nature of the metallic particles.

ACKNOWLEDGMENTS.

The author wishes to thank Professor S. Tolansky for the continued interest he has shown in this work, which was made possible by the receipt of a grant from the Department of Scientific and Industrial Research. He also wishes to acknowledge the loan of the reflectometer by Mr. D. G. Avery and the valuable assistance given by the workshop staff of the Physics Department, Royal Holloway College.

REFERENCES.

AVERY, D. G., 1949, *Nature, Lond.*, **163,** 916.
GOOS, F., 1936, *Z. Phys.*, **100,** 95 ; 1937, *Ibid.*, **106,** 606.
HAMY, M., 1906, *J. Phys. Radium*, **5,** 789.
HOLDEN, J., 1949, *Proc. Phys. Soc.* B, **62,** 405.
KHAMSAVI, A., and DONALDSON, W. K., 1947, *Nature, Lond.*, **159,** 228.
KRAUTKRÄMER, J., 1938, *Ann. der Phys.*, **32,** 537.
GARNETT, J. C. M., 1904, *Trans. Roy. Soc.* A, **203,** 385 ; 1905, *Proc. Roy. Soc.* A, **76,** 370.
MEGGERS, W. F., 1921, *J.O.S.A.*, **5,** 308.
v. D. PAHLEN, E., 1912, *Ann der. Phys.*, **39,** 1567.
ROUARD, P., 1937, *Ann. de Physique*, **7,** 291.
SENNETT, R. S., and SCOTT, G. D., 1950, *J.O.S.A.*, **40,** 203.
STRONG, J., and DIBBLE, B., 1940, *J.O.S.A.*, **30,,** 431.
TOLANSKY, S., 1945, *Proc. Phys. Soc.*, **36,** 225.

Fig. 3.

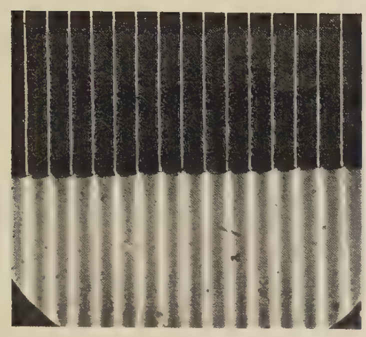

Fig. 5.

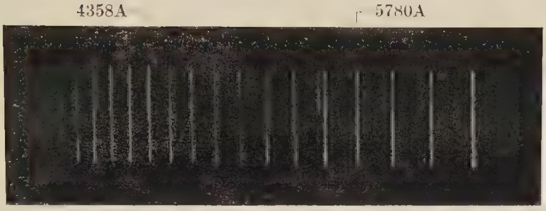

Fig. 6.

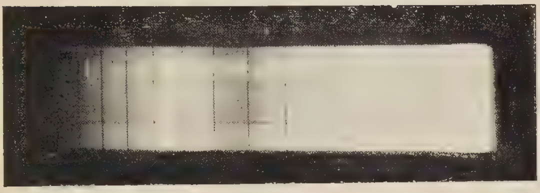

Fig. 8.

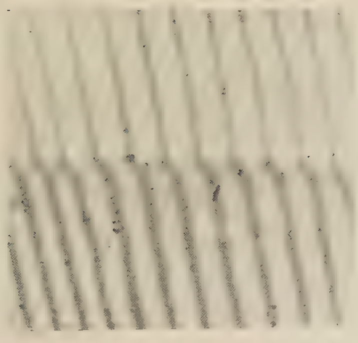

Fig. 9.

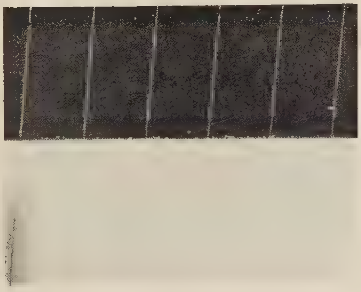

Fig. 10.

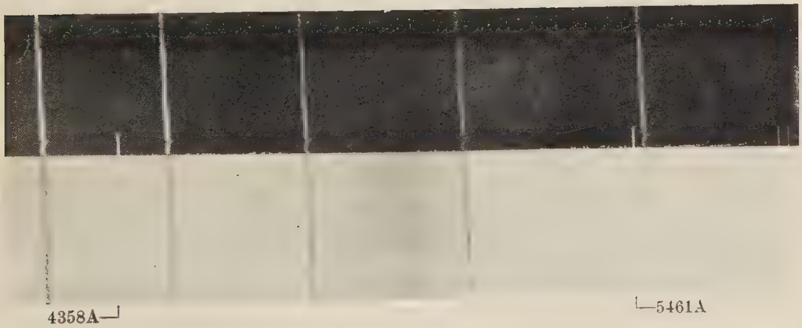

Fig. 11.

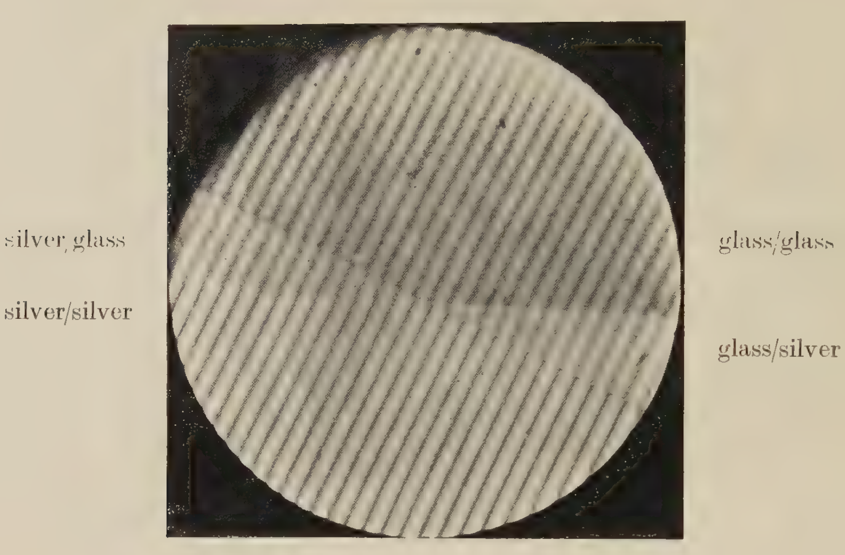

Fig. 13.

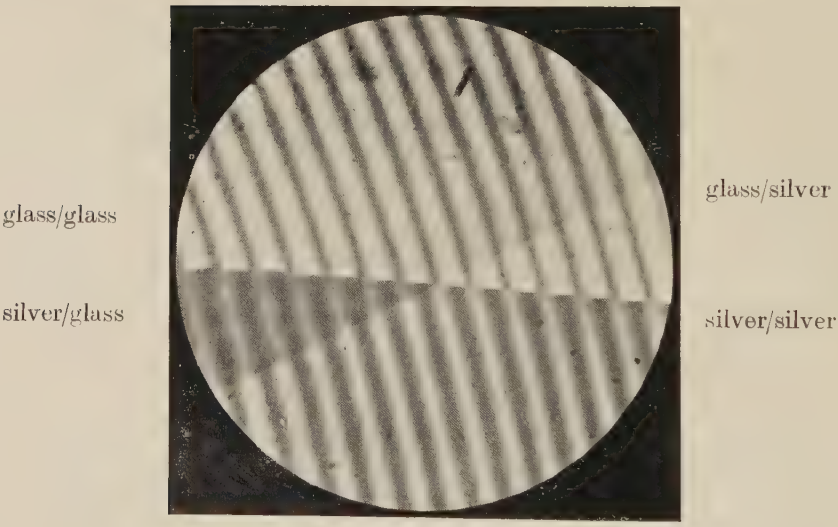

Fig. 14.

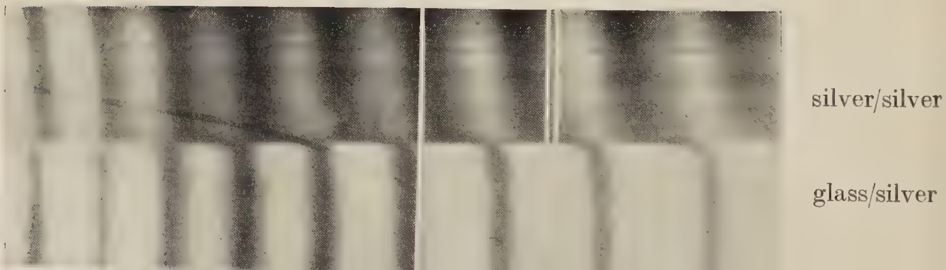

CXI. *The "Velocity" of Brownian Movement.*

By R. Fürth,
Birkbeck College, University of London†.

[Received September 1, 1950.]

Abstract.

The notion of the velocity of the random movement of a particle and the problem of its observation is discussed in view of certain incorrect statements in a recent paper by D. K. C. MacDonald.

The problem of how to define and to measure the velocity of the random movement of a particle has frequently been discussed in the past. Recently D. K. C. MacDonald (1950) has contributed to the problem by applying to it the modern notion of the "frequency spectrum" of a random movement and by deriving an expression for the "observable" mean square fluctuation $\overline{\delta_v^2}$ of the velocity which he attempts to test on some early observations of the Brownian movement of small particles by F. Exner (1900). However, his analysis rather confuses the real issue and the application to the observations of Exner is partly erroneous. I, therefore, wish to make the following brief remarks on the problem.

(1) Let x be a "unidimensional stochastic function" of time t. This means that a function $x(t)$ does not exist in the usual mathematical sense, but that there exists a probability density function $p(x,t)$ for observing a certain value x at time t. Consequently all moments $\overline{x^s}$ are ordinary functions of time and their derivatives exist. In particular, $V \equiv d(\overline{x})/dt$ is the so-called drift velocity (which may be zero), and the quantity $D \equiv \frac{1}{2}d(\overline{x^2})/dt$, which, in general, is different from zero, is a convenient measure for the rate of fluctuations of x (D can, of course, be independent of time). But the quantity dx/dt does *not* exist at all.

If in particular x is a coordinate, a corresponding velocity component in the strict sense of the word cannot be defined. *Vice versa*, if a velocity component v is primarily introduced as a stochastic variable the corresponding position co-ordinate has no meaning. This is the well known situation in quantum mechanics where either coordinates or momenta of particles can be chosen as representing variables, but not both at the same time. It leads directly to the uncertainty principle for the simultaneous measurement of position and velocity.

(2) There is, of course, no justification for regarding a physical quantity x as a stochastic variable under conditions where quantum effects can be neglected. For the random character of the variation of

---

† Communicated by the Author.

x in such a case is only due to the influence of "random external disturbances" on the observed system which are supposed to be not accessible to direct measurement. Thus x can be regarded as an ordinary function of time for an individual observed system, and the system, therefore, possesses at each moment a well defined velocity v which, in the absence of a drift velocity, will irregularly fluctuate in time.

One can, evidently, also define a "velocity" v^* by the difference quotient

$$v^* = \frac{\Delta x}{\Delta t} \quad . \quad . \quad . \quad . \quad . \quad . \quad . \quad . \quad . \quad . \quad (1)$$

over a finite time interval Δt. This v^* will be found to be practically identical with v as long as Δt is smaller than a certain time interval τ which depends on the mechanism of the observed system and which may appropriately be called its "characteristic time"(†).

If $\Delta t < \tau$, the statistical characteristics of v^* must be identical with those of v. If, on the other hand, Δt is considerably larger than τ the statistical characteristics of v^* may be very different from those of v. In any case, however, a statistical analysis of the behaviour of v^* is absolutely equivalent to a statistical analysis of a record of displacements Δx at equal time intervals Δt, and so no useful purpose is served by the introduction of the quantity v^*.

(3) So far we have assumed that x is measured by means of an "ideal" instrument. In actual fact, the result of the observation by a real measuring device will usually be in the form of a graph representing the dependence of a "reading" y on time, y being a suitable measure of x. The rate of change w of y is obtained at any point of this graph by constructing the tangent to the arc of the curve at that point. This, of course, is only psssible with a finite accuracy, depending on the "resolving power" δy of the instrument.

The problem of the accuracy of the simultaneous determination of y and w has been discussed in detail by the author (1935, 1948), and he has shown that it is limited by a relation which is analogous to the quantum mechanical uncertainty principle.

Within the limit δy of accuracy, one can also measure a quantity w^* defined by

$$w^* = \frac{\Delta y}{\Delta t}, \quad . \quad . \quad . \quad . \quad . \quad . \quad . \quad . \quad . \quad . \quad (2)$$

where Δt is again a finite time interval. As a rule, it will be found that w^* is identical with w as long as Δt is smaller than a certain time interval δt which we may call the "resolving power in time" of the instrument

---

(†) τ need not necessarily be the same as the so-called "relaxation time" which plays a decisive part in MacDonald's considerations ; this latter quantity is only defined for phenomena which are the outcome of the opposing influences of inertial and dissipating processes.

as the record can clearly give no indication whatsoever about the variation of the measured quantity x within time intervals smaller than δt(†). It has to be borne in mind, however, that both δt and δy cannot be defined precisely and that their values are necessarily arbitrary within considerable margins.

If one can make δt of the order of magnitude τ (or smaller) the record can be used for investigating the statistical properties of v. But if, as usual, δt is much larger than τ the record can only be used for the investigation of the statistical properties of Δx for time intervals Δt larger than δt. This holds *a fortiori* for discontinuous observations of y at equal time intervals Δt. Clearly no complicated mathematical analysis is required to come to this almost trivial conclusion, and no analysis can reveal anything beyond the above statement.

(4) Let us finally consider the practical example used by MacDonald to test his theoretical relations. The observations of Exner consisted in following, by means of a camera lucida, the movemnt of a Brownian particle as closely as possible with a stylus on a blackened glass plate. This curve was subsequently projected on a screen and the total length of the curve measured. The " velocity " of the Brownian movement was then taken to be this length divided by the total time taken for the observation.

Evidently in this case δt is the " reaction time " of the observer for this sort of observation which is large compared with τ. Thus, according to (2), the measured " velocity " is simply $(\overline{\delta s})/\delta t$ where $(\overline{\delta s})$ is the average arc of the curve described in time δt.

As the observed Brownian motion is a two-dimensional projection of the actual three-dimensional path, one finds easily for the probability density $p(\delta s, t)$ of δs in time t

$$p(\delta s, t) = \frac{\delta s}{2\mathrm{D}t} \exp\left(-\frac{(\delta s)^2}{4\mathrm{D}t}\right), \quad . \quad . \quad . \quad . \quad . \quad . \quad (3)$$

where D is the diffusion coefficient of a suspension of identical particles. From (3) one obtains at once

$$(\overline{\delta s}) = \int_0^\infty p(\delta s, t)\delta s d(\delta s) \quad \sqrt{(\pi \mathrm{D}t)}. \quad . \quad . \quad . \quad . \quad . \quad (4)$$

Thus finally

$$w^* = \sqrt{(\pi \mathrm{D}/\delta t)} \quad . \quad . \quad . \quad . \quad . \quad . \quad . \quad . \quad . \quad (5)$$

MacDonald, however, identifies his $\sqrt{\overline{\delta_v^2}}$ with w^* which is incorrect, as his $\overline{\delta_v^2}$ refers to a one-dimensional Brownian movement ; he also

---

(†) δt may have the character of a relaxation time but not necessarily so ; *e.g.* if the record is obtained by trying to follow the movements of a spot on a projection screen with a pencil, δt will mainly be determined by the time the nervous impulses take to travel from the eye to the brain and back to the muscles of the hand.

mixes up a mean absolute value with a root mean square value, a procedure he himself strongly criticises in his paper.

For spherical particles of radius a

$$D=\frac{kT}{6\pi\eta a}. \qquad (6)$$

From (5) and (6) an expression for w^* is obtained which, of course, is of the same order of magnitude as MacDonald's expression (16), but there is no justification for his different numerical factor, although it is allegedly obtained by a refined mathematical analysis.

From the values of w^* given in Exner's paper for particles of various sizes, one obtains from (5) and (6) values of δt between 0·1 and 0·2 sec. which are of the order of magnitude to be expected. No other conclusions can be drawn from these experiments.

REFERENCES.

EXNER, F., 1900, *Ann. d. Phys. Lpz.*, **2**, 843.
FÜRTH, R., 1935, *Zs. f. Phys.*, **81**, 143.
FÜRTH, R., 1948, *Science Progress*, **143**, 396.
MACDONALD, D. K. C., 1950, *Phil. Mag.*, **41**, 814.

CXII. *The Use of Atmospherics to Study the Propagation of Very Long Radio Waves.*

By F. F. Gardner,
Cavendish Laboratory, Cambridge *.

[Received October 5, 1950.]

Summary.

The "level" of integrated atmospherics received on narrow-band receivers tuned to a series of different frequencies between 3·5 and 50 kc./s. has been recorded. The band-width of the receivers was about 200 c./s. and the time of integration about one minute. The results were analysed so as to eliminate the unknown spectral distribution of energy at the source, and so as to show up the way in which propagation conditions changed with distance and with time of day. The results are shown in fig. 4, from which the most significant effect is seen to be a marked attenuation of waves of frequency below 10 kc./s. when travelling over distances of 1000 km. or more. This attenuation is discussed and is related to the quasi-sinusoidal waveform often assumed by atmospherics which have travelled great distances.

A decrease in the level of atmospherics has been found to occur during sudden ionosphere disturbances (S.I.D.'s) on frequencies below about 10 kc./s. This contrasts with the known increase on frequencies above about 20 kc./s.

§1. Introduction.

A study of the propagation of the very longest radio waves entails the use of powerful sending stations, using large ærials, since the difficulty of radiating appreciable power increases as the wavelength is increased. For this reason the senders which have been used are those available for commercial radio services, and the longest waves at present available in this way have a length of about 18 km. (16 kc./s.). Much useful information has been gained about the ionosphere by studying the waves emitted by these stations (Best, Ratcliffe and Wilkes 1936, Budden, Ratcliffe and Wilkes 1939) and it is desirable that observations should be made on even longer wavelengths. The construction of special experimental senders for this purpose would be a large and expensive undertaking and an attempt has therefore been made to use instead naturally occurring atmospherics as sources of very long waves. This paper gives some of the results obtained at Cambridge in this way during the years 1948 and 1949.

It is generally agreed that radio atmospherics have their origin in the electrical discharges associated with thunderclouds. The discharges, being impulsive in nature, radiate over a wide frequency range and can be used as senders for investigating the propagation of very long waves. The large energy available in atmospherics at these wavelengths renders them easily observable compared with man-made and circuit noise. One of the major difficulties encountered in the use of atmospherics in this way is that the " waveform " of the original discharge is not known, so that the power radiated on different frequencies by any one atmospheric is not known, and the experiments must be planned so that the results are either independent of, or give us information about, the distribution of radiated power amongst the different frequencies.

---

* Communicated by J. A. Ratcliffe.

Another difficulty is that atmospherics are produced at different distances from the receiving point, and without some knowledge of, or assumptions about, their location, it is impossible to make useful deductions about the propagation of the associated waves. Fortunately we have been able, thanks to the assistance of the Director of the Meteorological Office, to make use of the chain of widely-spaced radio direction-finders which the Meteorological Office use to locate lightning flashes in their so-called " Sferics " organization. In this way it was known when fairly localized storm-centres were in action at distances less than about 1500 km.

The method employed was to determine four points on the " spectrum " of the integrated received atmospherics, by recording the level on four different frequencies, and then to investigate how this spectrum changed from day to night, and with the distance of the storm centre. The assumption was then made that changes in the spectrum corresponded to changes in the propagation conditions, brought about either by the change from day to night, or by the change in the distance of the storm.

§2. METHOD OF OBSERVATION.

The results to be described were obtained from records of the average field strength of atmospherics on a number of different frequencies. The equipment used on one frequency is shown schematically in fig. 1 (*a*). A vertical ærial was connected to the common input of the various tuned receivers. Each receiver selected the appropriate frequency component from the atmospherics arriving. Its output was then rectified and averaged with a time constant of about one minute. The resulting voltage was recorded on paper moving at one inch per hour.

The receivers were all of similar type. Each consisted of a tuned input stage followed by two tuned amplifier stages, and had an overall bandwidth between half-power points of approximately 200 c./s. The radio frequency output fed the detector circuit and was also available for viewing on an oscilloscope. The detector circuit is shown schematically in fig. 1 (*b*). The time constant for discharge of the condenser C was about 80 seconds which was very long compared with the average interval between the arrival of atmospherics. Hence a fairly steady output was obtained which represented a running mean of the input signal. The voltage V_R across the condenser C at any instant therefore depended on the signals received

Fig. 1. (*a-c*)

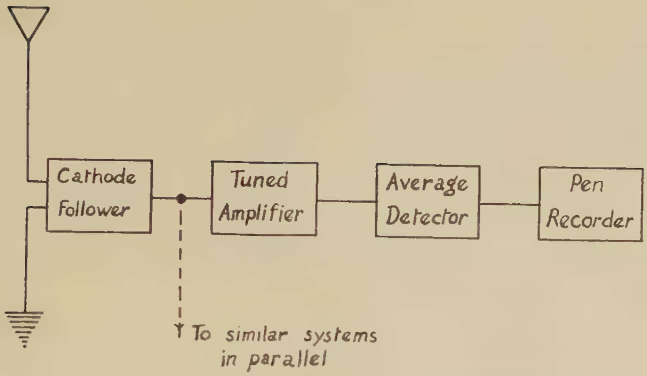

(*a*) Arrangement of atmospherics receiver.

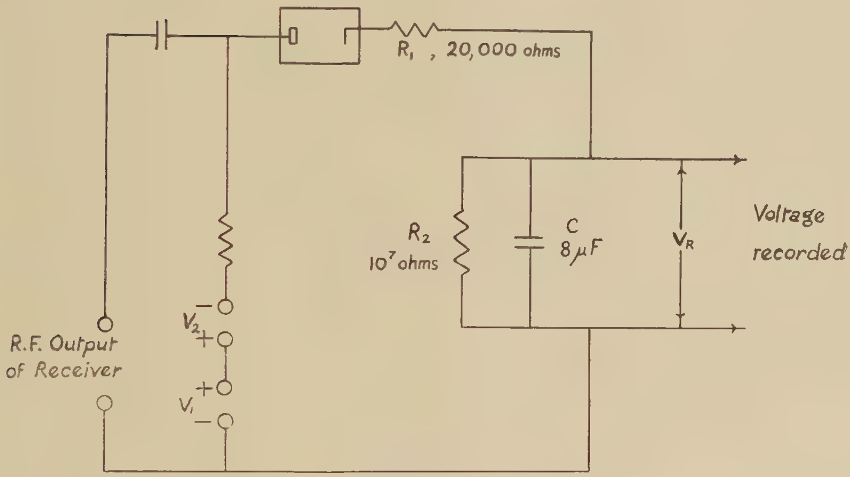

(*b*) Simplified form of detector circuit.

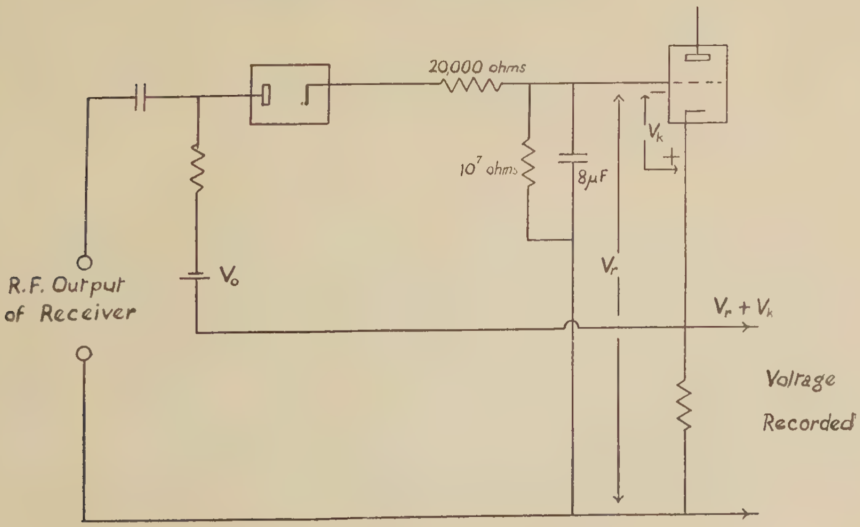

(*c*) Actual form of detector circuit.

during a time of the order of 80 seconds. In the simple circuit of fig. 1 (*b*) this voltage would affect the bias on the detector diode. To prevent this a voltage V_1 equal to V_R was connected in series with the diode. This was actually achieved, as shown in fig. 1 (*c*), by applying the voltage V_R to a cathode follower valve, and using the output of this valve to supply bias to the diode. The cathode voltage of a cathode follower exceeds the grid voltage by a small amount V_K which is roughly constant, so that the output voltage of the cathode follower was V_R+V_K. The excess voltage V_K was compensated as explained below.

When the radio frequency output was examined on an oscilloscope, it was found to consist of atmospherics of short duration and fairly large amplitude and of continuous " noise " of small amplitude, much of which was known to be due to " man-made " interference. On some frequencies, also, a small output due to signals from radio stations was sometimes observed. To reduce the effect of these unwanted voltages, an additional small voltage, V_2 in fig. 1 (*b*), was connected in series with the diode, which prevented it from conducting until the level of the signal output from the receiver exceeded a small threshold about equal to V_2. The voltage V_2 was actually derived, as shown in fig. 1 (*c*), from a constant voltage source V_0 which served also to compensate for the voltage V_K in the output of the cathode follower, so that $V_2=V_0-V_K$. V_2 was equal to 2 or 3 volts, which greatly reduced the contributions from the unwanted signals without appreciably affecting the wanted atmospherics.

The apparatus was set up at the Radio Field Laboratory in Cambridge, where the general level of man-made noise was known to be low. Records were made between February 1948 and December 1949, at first on two frequencies, and after June 1949 on four frequencies. The frequencies were selected from time to time from amongst 3·5, 5, 7·5, 10, 14, 22, 27, 33, 40 and 48 kc./s. The receivers were calibrated from time to time, at first by means of a C.W. signal generator, and later by means of a special impulse generator which produced a regular succession of pulses each of duration 1, 4 or 14 microseconds. These calibrations were only used to check the linearity of the receivers, and in the deductions to be described no use is made of the relative calibrations on the different frequencies.

§3. RESULTS OBTAINED.

The records were analysed so as to bring out effects which might be produced by changes in the conditions of propagation. For this purpose it was assumed, as a first approximation, that waves of all frequencies were propagated without appreciable attenuation from storm centres which were comparatively near (less than about 600 km.). It was next assumed that, in the absence of near storms, the atmospherics represented sources at a considerable distance (greater than 1000 km.) and that the recorded integrated levels measured relative to their values at the source would vary with frequency in a way which depended both on the nature of the source and on the propagation characteristics. The effect of the propagation characteristic at night was established by comparing the normal night-time level with the level produced by near storms, as explained in sub-section (b) below. If, next, propagation conditions change as we pass from night to day it should be possible to establish the change by comparing, in the absence of near storms, the levels recorded by day and by night at the different frequencies. This comparison is made in sub-section (a) below. It is convenient to consider these two comparisons in the reverse order.

Fig. 2. (*a*-*b*)

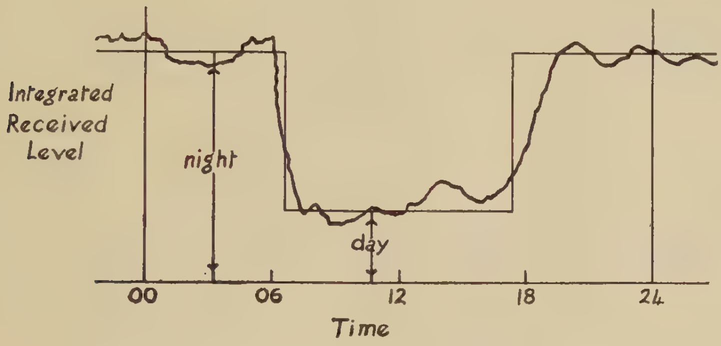

(*a*) Typical atmospherics record in the absence of near storms.

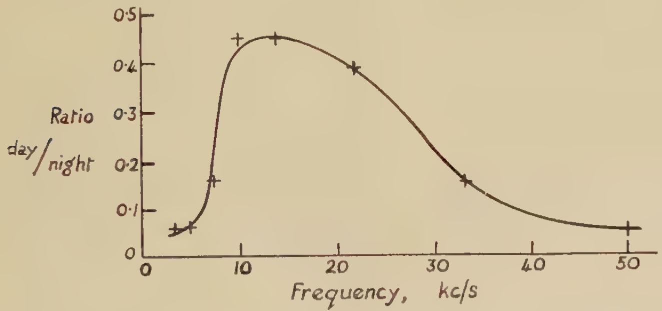

(*b*) Ratio, day level to night level as a function of frequency.

(a) *Change from day to night.*

Fig. 2 (*a*) shows a typical record for a 24-hour period when it was known that there was no storm centre within 1000 km. of Cambridge. From a record of this type it is possible to estimate, with some significance, the average level in the few hours before sunrise and the level in the few hours after sunrise, and to determine their ratio. The average value of this ratio, deduced from a large number of records obtained on different frequencies, is exhibited as a function of frequency in fig. 2 (*b*). Often local storm centres would develop during the afternoon so as to complicate the records, but by determining the daytime level from the few hours just after sunrise, and at the same time disregarding the spasmodic increases produced by isolated near discharges, a significant ratio was obtainable. Fig. 2 (*b*) appears to indicate that the onset of daylight conditions represents a marked increase of attenuation for frequencies less than 10 kc./s. and greater than 20 kc./s. but near 10 kc./s. there is little extra attenuation.

Fig. 3. (*a-b*)

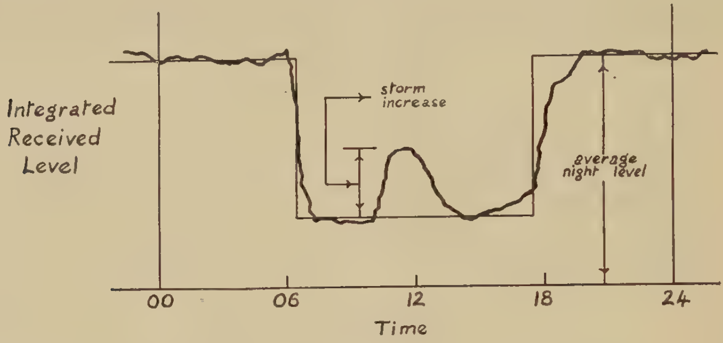

(*a*) Atmospherics record, showing effect of near storm.

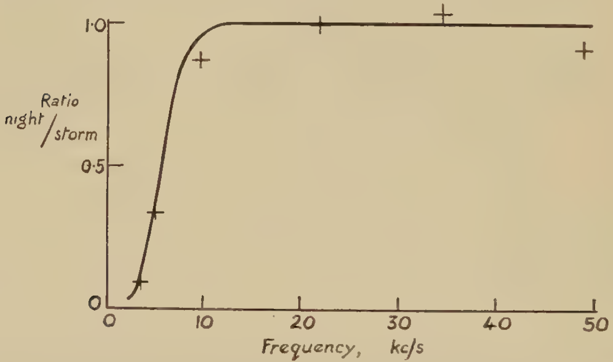

(*b*) Ratio, night level to increase due to storm, as a function of frequency.

(b) *Comparison of near and distant storms.*

Additional evidence is derivable from the increase in the average field strength which occurs when a comparatively close storm centre becomes active. The type of record then obtained is shown in fig. 3 (*a*). On several occasions records of this type were obtained, and it could be seen from the " Sferics " charts that a comparatively local storm centre had become active at some distance less than 1000 km. Under these conditions it was possible to estimate the increase in average field strength on the frequencies being recorded. The results were studied by computing the ratio (average night field strength) ÷ (increase due to storm). The absolute value of the ratio depends, of course, on the intensity of the particular storm being considered ; what is of interest, however, is not the absolute magnitude of the ratio but the way it changes with frequency.

For any one storm we have therefore normalized the ratios obtained on the different frequencies so that the ratio for a frequency of 22 kc./s. is put equal to unity. During the short period of recording on 3·5 kc./s., only three storms of short duration and completely localized within 600 km. were available, and these provided the mean " night-to-storm " ratios for 3·5, 5 and 22 kc./s. shown in fig. 3 (*b*). Other storms, more extensive in range or duration, yielded values showing the same general trend at the low frequency end, while records made at different times on other frequencies yielded the points shown on the curve for frequencies between 10 and 50 kc./s. In interpreting these results it should be remembered that the field on 3·5 kc./s. is predominantly the radiation field at distances greater than about 20 km. and all the storms considered were further away than that.

§4. Discussion of Results.

We start our discussion of the results by considering the implications of fig. 3 (*b*). We first make the assumption, previously mentioned, that all frequencies are propagated equally well from a near storm centre, and that the normal night-time level represents storms at a great distance. Then fig. 3 (*b*) gives a measure of the relative attenuation suffered by waves of different frequency as they travel over great distances at night. The results are normalized so that the attenuation factor for a frequency of 22 kc./s. is taken as unity. Of course the distances of the sources at night are very indefinite, but the results appear to show that, when the sources are at a considerable distance (greater than 1000 km.), the lower frequencies are much more heavily attenuated than the higher and that the " low-frequency cut-off " occurs just below 10 kc./s. Although this conclusion rests mainly on observatious made on a few occasions only, we consider it to be quite sound because it is supported by observations made on several other occasions when different frequencies were in use, or when the storm centre was not accurately located.

We next consider the curve of fig. 2 (*b*) which shows the extra attenuation introduced on the different frequencies as we pass from night-time to daytime. Since this curve refers to conditions when there were no storms within 1000 km. we assume that it represents propagation over great distances. Fig. 2 (*b*) is the result of a preliminary analysis covering the midsummer months of 1949 (more than 60 days' observations are involved in the determination of the value for 5 kc./s.), and we consider that it represents a well-established result and shows that the incidence of daylight has the effect of producing a considerable increase in the attenuation of waves propagated over great distances on frequencies below about 10 kc./s.

Fig. 4 (*a*) shows the attenuation curve of fig. 3 (*b*) for night, re-plotted on a logarithmic basis. Fig. 4 (*b*) represents the product of the curves of figs. 2 (*b*) and 3 (*b*), plotted in a similar way, and therefore represents the attenuation curve for day.

Although there may be some doubt about the absolute magnitudes of the attenuation factors shown in this figure, we feel reasonably confident that it indicates, in a general way, how the attenuation factor depends on frequency for transmission over distances of 1000 km. or more. We shall here concern ourselves with the results represented by the portion of the curve below 10 kc./s.

In considering these results it is convenient to think of the space between the ground and the ionosphere as forming a four-terminal network, with the input terminals at the lightning flash and the output at the receiving ærial. Our experimental results provide a description of the overall frequency characteristics of this network and, in particular, show that there is a sharp cut-off at frequencies below about 10 kc./s., but do not indicate how these characteristics come about. It might, for example, result from the combination of separate ground- and sky-waves. In this connection, however, one point of significance emerges. The attenuation of a ground wave of frequency 5 kc./s. by absorption and diffraction, when travelling over a distance of 2000 km., can be calculated and the attenuation factor is found to be about 0·3. But the daytime attenuation factor measured on this frequency is much lower, about 0·02, as shown in fig. 4 (*b*). We deduce that the strength of the daytime field is much less than that of

Fig. 4.

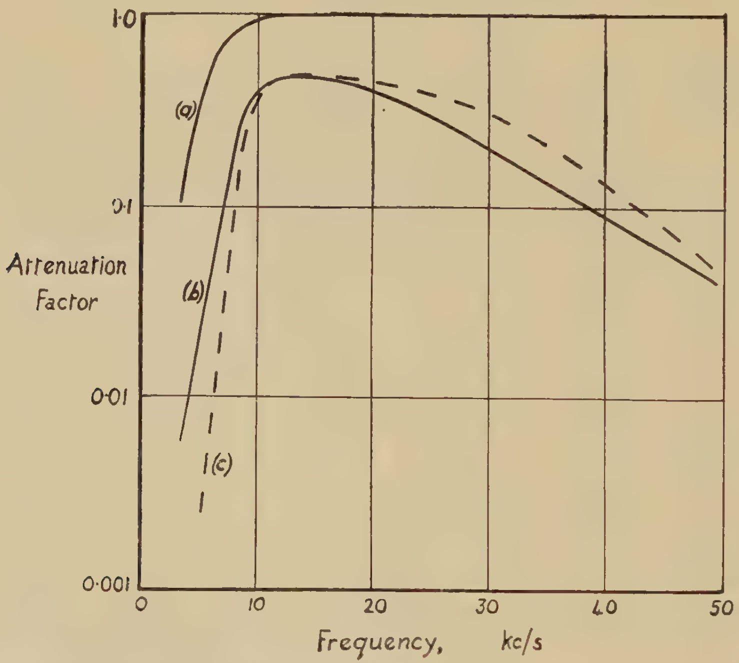

Attenuation factor as a function of frequency for (*a*) night, (*b*) day, (*c*) day during a Sudden Ionospheric Disturbance.

the ground-wave alone. In explaining this result it will probably be necessary to remember that the wavelength (60 km.) at this frequency is comparable with the distance between the ground and the " reflecting " region, so that it is doubtful whether we are entitled to think of the problem in terms of separate ground- and sky-waves.

It is not the purpose of this paper to discuss the explanation of the results here presented, but I understand that Dr. K. G. Budden is preparing a paper in which he suggests a theoretical explanation.

Before leaving the discussion of the curves of fig. 4 it is of interest to relate them to the waveform of an atmospheric received on an aperiodic amplifier. If we assume that the atmospheric is a sharp impulse lasting considerably less than 2×10^{-4} sec. (the time period corresponding to a frequency of 5 kc./s.), then simple transient analysis tells us what output we should expect if it is applied to a four-terminal network having the transmission characteristic of fig. 4. The result would be a quasi-sinusoidal oscillation with " period " roughly equal to the cut-off frequency of the network.

Fig. 5.

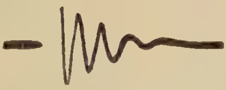

Waveform of atmospheric from a distant source.

Now it is well-known (Appleton and Chapman 1937) that atmospherics received from the greater distances very frequently show a smooth quasi-sinusoidal waveform with a period of the order of 150 microseconds. An example of one of these waveforms is shown in fig. 5 and it is clear that since it is so smooth and regular it would be difficult to interpret it in terms of a series of separate reflections from the ionosphere. It is, however, very much what we should expect as the result of applying an impulse to a transmission system with an attenuation curve as shown in fig. 4, and it seems probable that, once this attenuation curve can be explained, the origin of the quasi-sinusoidal atmospheric waveforms will be clear.

§5. Effect of Sudden Ionosphere Disturbances (S.I.D.'s).

Bureau (1937) has shown that the Sudden Ionospheric Disturbances (S.I.D.'s) of the type associated with solar flares, and frequently with " Dellinger Fadeouts ", very often coincide with an increase of the average field strength of atmospherics recorded on frequencies in the range 20–40 kc./s. We have confirmed his observations in this range, but our records on the lowest frequencies have revealed the unexpected phenomenon that there the average field strength often *decreases* during the S.I.D. This effect has been observed most frequently on 5 kc./s. Examples are shown in fig. 6.

We have already seen that, during the day, the average field strength on the lowest frequencies is very small, unless there is a fairly near storm, and indeed if there are no storm centres within 2000 km. the average field strength recorded on 5 kc./s. is so low that a further decrease due to an S.I.D., if it does occur, is not noticeable. For a frequency of 3·5 kc./s. the corresponding distance is about 1400 km.

If the storm centre is at distances between 1500 and 2000 km., it has been observed that S.I.D.'s can reduce the mean field strength by a factor of 10 : 1 on a frequency of 5 kc./s., and for distances between 600 and 1500 km. a reduction of 3 : 1 has been observed. Observations on 3·5 kc./s. have been less extensive, but on one occasion the field due to a storm centre at a distance of 800–1500 km. was reduced to one fifth during an S.I.D.

Fig. 6.

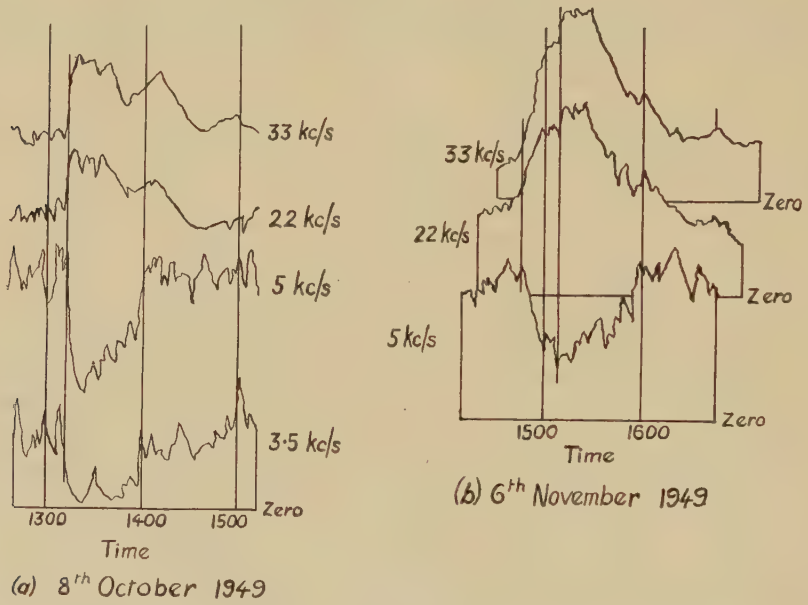

Records of integrated atmospherics at times of Sudden Ionospheric Disturbances.
(*a*) 8th October, 1949 (zero level shown only for 3·5 kc./s.);
(*b*) 6th November, 1949.

Although the effects associated with S.I.D.'s have depended on the distance of the storm centres, we have attempted to represent them in a general way by the curve (*c*) in fig. 4. In examining this curve it is interesting to notice the different effect of an S.I.D. on the resultant signal produced at a great distance on different frequencies. For frequencies below 10 kc./s. the signal decreases : for frequencies between 10 kc./s. and about 200 kc./s. the signal increases : for frequencies above about 1 Mc./s. the signal decreases (Dellinges effect). A satisfactory theory of propagation will have to explain these results.

§6. ACKNOWLEDGMENTS.

This work was done as part of a programme of radio research supported by the Department of Scientific and Industrial Research at the Cavendish Laboratory, Cambridge. I wish to thank Mr. J. A. Ratcliffe for much advice and encouragement during the experiments and assistance with the writing of this paper. I am indebted also to the Commonwealth Scientific and Industrial Research Organization of Australia, to Sidney Sussex College, Cambridge, and to the Director of the Cavendish Laboratory for grants which enabled me to work in Cambridge.

REFERENCES.

APPLETON and CHAPMAN, 1937, *Proc. Roy. Soc.* A, **158**, 1.
BEST, RATCLIFFE and WILKES, 1936, *Proc. Roy. Soc.* A, **156**, 614.
BUDDEN, RATCLIFFE and WILKES, 1939, *Proc. Roy. Soc.* A, **171**, 188.
BUREAU, 1937, *Nature, Lond.*, **139**, 110.

CXIII. *The Force Acting on a Body Moving Uniformly through a Gas containing Sound Waves.*

By F. R. N. NABARRO,
Department of Metallurgy, The University of Birmingham *.

[Received September 25, 1950.]

SUMMARY.

When a body travels through a gas containing an isotropic distribution of sound waves it suffers a retarding force proportional to its area, to the energy density of the sound, and to its velocity. Three effects might contribute to this force : (*a*) the distribution of sound with respect to the moving body is no longer isotropic ; (*b*) the apparent wavelength of the sound is altered by the motion of the body ; (*c*) the non-linear terms in the equation of motion lead to a coupling between the sound waves and the steady flow of gas round the body. Effect (*c*) is shown to produce no force. Effects (*a*) and (*b*) are evaluated in the case of a sphere, and the force is shown to be expressible in terms of the force exerted by a single sound wave on a stationary sphere, already calculated by L. V. King.

§ 1. INTRODUCTION.

IT is well known that a body moving uniformly through a non-viscous fluid at rest is not acted on by any force. The resultant couple also vanishes if the body is symmetrical (Lamb 1932). If the body is at rest, and a plane sound wave impinges on it, the sound wave is scattered, and a force is exerted on the body. This force has been calculated by Rayleigh (1905) in the case where the obstacle is the flat end of a cylinder containing the gas, and by King (1934) for the case of a spherical obstacle. (King actually treats the more general problem of a free sphere of density ρ. The result for a fixed sphere is obtained by taking ρ infinite.) An apparent discrepancy between their results is discussed in § 2 of the present paper.

If a symmetrical body lies at rest in a gas containing an isotropic distribution of sound waves, the resultant force on it clearly vanishes. If it moves with velocity v, it experiences a retarding force proportional to its area, to the energy density of the sound waves, and to v/c, where c is the speed of sound. In § 3 a plausible argument is advanced for believing that this force should vanish. The exposure of this fallacy illustrates an unexpected difficulty which arises if the thermal motion of the molecules of a gas is analysed into Fourier components in the way customarily used for solids. The result to be obtained is proportional both to the speed of the body and to the energy density of the sound waves, and therefore involves terms of the third order of small quantities in the equations of motion. In § 4 the equations are developed to the necessary order. In § 5 the explicit interaction between the uniform motion of the body and a single sound wave is evaluated and found to lead to no resultant force. However, an isotropic distribution of sound waves in the gas is not isotropic in axes attached to the moving body, and in § 6 it is shown that this anistropy leads to a force of the kind expected.

---

* Communicated by the Author.

This problem has a certain intrinsic interest. I was actually led to study it by reading a paper by Leibfried (1950) in which he applies similar considerations to estimate the resistance to the motion of a dislocation in a crystal caused by its scattering of sound waves in that solid. His result for this more complicated problem depends upon several drastic simplifying assumptions. He finds a resistance so large that the terminal velocity of a dislocation in a crystal under a reasonable stress could never become comparable with that of sound. Since this result would render impossible a type of process which plays an important rôle in some modern theories of plastic deformation (Frank 1948), it seemed worth while to treat this related, but simpler, problem in detail. The results are compatible with that of Leibfried.

§ 2. DISCUSSION OF RAYLEIGH'S AND KING'S FORMULÆ FOR THE PRESSURE OF A SOUND WAVE.

King considers a single plane wave of wavelength λ incident on a sphere of radius a. If the energy density of the sound wave is E, the force P on the sphere is given by

$$P=\pi a^2 E L(ka), \qquad (1)$$

where

$$k=2\pi/\lambda, \qquad (2)$$

and it is easy to see that the function L must tend to the value $\frac{1}{2}$ when ka is large. King's computation leads to $L(1)=0{\cdot}425$. The distribution of scattered radiation from a large sphere may be resolved (Morse 1948) into a forward lobe which interferes with the incident beam to form the shadow and an isotropic reflected beam. Thus, of the radiation intercepted by the scattering cross-section $2\pi a^2$, half continues in the forward direction with unchanged momentum, and half is scattered isotropically with zero total momentum. If the momentum in unit volume of the incident wave is m, the change of momentum in unit time caused by the sphere is $mc\pi a^2$, and comparison with (1) leads to

$$m=E/2c. \qquad (3)$$

This appears to disagree with Rayleigh's result. Both authors assume that the pressure p in the gas depends only on its density ρ according to the law

$$p=f(\rho). \qquad (4)$$

If the density of the undisturbed gas is ρ_0, the velocity of sound c is given by

$$c^2=f'(\rho_0). \qquad (5)$$

Rayleigh's formula for the momentum is, in the present notation,

$$m=[1+\rho_0 f''(\rho_0)/2c^2]\mathrm{E}/2c. \qquad (6)$$

The discrepancy between (3) and (6) does not arise from an implied assumption $f''(\rho_0)=0$ (corresponding to Boyle's Law) in the derivation of (3), but from a difference in the physical situations considered. A similar ambiguity is known (Andrejew 1940) to arise in the determination of the energy density in a sound wave. King treats a finite obstacle in an infinite gas. Because the plane sound wave is disturbed by the obstacle, the time average of the density of the gas varies from place to place, and this variation contributes to the resultant force. Rayleigh considers a fixed quantity of air in a cylindrical pipe, either at rest or containing a resonant sound wave in a quasi-stationary state. The pipe is closed by a piston at one end and by a rigid wall at the other. Rayleigh's argument will be developed here in the notation which will be convenient in later work.

In Cartesian coordinates x_i, the components of velocity u_i are given by the equations of motion :

$$\rho\frac{\mathrm{D}u_i}{\mathrm{D}t}=-\frac{\partial p}{\partial x_i}, \qquad (7)$$

where

$$\frac{\mathrm{D}}{\mathrm{D}t}=\frac{\partial}{\partial t}+u_i\frac{\partial}{\partial x_i}. \qquad (8)$$

The repeated suffix i implies a summation over the values $i=1, 2, 3$.

If a function ϖ is introduced by the relation

$$\varpi=\int\frac{dp}{\rho}, \qquad (9)$$

the equations of motion become

$$\frac{\mathrm{D}u_i}{\mathrm{D}t}=-\frac{\partial\varpi}{\partial x_i}. \qquad (10)$$

If the motion is irrotational, there is a velocity potential ϕ satisfying

$$u_i=-\frac{\partial\phi}{\partial x_i} \qquad (11)$$

(Rayleigh here uses $-\phi$.)

The equations of motion are satisfied if

$$\varpi=\frac{\partial\phi}{\partial t}-\frac{1}{2}\left(\frac{\partial\phi}{\partial x_i}\right)^2=\frac{\mathrm{D}\phi}{\mathrm{D}t}+\frac{1}{2}\left(\frac{\partial\phi}{\partial x_i}\right)^2. \qquad (12)$$

Changing only the notation, Rayleigh's argument now proceeds: "If we integrate over a long period of time, ϕ disappears, and we see that $\int\varpi\,dt+\frac{1}{2}\int(\partial\phi/\partial x)^2\,dt$ retains a constant value at all points of the cylinder.

The value at the piston is accordingly the same as the mean value taken over the length of the cylinder. ” The pressure on the piston is derived from the value of ϖ at that point. According to (9), the definition of ϖ involves an arbitrary constant of integration. Rayleigh determines this constant from his “mean value” result just quoted, using his assumption that the total mass of gas, and hence the mean density taken over the length of the cylinder, is unaltered by the presence of the sound wave. The term in Rayleigh's formula for the pressure on the piston which depends only on conditions near the piston would lead to (3). The term in f'' in (6) arises from integrals over the length of the tube, expressing the constancy of the total mass of gas.

Two points in the argument quoted deserve rather more attention. Firstly, it is obvious that ϕ does not vanish in the time integral. It is necessary to take the time average before ϕ can disappear. If ϕ actually did “disappear” in the integration, the time average of $\varpi+\frac{1}{2}(\partial\phi/\partial x)^2$ would not be a determinable constant but zero, leading again to (3). In fact the arbitrary constant of integration in ϖ corresponds to an arbitrary addition to ϕ of the form $t\psi(x)$. This gives an aperiodic contribution $-t\, d\psi/dx$ to u_x, and the postulate of a steady state leads to $\psi(x)=\text{constant}$, which justifies Rayleigh's method.

The second point is that when terms of the second order in the wave equation are considered, a true stationary state almost certainly does not exist (Rayleigh 1910). Time averages can only be given a meaning by a special process. If the unperturbed motion is represented by a sufficiently small periodic function ϕ_0, the second order terms are small perturbations. After time t, ϕ becomes $\phi_0+\delta\phi$, where $\delta\phi$ is in general of order $\phi_0^2 t$. If $\delta\phi$ in fact has this form, the time average of $\partial\phi/\partial t$ does not tend to zero, but tends to an unknown quantity of order ϕ_0^2, which is of the same order as the terms to be evaluated. A periodic state may be maintained near the piston by using a train of waves in an infinite tube, but this no longer requires that the mean density should be unchanged. Alternatively, the rigid end wall of the cylinder may be replaced by another piston which is controlled from outside in an attempt to maintain a periodic state in the tube. This artifice can only be used if it can be shown to be possible, and in particular it must be shown that the piston will not continuously supply energy to the gas in the tube. The second order terms in the wave equation lead to an irreversible change, and thus entropy is continuously generated in the gas. In a steady state this entropy flows out through the walls of the tube as heat, while the controlled piston supplies energy at the same rate. This is exactly the experimental arrangement which would normally be adopted to measure the pressure of radiation in a closed tube. It is remarkable that a constant flow of mechanical work into the tube and of heat out is not a result of experimental imperfections, but is essential to a self-consistent interpretation of the results.

§ 3. RELATION BETWEEN THE RESULTS OF THIS PAPER AND THE KINETIC THEORY OF GASES.

Equation (1) gives the force on a sphere at rest in a single sound wave. If there is an isotropic distribution of sound waves of the same wavelength and of energy density $\bar{E}$, the force on a sphere at rest clearly vanishes. It will be shown in § 6 that if the sphere moves with velocity v it is subject to a retarding force $\bar{P}$ given by

$$\bar{P}=\pi a^2\bar{E}(v/c)\bar{L}(ka), \quad . \quad . \quad . \quad . \quad . \quad . \quad . \quad . \quad . \quad (13)$$

where
$$\bar{L}(ka)=\tfrac{1}{3}[4L(ka)+kaL'(ka)]. \quad . \quad . \quad . \quad . \quad . \quad . \quad . \quad (14)$$

The first term in (14) arises from the " aberration " of the sound waves, the moving sphere meeting a larger flux of sound waves on the leading than on the trailing hemisphere. The second term arises from the Doppler effect, the waves incident from ahead having a shorter effective wavelength and a correspondingly larger scattering cross-section than those incident from behind.

Consider a large sphere moving through a monatomic gas at rest. The pressure of the gas is caused by the motion of the gas atoms. In the case of a solid it is customary to resolve the thermal motion of the atoms into normal modes of vibration of the lattice, and it is plausible to do the same in the case of a gas. In both cases it is necessary to consider vibrations of wavelengths as short as twice the interatomic spacing, and nevertheless the vibrations are regarded as those of a continuous medium. These short waves are far more numerous than the larger waves, for which such an approximation is reasonably accurate. In both cases the scattering of short waves is so large that their mean free path is of the order of one wavelength. Since this theory is reasonably successful for solids, it might be expected also to succeed for gases. If the whole thermal energy of the gas is resolved into sound waves in this way, the moving sphere is retarded according to (13), with $ka \gg 1$. If the pressure of the gas is p, then $\bar{E}=\tfrac{3}{2}p$, while $L(\infty)=\tfrac{2}{3}$. So

$$\bar{P}=\pi a^2 pv/c. \quad . \quad . \quad . \quad . \quad . \quad . \quad . \quad . \quad . \quad . \quad (15)$$

A retardation of this enormous value would leave billiards as the only practicable ball game. While the approximations leading to (15) could alter the value of $\bar{P}$ appreciably, it is obvious that the derivation is not merely inaccurate, but basically wrong.

The same problem may be treated in a more orthodox way by regarding the pressure of the gas on the sphere as being produced, not by the impact of sound waves, but by the impact of atoms. Again, more atoms strike on the leading hemisphere than on the trailing, and, if the sphere is smooth, formula (15) is again obtained. In this case the error in the assumptions is obvious. The result can only be expected to hold if a is much less than the mean free path of atoms in the gas. The distribution of momenta among atoms striking an element of the surface of the sphere is then the superposition of two distributions, corresponding to incident and reflected streams of gas. If a is large compared with the mean free path, the distribution of momenta among atoms reaching the surface is not that corresponding to distant parts of the gas, but corresponds to the pressure and mean velocity of the gas (which is parallel to the surface) at that point in the ordinary hydrodynamical theory. Forces of the kind just considered arise only when v changes, and give rise to an increase in the effective mass of the sphere.

In the original derivation of (15), where the thermal motion of the gas was resolved into sound waves, it is now clear that the short waves, which contribute most of the pressure p, do not contribute to $\overline{\mathrm{P}}$ because of their short free path, but there remain enough long waves of very long free path to give a retardation far greater than is observed. The basic difficulty in regarding the pressure of a gas as the sum of the pressures of all the sound waves in the gas now appears. It follows from (9) and (12) that in any standing wave the time average of the pressure is greatest at the nodes, where $(\partial\phi/\partial x_i)^2=0$, and least at the antinodes. Since the wall is a node for every wave, the pressure on the wall exceeds the pressure in the interior, which is equal to the "internal pressure" of the gas, that is, zero for a perfect gas. In a solid, this resolution of the thermal motion into independent sound waves is an acceptable approximation, because each sound wave can be propagated alone through the elastic solid. This is not true in the gas. The velocity of propagation of a sound wave is proportioanl to $\mathrm{T}^{\frac{1}{2}}$, where T is the absolute temperature. If the whole thermal energy of the gas is resolved into sound waves, T is a measure of the number of sound waves already present, and the propagation of one sound wave depends essentially on the presence of others. To analyse the motion into independent sound waves is therefore meaningless. If, in the problem of a sphere moving through a gas at rest, the thermal motion of the gas is resolved into sound waves, the disturbance of one particular sound wave by the sphere is produced not only directly, but also indirectly by the interaction of this sound wave with other sound waves already disturbed by the sphere. In the hydrodynamic solution, the points of stagnation are points of high pressure and so, in adiabatic flow, of high temperature and of high sound velocity, while the equator is a region of low sound velocity. This temperature distribution refracts sound waves so that they tend to travel along the lines of flow, in the same way that, in the molecular picture, incident molecules are deviated by collisions towards the lines of flow. Thus (13) cannot be disproved by deducing from it the absurd consequence (15).

§ 4. THE BASIC EQUATIONS.

The motion of the gas is governed by the equation of continuity,

$$\frac{\partial\rho}{\partial t}+\frac{\partial(\rho u_i)}{\partial x_i}=0, \quad . \quad . \quad . \quad . \quad . \quad . \quad . \quad . \quad . \quad (15)$$

which may be written

$$\frac{\mathrm{D}\ln\rho}{\mathrm{D}t}=\frac{\partial^2\phi}{\partial x_i^2}. \qquad (16)$$

It follows from (4) and (9) that ρ may be expressed as a function of ϖ alone, and then from (12) that ρ may be expressed in the form

$$\rho=\rho(\phi). \qquad (17)$$

The function $\rho(\phi)$ involves both ϕ and its derivatives. The equation of motion (16) may now be written in terms of ϕ alone as

$$\frac{\mathrm{D}\ln\rho(\phi)}{\mathrm{D}t}=\frac{\partial^2\phi}{\partial x_i^2}, \qquad (18)$$

while the pressure is given by

$$p=f[\rho(\phi)]. \qquad (19)$$

These equations will now be expanded in powers of ϕ, using as an auxiliary variable the condensation s, a pure number of the same order as ϕ, defined by

$$\rho=\rho_0(1+s). \qquad (20)$$

To the third order (4) becomes

$$p=p_0+\rho_0c^2s+\tfrac{1}{2}\rho_0^2f''s^2+\tfrac{1}{6}\rho_0^3f'''s^3, \qquad (21)$$

where

$$p_0=f(\rho_0) \qquad (22)$$

and the derivatives f'' and f''' are evaluated at $\rho=\rho_0$. To the same order (9) becomes

$$\varpi=c^2s-\tfrac{1}{2}(c^2-\rho_0f'')s^2+\tfrac{1}{3}(c^2-\rho_0f''+\tfrac{1}{2}\rho_0^2f''')s^3. \qquad (23)$$

Inverting (23),

$$s=\frac{\varpi}{c^2}+\tfrac{1}{2}(c^2-\rho_0f'')\frac{\varpi^2}{c^6}+\tfrac{1}{6}(c^4-4\rho_0c^2f''+3\rho_0^2f''^2-\rho_0^2c^2f''')\frac{\varpi^3}{c^{10}}. \qquad (24)$$

Using (12) and (24), (17) becomes

$$\begin{aligned}\rho=\rho_0&+\frac{\rho_0}{c^2}\frac{\partial\phi}{\partial t}-\frac{1}{2}\frac{\rho_0}{c^2}\left(\frac{\partial\phi}{\partial x_i}\right)^2+\frac{1}{2}\frac{\rho_0}{c^6}(c^2-\rho_0f'')\left(\frac{\partial\phi}{\partial t}\right)^2\\&-\frac{1}{2}\frac{\rho_0}{c^6}(c^2-\rho_0f'')\frac{\partial\phi}{\partial t}\left(\frac{\partial\phi}{\partial x!}\right)^2\\&+\frac{1}{6}\frac{\rho_0}{c^{10}}(c^4-4\rho_0c^2f''+3\rho_0^2f''^2-\rho_0^2c^2f''')\left(\frac{\partial\phi}{\partial t}\right)^3. \qquad (25)\end{aligned}$$

It is convenient to introduce the abbreviations

$$\frac{\partial\phi}{\partial t}=\dot\phi;\quad \frac{\partial\phi}{\partial x_i}=\phi_i,\quad \frac{\partial^2\phi}{\partial x_i\partial t}=\dot\phi_i,\quad \frac{\partial^2\phi}{\partial x_i\partial x_j}=\phi_{ij},\ \text{etc.} \qquad (26)$$

With this notation the equation of motion (18) becomes, to second order,

$$c^2\phi_{ii}-\ddot{\phi}=-2\phi_i\dot{\phi}_i-\rho_0c^{-4}f''\dot{\phi}\ddot{\phi}, \quad . \quad . \quad . \quad . \quad . \quad (27)$$

and (21) becomes, to third order,

$$p=p_0+\rho_0\dot{\phi}-\tfrac{1}{2}\rho_0\phi_i^2+\tfrac{1}{2}\rho_0c^{-2}\dot{\phi}^2-\tfrac{1}{2}\rho_0c^{-2}\dot{\phi}\phi_i^2+\tfrac{1}{6}\rho_0c^{-6}(c^2-\rho_0f'')\dot{\phi}^3. \qquad (28)$$

It is noteworthy that f''', which appears explicitly in (21), is absent from (28).

§ 5. A Body Moving with Uniform Velocity through a Gas containing a Single Progressive Sound Wave.

In treating the interaction of a sound wave with a body moving with uniform velocity v, it is convenient to use axes $(x_1'\ x_2'\ x_3')$ travelling with the body, and also to make a Lorentz transformation of the time. The new coordinates are given by

$$\left.\begin{aligned}(1-v^2/c^2)^{\frac{1}{2}}x_1'&=x_1-vt,\\ x_2'&=x_2,\\ x_3'&=x_3,\\ (1-v^2/c^2)^{\frac{1}{2}}t'&=t-vx_1/c^2.\end{aligned}\right\} \quad . \quad . \quad . \quad . \quad . \quad . \quad (29)$$

If v/c is treated as a small quantity of the first order, the wave equation (27) takes the same form, to second order, in primed coordinates. In (28) the term $\rho_0\dot{\phi}$ does not contribute to the time average of p, and the remaining terms are unaltered, to third order, by the change of coordinates. (By the argument of § 2, a term in ϕ proportional to t can only lead to a change in pressure which is independent of position, and so produces no force on a closed surface.) Equations (27) and (28) may therefore be considered to hold in moving coordinates. They are "mixed" equations, in which p and ϕ retain their original values measured in fixed coordinates, while the differentiations are carried out in moving coordinates.

The present problem is concerned with the interaction between two disturbances. One, representing the uniform motion of the body with speed v, is independent of time; the other is, in first order, a sinusoidal function of frequency ω. The first order solution of (27) is then expressible in the form

$$\phi^{(1)}=\mathrm{V}(x_i)+\mathrm{C}(x_i)\cos\omega t+\mathrm{S}(x_i)\sin\omega t.$$

In moving coordinates, the disturbance represented by C and S is still periodic, and the first order solution may be written

$$\phi^{(1)}=\mathrm{V}[(x_1'+vt')(1-v^2/c^2)^{-\frac{1}{2}},\ x_2',\ x_3']+\mathrm{C}'(x_i')\cos\omega't'+\mathrm{S}'(x_i')\sin\omega't'. \quad . \quad . \qquad (30)$$

If the solution to second order is $\phi=\phi^{(1)}+\phi^{(2)}$, $\phi^{(2)}$ is a solution of the equation

$$\begin{aligned}c^2\phi_{ii}^{(2)\prime}-\ddot{\phi}^{(2)\prime}=&-2\omega'(\mathrm{V}_i'+\mathrm{C}_i'\cos\omega't'+\mathrm{S}_i'\sin\omega't')(-\mathrm{C}_i'\sin\omega't'+\mathrm{S}_i'\cos\omega't')\\ &+\rho_0c^{-4}f''\omega'^3(-\mathrm{C}'\sin\omega't'+\mathrm{S}'\cos\omega't')(\mathrm{C}'\cos\omega't'+\mathrm{S}'\sin\omega't').\end{aligned}$$

$$. \quad . \quad . \quad . \quad . \quad (31)$$

Here ϕ'_{ii} is an abbreviation for $\partial^2\phi/\partial x_i'^2$, and C'_i is an abbreviation for $\partial C'/\partial x'_i$, etc. Terms in $\partial V/\partial t'$ in (31) are of the third order, and have been neglected.

All terms in $\phi^{(2)}$ are of frequency 2ω, except those arising from the term $2\omega' V'_i(C'_i \sin \omega' t' - S'_i \cos \omega' t')$, and the solution for ϕ may be written to second order as

$$\begin{aligned}\phi &= \phi^{(1)} + \phi^{(2)} \\ &= V + C' \cos \omega' t' + S' \sin \omega' t' + C^{(2)\prime} \cos 2\omega' t' + S^{(2)\prime} \sin 2\omega' t' \\ &\quad + (VC)' \sin \omega' t' + (VS)' \cos \omega' t', \qquad (32)\end{aligned}$$

where $(VC)'$ is a solution of

$$c^2 (VC)'_{ii} + \omega'^2 (VC)' = 2\omega' V'_i C'_i, \qquad (33)$$

and $(VS)'$ is a solution of

$$c^2 (VS)'_{ii} + \omega^2 (VS)' = -2\omega' V'_i S'_i. \qquad (34)$$

When this solution is substituted in (28), and terms of higher order than the third are neglected, it is readily seen that the time average p_m of p is given by

$$\begin{aligned}p_m = p_0 &- \tfrac{1}{2}\rho_0 V_i^2 - \tfrac{1}{4}\rho_0 (C_i'^2 + S_i'^2) + \tfrac{1}{4}\rho_0 c^{-2} \omega'^2 (C'^2 + S'^2) \\ &+ \tfrac{1}{2}\rho_0 [C'_i (VS)'_i + S'_i (VC)'_i] + \tfrac{1}{2}\rho_0 c^{-2} \omega'^2 [C'(VS)' + S'(VC)'] \\ &- \tfrac{1}{2}\rho_0 c^{-2} \omega' [V'_i (C'_i S - S' C)]. \qquad (35)\end{aligned}$$

Here p_0 is the pressure of the undisturbed gas, the second term is the pressure due to the steady flow, which gives no force and, for a symmetrical body, no couple. The next two terms give the acoustic radiation pressure, as calculated by King, and the remaining three terms give the pressure produced by the interaction of the steady flow and the sound wave.

Using equations (33) and (34), together with the fact that C and V satisfy equations of the form

$$c^2 C'_{ii} + \omega'^2 C = 0, \qquad (36)$$

reduces the last three terms in (35) to the form

$$-\tfrac{1}{4}\rho_0 [C'(VS)' + S'(VC)']_{ii}. \qquad (37)$$

It may be shown that this term gives no resultant force on the body. For a smooth function Q may be defined inside the body, which has on the surface of the body the same first and second derivatives as $[C'(VS)' + S'(VC)']$. If $d\Sigma'_j$ is an element of area of the surface, the total force on the body in the direction x_j is

$$-\tfrac{1}{4}\rho_0 \iint Q'_i \, d\Sigma'_j = -\tfrac{1}{4}\rho_0 \iiint (\partial Q'_{ii}/\partial x'_j) \, d\tau',$$

where the integral $d\tau'$ is taken through the volume of the body. This may be written

$$-\tfrac{1}{4}\rho_0 \frac{\partial}{\partial x'_j}\iiint Q'_{ii}\,d\tau' = -\tfrac{1}{4}\rho_0 \frac{\partial}{\partial x'_j}\iint Q'_i\,d\Sigma'_i.$$

At each point of the surface,

$$Q'_i = C'_i(VS)' + C'(VS)'_i + S'_i(VC)' + S'(VC)'_i,$$

and each of the derivatives in this expression is orthogonal to $d\Sigma'_i$ because each term C', $(VS)'$, S', $(VC)'$ represents the velocity potential of a flow with the surface of the body as a fixed boundary.

§ 6. A BODY MOVING THROUGH AN ISOTROPIC FLUX OF SOUND WAVES.

Consider a body moving with velocity v through a large space containing an isotropic flux of sound waves of frequency ω. It follows from § 5 that the third order terms in (35) do not produce a force on the body. However, the radiation is not isotropic in coordinates moving with the body, and, even in the case of a sphere or a cylinder, the pressures corresponding to the second order terms in (35) lead to a resultant force.

In a fixed coordinate system a typical sound wave has the velocity potential

$$\phi = \phi_0 \cos(k_1x_1 + k_2x_2 + k_3x_3 - \omega t), \quad \dots \dots \quad (38)$$

where

$$k^2 = k_1^2 + k_2^2 + k_3^2 = \omega^2/c^2. \quad \dots \dots \quad (39)$$

Referred to axes moving with the body, as given by (29), the velocity potential is

$$\phi = \phi_0 \cos\left[(k_1 - \omega v/c^2)(1 - v^2/c^2)^{-1/2}x'_1 + k_2x'_2 + k_3x'_3 - (\omega - k_1v)(1 - v^2/c^2)^{-1/2}t'\right]. \quad \dots \quad (40)$$

Neglecting terms of order v^2/c^2, this is a wave travelling in the direction

$$\left.\begin{aligned} l'_1 &= \frac{k_1}{k} + \frac{k_1^2 v}{k^2 c} - \frac{v}{c}, \\ l'_2 &= \frac{k_2}{k} + \frac{k_1k_2v}{k^2c}, \\ l'_3 &= \frac{k_3}{k} + \frac{k_1k_3v}{k^2c}, \end{aligned}\right\}, \quad \dots \dots \quad (42)$$

with frequency

$$\omega' = \omega - k_1v \quad \dots \dots \quad (42)$$

and wave number

$$k' = \omega'/c. \quad \dots \dots \quad (43)$$

Equation (1) may be written in the form

$$P = \tfrac{1}{2}\pi\rho_0\phi_0^2(ka)^2L(ka), \quad \dots \dots \quad (44)$$

and by substituting (40) in (30) and (35) it is clear that the force on a moving sphere is given by (44) with k replaced by k'. The resultant force produced by the isotropic radiation must act in the direction x_1. The force produced by the wave $(k_1k_2k_3)$ has a component in this direction of

$$l_1'\tfrac{1}{2}\pi\rho_0\phi_0^2(k'a)^2\mathrm{L}(k'a). \qquad (45)$$

On setting $l_1=k_1/k$, this may be written, to first order in v/c, as

$$\tfrac{1}{2}\pi\rho_0\phi_0^2\{l_1k^2a^2\mathrm{L}-(v/c)[(1+l_1^2)k^2a^2\mathrm{L}+l_1^2k^3a^3\mathrm{L}']\}. \qquad (46)$$

If $\phi_0\,d\Omega$ is now taken to represent the velocity potential of waves in a small solid angle $d\Omega$, the total force $\overline{\mathrm{P}}$ on the sphere is obtained by integrating (46) over all directions as

$$\overline{\mathrm{P}}=-\frac{2\pi^2\rho_0\phi_0^2k^2a^2v}{3c}[4\mathrm{L}(ka)+ka\mathrm{L}'(ka)]. \qquad (47)$$

The energy density in the sound flux is

$$\overline{\mathrm{E}}=2\pi\rho_0\phi_0^2k^2, \qquad (48)$$

and (47) may thus be written

$$\overline{\mathrm{P}}=-\frac{\pi a^2\overline{\mathrm{E}}v}{3c}[4\mathrm{L}(ka)+ka\mathrm{L}'(ka)]. \qquad (49)$$

This agrees with (13) and (14).

REFERENCES.

Andrejew, N., 1940, *J. Phys. U.S.S.R.*, **2,** 305.

Frank, F. C., 1948, 1947 *Bristol Conference Report*, p. 46 (London: The Physical Society).

King, L. V., 1934, *Proc. Roy. Soc.* A, **147,** 212.

Lamb, Sir H., 1932, *Hydrodynamics* (Cambridge).

Leibfried, G., 1950, *Z. Physik*, **127,** 344.

Morse, P. M., 1948, *Vibration and Sound*, p. 355 (New York: McGraw-Hill).

Rayleigh, Lord, 1905, *Phil. Mag.*, [vi], **10,** 364; 1910, *Ibid.*, [vi], **20,** 450.

CXIV. *A Note on the Decay of Current in Germanium Diodes.*

By J. R. Tillman and H. Yemm,
The Post Office Engineering Research Station, London*.

[Received October 4, 1950.]

A modulator using germanium crystal diodes, for use in time division multiplex systems, shows an effect which enables a property of the crystal diode—not hitherto reported on—to be investigated.

Fig. 1 (*a*) shows part of a multiplex system consisting of two channels only. $(E_i)_1 = A \sin \omega_1 t$ is the source of modulation for channel 1. At all times other than when a P1 pulse is applied the diode W1A passes about 1 ma. and has low impedance, R_f ($\simeq 150\Omega$), to a.c.; the diode W1B is therefore subject to a "reverse" voltage of about 1 and presents a high impedance, R_r, to a.c. When a P1 pulse is applied W1B passes a pulse of current whose value lies between 2·2 and 3·8 ma. according to the instantaneous value of $A \sin \omega_1 t$; W1A becomes of high impedance. The modulator of channel 2 works in a similar way, with $\sin \omega_2 t$ for $\sin \omega_1 t$, P2 for P1, etc.; its output is connected in parallel with that of channel 1. The pulse length is fixed at 0·2 μsec. but the relative timing of P1 and P2, t_c, is controllable. The trains of pulses, designated HP1, HP2, are together transmitted to the receiving end of the system where they are separated and demodulated by low pass filters. The two outputs $(E_0)_1$ and $(E_0)_2$ substantially reproduce the waveforms of $(E_i)_1$ and $(E_i)_2$ respectively, with equal efficiency. Each, however, contains components, at low levels, in addition to that wanted. These include a crosstalk component; thus $(E_0)_1$ contains a component C_{21} in $\omega_2 t$ and $(E_0)_2$ a component C_{12} in $\omega_1 t$.

The circuit is so designed that the crosstalk ratio C_{12}/E_0, expected, is small: the crystal diode W1B is chosen to have $R_r > 1 M\Omega$ in order that the component of C_{12} arising from the finite values of R_f and R_r is $< E_0/5000$. Only for values of $t_c < 0{\cdot}5$ μsec. will the attenuation distortion at high frequencies, introduced by residual shunt capacitances in the common path, cause C_{12} to exceed $E_0/5000$.

However, in practice, values of C_{12} of up to $E_0/100$ have been noted at $t_c = 1{\cdot}0$ μsec., depending on the sample of diode used as W1B. These values decay approximately exponentially, falling to 1/eth in about 0·4 to 1·2 μsec. (see fig. 2). The use of either a thermionic diode or some other samples of crystal diodes as W1B reduces the crosstalk to about the expected low level residual.

The newly noted crosstalk voltage is always out of phase, by π, with the signal obtained with $t_c = 0$, and hence with any leak due to the finite value of R_r. Any failure on the part of R_r rapidly to reach its steady state value after the cessation of P1 is, therefore, not the cause of the new crosstalk voltage. This conclusion is supported by experiments with the modulator of channel 1 changed to that of fig. 1 (*b*). Here W1B is a thermionic diode, or a crystal giving no significant crosstalk when used as W1B in the circuit of fig. 1 (*a*). Crosstalk still arises when a crystal giving crosstalk in the position of W1B of fig. 1 (*a*) is used as W1D in fig. 1 (*b*), despite the fact that signal leak is now adequately suppressed by W1A and W1B.

---

* Communicated by the Author.

Fig. 1.

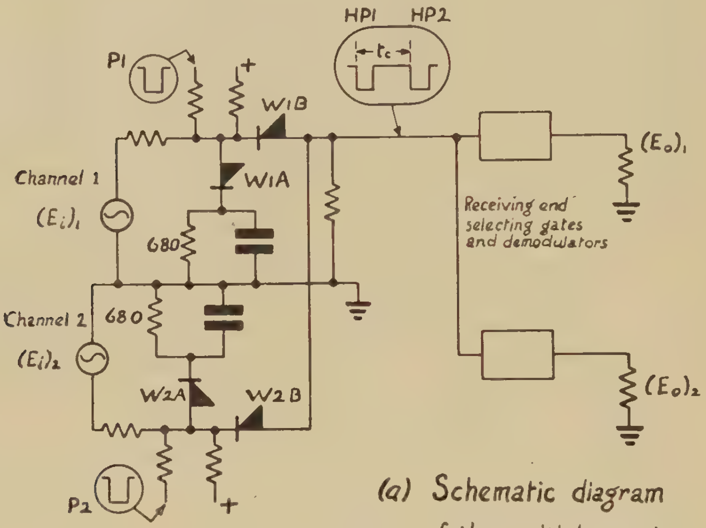

(*a*) Schematic diagram of the multiplex system

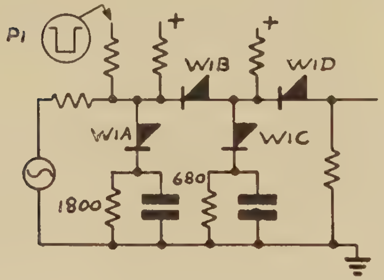

(*b*) The modified modulator

The explanation of the new crosstalk seems to lie in the slowness of dispersal of the charge carriers. But the evidence available on transit times does not afford a simple explanation.

Lark Horovitz (1946) has noted that the rise of current through a germanium diode is noticeable slower than the rise of an applied voltage, when the latter takes place in 10^{-7} sec. ; the decay of his voltage pulses was so slow as to obscure the effect now noted. Douglas and James (in press) suggest that the finite transit time of the charge carriers may be responsible for the decrease of rectification efficiency noted at frequencies above about 10 Mc/s. They have correlated this falling-off with increasing "turnover" voltage, V_t, and have pointed out that turnover voltage may well be a measure of the thickness of the barrier layer. They do not give a value to any transit time, but in view of the fact that the rectification efficiency is not grossly impaired at 50 Mc/s., a time of 10^{-8} sec. rather than 10^{-6} sec. seems to be indicated.

Correlation between the crosstalk voltage and other properties of the crystal diodes was sought, even though the large differences of crosstalk voltage noted (see fig. 2) could be obtained from units differing little in V_t. In general, the crosstalk voltage was smaller the lower the turnover voltage ; two batches of crystal rectifiers type CG5 supplied by Mr. Kinman of the B.T.H. Co., Rugby, having V_t less than 80 volts, consistently gave $C_{12}<E_0/2000$ at $t_c=1\,\mu$sec., whereas some CG4's ($V_t>100$ volts) gave $C_{12}=E_0/200$ at $t_c=1\,\mu$sec. At the same time some other CG4's gave $C_{12}<E_0/3000$. Units with low turnover voltages often have low values of R_r. There seemed no correlation between C_{12} and R_r, however ; in fact, one of the two batches of CG5's giving small values of C_{12} had, in the main, values of R_r of about 100kΩ, whereas the other batch was specially made to have values of $R_r>1$ MΩ.

Fig. 2.

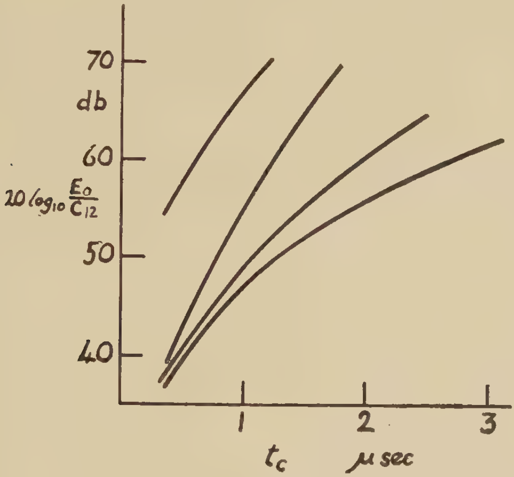

The variation of C_{12} with time for four samples of diode.

Some of these experiments point, therefore, to the effect being independent of the operation of the diodes which gives them their better known properties ; further work based on this indication is in hand.

References.

Horovitz, K. Lark, 1946, National Defence Research Committee Report 14–585, "Preparation of Semi-Conductors and Development of Crystal Rectifiers."

Douglas, R. W., and James, E. G., *Proc. Inst. Elect. Eng.* To be published shortly.

CXV. CORRESPONDENCE.

Superconductivity of Niobium.

By L. C. Jackson and H. Preston-Thomas*.
H. H. Wills Physical Laboratory, University of Bristol.

[Received October 10, 1950.]

Until recently, published data on the properties of the "hard" superconductors were both scanty and inconsistent, particularly in the case of niobium. Studies have been made in this laboratory of the properties of the latter metal, both before and after heat treatment. At the start of the investigation the only published measurements of the critical magnetic field of niobium were those of Daunt and Mendelssohn (1937) in the liquid helium region. A cryostat was therefore constructed to extend the measurements to the region between 4·2° K. and the normal transition temperature, given by Meissner, Franz and Westerhoff (1933) as 9·2° K. A description of this apparatus is to appear elsewhere. Three methods have been used to determine the superconducting properties; resistance measurements, an A.C. inductance method identical in essentials with that of Webber, Reynolds and McGuire (1949) and the ballistic method of Keeley and Mendelssohn (1936). The satisfactory operation of the apparatus was checked by carrying out measurements on pure lead (H.S. Lab. no. 11,116) by the three methods mentioned above.

The critical magnetic fields obtained by the ballistic method for a sample of niobium (Johnson, Matthey and Co. H.S. Lab. no. 1673—spectroscopic examination showed the presence of traces of molybdenum, nickel and silicon together with a very slight trace of aluminium—used as received, not heat treated) are given in fig. 1; curve A, beginning of penetration of magnetic field, curve B completion of penetration. The amount of frozen-in flux is not large, of the order 10 to 15 per cent and varies with the temperature. Curve C of fig. 1 is derived from the alternating magnetic field measurements and agrees closely with the curve determined from measurements of the electrical resistance of niobium tape rolled from the same sample. The spread of the transition curve in the absence of a magnetic field is about 0·07 deg.

---

* Communicated by the Authors.

Curves A′, B′ and C′ of fig. 1 give the corresponding results for another sample of niobium. (Johnson, Matthey and Co. H.S. Lab. no. 2088—trace of silicon and very slight trace of aluminium detected spectroscopically—used as received, no heat treatment.) Curve D, fig. 2 is the critical field curve for niobium recently determined by Cook, Zemansky and Boorse (1950) using the alternating magnetic field method.

Fig. 1.

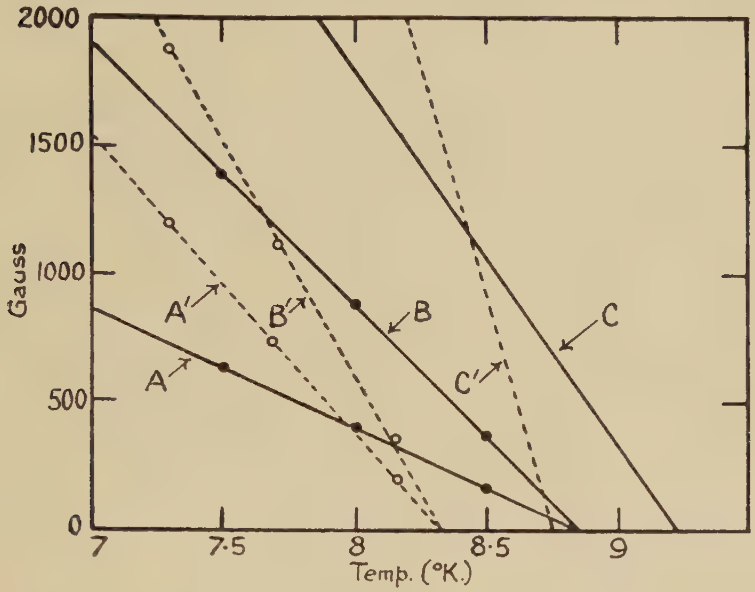

Fig. 2.

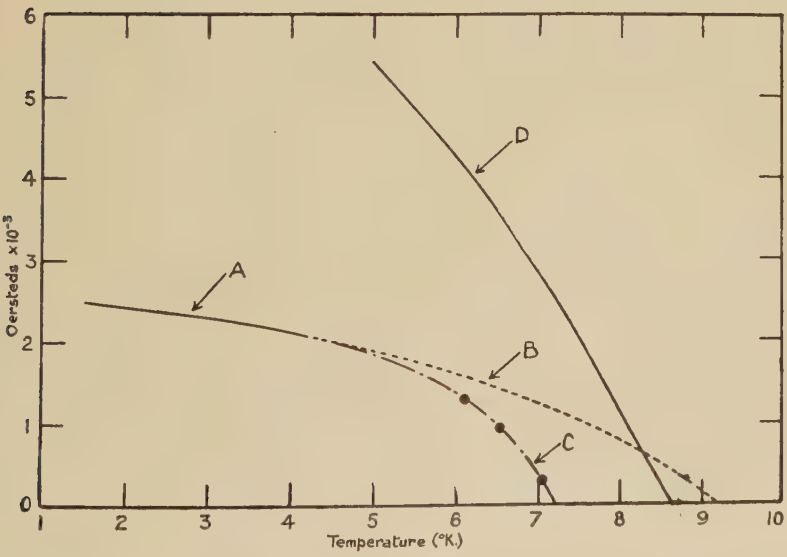

Fig. 2 shows the results of the ballistic method for an older, less pure specimen of niobium (Hilger H.S. Lab. no. 8290—spectroscopic analysis showed the presence of about 0·2 per cent tin and possibly slight traces of copper, iron and gold—used as received, not heat treated). This is also the Lab. no. of the sample used by Daunt and Mendelssohn (1937) in their determination of the critical magnetic field between 1·5 and 4·2° K. Their measurements showed that about 20 per cent of the critical field remained frozen in the specimen. The solid line A in fig. 2 gives their results. The dotted line B is the interpolation between 4·2° K, and the normal transition temperature determined by Meissner *et al.* (1933) as given in Shoenberg's " Superconductivity " (1938). The points on the dotted line C are those at which the penetration of the magnetic field into the specimen is complete. Alternating magnetic field measurements with the same specimen gave a normal transition beginning at approximately 8° K. and becoming complete at approximately 7° K. The spread of the transition appears to become smaller as the applied field is increased but it is still too great to provide useful data for the H_c—T curve. The material is, moreover, so brittle that it is impossible to roll tape specimens from it suitable for resistance measurements.

There is a considerable similarity between the above results for niobium and recently published observations on vanadium by the alternating magnetic field method (Webber *et al.* 1949) and the ballistic method (Wexler and Corak 1950).

The form of the results given above—for samples 1673 and 2088—can be explained on the basis of an extension of Mendelssohn's model of an " alloy type " superconductor (Mendelssohn 1935). This considers such a superconductor to have filaments running through it which have a much higher critical field (H_f) than that characteristic of the bulk of the material (H_c). This results in the internal field of the specimen lagging behind that which would occur in the absence of the filaments by an amount (H_a) depending on the capacity of the filaments to carry resistanceless currents.

If we now also postulate a higher normal transition temperature (T_{cf}) for the filaments than that for the bulk metal (T_c) and an inhomogeneous distribution of the frozen-in flux the following results are obtained.

The value of H_a is a function of the temperature. A graph of the frozen-in flux, which in our use of the ballistic method is equal to $2H_a$, against temperature shows that for the two niobium specimens (nos. 1673 and 2088) for which complete data have been obtained this function may be represented by $H_a = K(T_{cf} - T)$ where K is a constant. In alternating magnetic field measurements the width of the transition curve is a function of dH_a/dT.

The critical field of the filament material is given by the alternating magnetic field (and resistance) curve (curve C) and that of the bulk material by the higher of the ballistic curves (curve B). The transition temperatures and the initial slopes of the critical field curves are given in Table I.

TABLE I.

Sample	T_c°K.	T_{cf}°K.	$\frac{dH_f}{dT}$	$\frac{dH_c}{dT}$	$\frac{dH_a}{dT}$	n
1673	8·85	9·20	1,300	1,050	45	0·55
2088	8·35	8·75	4,000	1,900	60	0·39

The inhomogeneous distribution of field in the material results in an effective bulk demagnetizing factor ($4\pi n$) for the specimen. If the higher and lower of the two values of the critical field slopes given by the ballistic measurements (curve B and curve A) are dH_c/dT and dH_b/dT respectively we have $dH_b/dT=(1-n)\,(dH_c/dT)$.

REFERENCES.

COOK, D. B., ZEMANSKY, M. W., and BOORSE, H. A., 1950, *Phys. Rev.*, **78,** 820.
DAUNT, J. G., and MENDELSSOHN, K., 1937, *Proc. Roy. Soc.* A, **160,** 127.
MEISSNER, W., FRANZ, H., and WESTERHOFF, H., 1932, *Ann. der. Phys.*, **17,** 593.
MENDELSSOHN, K., 1935, *Proc. Roy. Soc.* A, **152,** 34.
WEBBER, R. T., REYNOLDS, J. M., and MCGUIRE, T. R., 1949, *Phys. Rev.*, **76,** 293.
WEXLER, A., and CORAK, W. S., 1950, *Phys. Rev.*, **79,** 737.

Lattice Sums for Ionic Crystals.

By F. C. FRANK,
The H. H. Wills Physical Laboratory, University of Bristol.*

[Received November 1, 1950.]

THE most important of lattice sums have by now been evaluated, at the cost of considerable labour: but there are still many which one often needs or would like to know, especially for bounded lattices or for off-lattice points. It is not too late to welcome an improved method.

In so far as the ionic charges can be regarded as distributed with spherical symmetry about the lattice points, they may be replaced (so far as the electrostatic field at any exterior point is concerned) by any other spherical distributions about the same points, or by point charges. This note is concerned with the evaluation of the potentials of the resulting lattice arrays of positive and negative point charges.

Consider the NaCl lattice as an example. Let space be divided into cubical cells, each having one ion at its centre. The point charge (positive, say) is equivalent to the sum of two charge groups: (*a*) 8 point charges of $e/8$, placed at the corners of the cell, and (*b*) one charge of e

---

* Communicated by the Author.

at the centre together with eight of $-e/8$ at the corners. We require the sum of the lattice sums for charge systems (*a*) and (*b*). The summing of (*a*) is easy, since the charges cancel at all interior points and in all cube faces and cube edges of the crystal. In a cuboid bounded by $\{001\}$ faces there remain from (*a*) only eight charges of $\pm e/8$ at the corners, situated $\frac{1}{2}\sqrt{3}\,.\,d$ cube-diagonally outwards from the corner lattice-points, and having the signs of the corner ions. An [0, 1] step in the cube face has no charge, but a Kossel kink in the step has four charges of $\pm e/8$, situated at the corners of a square of side d (the interionic distance) midway between the last ion in the incomplete step and the first missing one ; *i. e.* at the corners of the end face of the cube cell surrounding the last ion. The sign of these charges is that of the last ion.

The charge groups (*b*) are equivalent to multipole systems at the lattice points, those of lowest order being hexadecapoles. Their potentials therefore decay with distance like r^{-5}. Moreover they are of alternating sign. The lattice sum is therefore highly convergent, and can be neglected save for a few lattice points close to the point of observation. However, it is not necessary to evaluate these multipole lattice sums as such. One may cut out a cuboid containing the non-negligible lattice points and evaluate by direct summation the potential due to the ions within it, together with charges of $\pm e/8$ at its corners (each opposite in sign to the ion in that corner), and at any other corners and kinks of the crystal. This is the required sum. If the calculation is to be physically realistic there are of course surface double layers, due to the Verwey effect, and additional multipoles due to ionic distortions which also have to be brought into account. These effects apart, the corner and kink charges arising from (*a*) reproduce exactly the charge, dipole, quadrupole and octopole moments of a bounded crystal.

To test the method we use it to evaluate

$$\log_e 2 = 0{\cdot}693\ 147\ 181\ \ldots .$$

This corresponds to the potential at the next lattice point of a semi-infinite one-dimensional sodium chloride crystal. By our method the $(n+1)$th approximation (requiring the addition of $n+1$ terms) is

$$\sum_{p=1}^{n} (-1)^{p+1} p^{-1} + [(2n+1)^2+2]^{-\frac{1}{2}},$$

$n=0$ (no summation) gives 0·57735, $n=1$ gives 0·69849, $n=4$ gives 0·693085, $n=8$ gives 0·693145 and the 6th place would then be correctly estimated by inspecting the alteration of terms.

As a second test we evaluate Madelung's sum for NaCl, which gives the potential at a lattice point due to the rest of the ions in an infinite crystal. Madelung evaluated this as 1·74(2) and Emersleben as 1·74755(7±2). Treating no ions individually we have

$$2/\sqrt{3} = 1{\cdot}1547\ \ldots$$

Treating individually the first cube shell of ions we have

$$-6+12/\sqrt{2}-8/\sqrt{3}+2/3\sqrt{3}=1\cdot748619\ldots$$

Taking one more shell (a total of 10 terms) gives 1·747626. The four term sum is sufficiently accurate for most physical applications.

Besides possessing the merits of simple physical interpretation and easy application to bounded crystals or to summation for off-lattice points, the method appears to be more efficient for computation than any hitherto suggested, whether of higher or lower mathematics. The former methods provide admirably convergent series, but the labour comes in interpolating values of uncommon functions which are not tabulated at close intervals. The neutral shell summation methods of Evjen and Slater (split shells) and of Højendahl (eccentric shells) converge much more slowly, having errors of nearly 2 per cent (1·77681) and 0·3 per cent (1·75177) after adding 9 and 12 terms respectively.

When this method is applied to lattices of lower symmetry, the residual charge groups (*b*) will have multipoles of lower order, *e. g.* quadrupoles, making the convergence of the method slower (alternating r^{-3} terms). It may then be profitable to repeat the device, so placing quadrupoles at kink and corner points to secure rapid convergence in the residue.

REFERENCES.

EMERSLEBEN, O., 1923, *Phys. Zeits.*, **24,** 73, 79.
EVJEN, H. M., 1932, *Phys. Rev.*, **39,** 680.
HØJENDAHL, K., 1938, *K. Danske. Videns. Selskab.*, **16** (2), 138.
MADELUNG, E., 1918, *Phys. Zeits.*, **19,** 524.
PAULING, L., 1945, *Nature of the Chemical Bond* (Ithaca N.Y.: Cornell Univ. Press), p. 338 (contains general references).
SLATER, J. C., 1939, *Introduction to Chemical Physics* (New York : McGraw-Hill), 387.
VERWEY, E. J. W., 1946, *Rec. Trav. Chim. des Pays-Pas*, **65,** 521.

October 7, 1950.

Some Extensions in the Use of Resistance Thermometry in the Study of Gaseous Explosions.

By A. S. LEAH, C. ROUNTHWAITE and D. BRADLEY,
University of Leeds*.

[Received October 20, 1950.]

IN a recent communication to the *Philosophical Magazine* (1950, **41**, 729–30) Messrs. Daish, Fender and Woodall have raised some interesting points concerning a method we described in a recent paper to this Journal (1950, **41**, 468–77) for determining flame gas temperatures by the resistance thermometer method. For reasons of economy in space we were constrained to omit a lengthy discussion of certain aspects of the work, but it would now seem profitable to add a few words in amplification.

---

* Communicated by the Authors.

We are entirely in agreement with them when they assert that there will be considerable distortion of the temperature-time curves due to lag in response of the wires. Indeed, it was for this reason that full allowance was made for the effect as they will find by referring to expression (1) on page 472 of our paper. In actual fact, the thermal capacities of the two types of wires are very little different and although the effect of the quartz owing to the low conductivity of quartz, this is hardly an appreciable effect coating might be expected to increase the time constant of the coated wires, as we found from the results of a simple experiment.

Fig. 1.

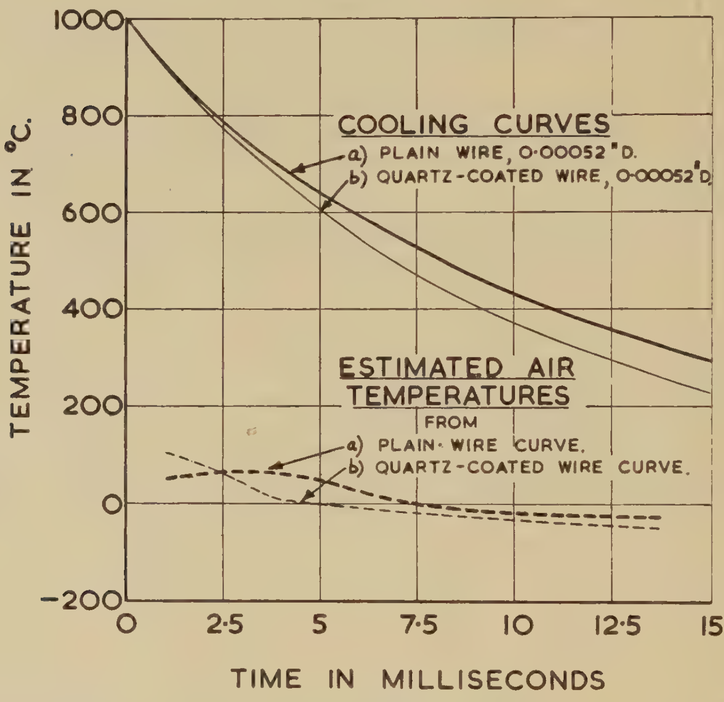

A quartz-coated wire and then a plain platinum wire, each of 0.0005 inch diameter, were heated electrically up to a high temperature in stagnant air at atmospheric pressure within a closed vessel. A rapid-acting relay switch was made to cut off the heating current and switch the wire into the oscillograph recording circuit described in the previous paper. The oscillograph trace gave the cooling curves in each case and these, with the temperature scale, are reproduced in fig. 1. It will be noted that the cooling rates are not very different, in fact the time constants are 0.0100 sec. for the coated wire and 0.0115 sec. for the plain wire.

These tests, however, provide a very excellent check upon the accuracy of our method of correction, as will be seen from the broken line curves of fig. 1, which give the temperature of the surrounding air as deduced by exactly the same analysis as that employed in the estimation of flame gas temperatures. This temperature should have been the constant value of approximately 20° C. The discrepancy is not large even under the exacting conditions at the beginning of our records when the wire temperature was of the order of 1000° C. In fact, these experiments gave us full confidence in the method of correction we used.

Thus, we disagree with the speculation of Messrs. Daish, Fender and Woodall that there is a large difference in the time constants of the two wires and that this difference could account for the catalytic heating we observed on the plain platinum wires, especially as full correction for the small difference there is in time constant was made.

Concerning the effect of cooling of the wires by the heavier leads there is little we need add to what has already been said. We chose a length of 1 inch for our wires not for ease of measurement but because repeated tests had shown that with lengths of 1 inch or more, the cooling effect was negligibly small for the quartz-coated wires. For plain wires, calculations and tests have shown that the mean temperature exceeds 97 per cent of the maximum temperature, suggesting an error of 3 per cent. But in our experiments this error is automatically corrected because the method of calibration simulates the explosive conditions very closely in so far as cooling by the leads is concerned (the leads, of course, do not heat up appreciably in 2 seconds in view of the large time constant).

The problem of determining the true convection losses from wires in the explosions is one with which we have experienced difficulty. It is true that in the explosion there will be a certain degree of forced convection past the wires, as we pointed out previously. In addition, it may be that the equilibrium natural convection conditions have not had time to become fully established, although we have photographic evidence of the bodily convective rise of the whole flame volume in times of only a few milliseconds. Nevertheless, experiments made by Mr. N. Carpenter in these laboratories (unpublished) have shown that the heat loss from electrically heated, 0.0005 inch diameter wires, in a stream of flame gas (at varying temperatures) hardly varies at all with gas velocity past the wires up to values of 30 in. per sec. This phenomenon appears to indicate that the loss of heat is mainly dependent upon conduction through a stagnant film of gas around the wires. In view of this, we feel confident that our assumptions regarding the convective heat loss will involve no substantial error in the derived temperatures and catalytic heating rates.

CXVI. *Notices of New Books and Periodicals received.*

Structure of Molecules and the Chemical Bond. By J. K. Syrkin and M. E. Dyatkina, translated and revised by M. A. Partridge and D. O. Jordan. (Butterworths Scientific Publications.)

This book describes the properties of the chemical bond and interprets them in terms of quantum mechanics.

It is clearly addressed mainly to experimental workers and therefore starts with an account of the quantum mechanics necessary to interpret the experimental results, the less essential part of the mathematics being relegated to an appendix. There are two different approximate solutions of the wave equation that will give a semi-quantitative interpretation of the chemical bond; these are the electron-pair bond plus resonance approximation, and the molecular orbital approximation. Both these approximations are described and compared, but in the subsequent discussion of experimental results it is usually the first approximation that is used. The latter chapters of the book consist of a large amount of experimental data on the chemical bond and the interpretation of this data in terms of the theory given in the first chapters. The subjects considered include bond lengths, bond energies, dipole moments, van der Waals forces, and the general arrangement of bonds in complex molecules and crystals. A minor criticism is that in Chapter 10 the word polarization and the symbol P are used in an unusual sense that makes the discussion rather puzzling at first.

Although this book is addressed mainly to experimentalists, the theoretical worker will also find the collection of experimental data of great value. A. F. D.

Calculating Instruments and Machines. By D. R. Hartree. (Urbana: University of Illinois Press.)

The English edition of this book is now obtainable, price 21*s*. Published by Cambridge University Press, London.

BOOKS RECEIVED.

A new scientific publication has been received—' Geochimica et Cosmochimica Acta', edited with the assistance of an Advisory Board. Published by Butterworth-Springer Ltd. (London). Price per vol. (approx. 300 pp.) £3 10*s*. 0*d*.

[The Editors do not hold themselves responsible for the views expressed by their correspondents.]

INDEX TO VOL. XLI.

ADAMS (N.), temporary increase in neutron compound of cosmic rays, 503.

——, —— (with Braddick, H. J. J.), 505.

Atkins (K. R.) and Osborne (D. V.), the velocity of second sound below 1° K., 1078.

Alpha particles, short range emission.—II. and III. (Burcham and Freeman), 337, 873.

——, —— .—IV. (Freeman), 1225.

——, ——, from break up of ^{8}Li (Baxter, Burcham and Paul), 937.

Alternant hydrocarbons, molecular-orbital calculations (de Heer), 370.

Atmospheric absorption of heat radiation by water vapour (Cowling), 109.

Atmospherics, use to study very long radio waves (Gardner), 1259.

Atomic oxygen in CO explosions (Leah, Rounthwaite and Bradley), 478.

Avery (D. G.), some optical properties of evaporated layers of silver, copper and tin, 1018.

Baxter (A. S.), Burcham (W. E.) and Paul (E. B.), short range alpha particles from the break up of ^{8}Li, 937.

Benson (A. C.), *see* Runcon *et al.*, 783.

Berz (F.), potentials derived from axial values in electron optics, 209.

Betatron-starting in electron synchrotrons (Wilkins), 34.

Books, new:—Bangham (D. H.), Progress in coal science, 1197; Born (M.) and Green (H. S.), General theory of liquids, 506; Bridgman (P. W.), The nature of physical theory, 619; Butterfield (H.), Origins of modern science, 107; Cauchois (Yvette), Les spectres de rayons X et la structure electronique de la matière, 731; Centre National de la Recherche Scientifique colloquia, 730; Chandrasekhar (S.), Radiactive transfer, 855; Computation Laboratory, Tables of inverse hyperbolic functions, 620; Crowther (J. A.), Ions, electrons and ionizing radiations, 208; Dingle (H.), Practical applications of spectrum analysis, 1196; Dyson (G.), Organic chemistry for advanced students, 856; Fishenden (M.) and Saunders (O. A.), Introduction to heat transfer, 732; Geochimica et Cosmochimica Acta, 1292; Hartree (D. R.), Calculating instruments and machines, 1292; Haward (R. N.), Strength of plastics and glass, 312; Jánossy (L.), Cosmic rays, 856; Johnson (M.), Astronomy of stellar energy and decay, 1197; Jessop (H. T.) and Harris (F. C.), Photoelasticity, 620; (Kniper (G. P.), Atmospheres of the earth and planets, 508; Kruyt (H. R.) Colloid science, 312; Lanczos (C.), Variational principles of mechanics, 620; Von Lane (M.), History of Physics, 856; Lothian (G. F.), Absorption spectrophotometry, 855; Martin (T.), Faraday's discovery of electromagnetic induction, 208; Milne (W. E.), Numerical calculus, 619; Milne-Thomson (L. M.), Theoretical hydrodynamics, 411; M.I.T. Technical report, supersonic flow around cones, 107; Mott (N. F.) and Massey (H. S. W.), Theory of atomic collisions, 108; Partington (J. R.), Advanced treatise on physical chemistry, Vol. I., 107; Reiner (M.), Twelve lectures on theoretical rheology, 412; Richardson (E. G.), Dynamics of real fluids, 732; Rides (J. F.), Electronic Engineering Master Index 1947–8, 619; Schelkunoff (S. A.), Applied mathematics for engineers and scientists, 108; Shannon (C. E.) and Weaver (W.), Mathematical theory of communications, 508; Sidgwick (N. V.), The chemical elements and their compounds, 731; Stoker (J. J.), Non linear vibrations in mechanical electrical systems, 731; Syrkin (J. K.) and Dyatkina (M. E.), Structure of molecules and the chemical bond, 1292; Tolansky (S.), Introduction to atomic physics, 208; Treloar (L. R. G.), Physics of rubber elasticity, 412; Wiener (N.), Stationary Time Series with engineering applications, 411.

Bourne (L.) and Hill (R.), rolled sheet in tension and cupping tests, 671.

Bowden (K. F.), effect of eddy viscosity on ocean waves, 907.

Braddick (H. J. J.), *see* Adams and Braddick, 505.

Bradley (D.), *see* Leah *et al.*, 468, 478, 1289.

Brinkley (T. A.), *see* Titterton and Brinkley, 500.

Buchdahl (H. A.), thermal equilibrium in gravitational sphere fluid, Tolman's equation, of 362.

Burcham (W. E.) and Freeman (Joan M.), emission of short range alpha particles from light elements under proton bombardment.—II., 337.

——, —— .—III., 873.

——, *see* Baxter, Burcham and Paul, 937.

Burge (E. J.) and Jackson (L. C.), transfer rates for surface films of HeII, 205.

Burton (P. C.), *see* Farnell, Burton and Hallama, 157, 545.

Calnan (E. A.) and Clews (C. J. B.), deformation textures in face centred cubic metals, 1085.

Camerini (U.), Fowler (P. H.), Lock (W. O.) and Muirhead (H.), nuclear transmutations produced by cosmic particles of great energy.—Part IV., 413.

Canetti (G. S.), *see* Whitehead and Canetti, 988.

Carlson (A. G.), Hooper (J. E.) and King (D. T.), cosmic ray particles of great energy.—Part V. The neutral mesons, 701.

Chess, programming a computer for playing (Shannon), 256.

Chester (W.), propagation of sound waves in an open-ended channel, 11.

Clegg (J. A.) and Davidson (I. A.), radio echo method for measurement of heights of meteor trails, 77.

Clews (C. J. B.), *see* Calnan and Clews, 1085.

Cockroft (A. L.), *see* Curran *et al.*, 517.

Coleman (B. L.), propagation of E.M. disturbances along a thin wire in stratified medium, 276.

Communication theory and physics (Gabor), 1161.

Compressible fluid, velocities and local Mach numbers (Tempest), 382.

Conn (G. K. T.), *see* Donovan and Conn, 770.

Corinaldesi (E.) and Field (G.), scattering of pseudoscalar charged mesons by nucleons.—II., 364.

Cosmic Radiation, heavy nuclei (Dainton and Kent), 963.

—— ——, mass of charged particles in (Franzinetti), 86.

—— ——, nuclear transmutations by particles of great energy.—Pt. III. (Fowler), 169.

—— —— .—Pt. IV. (Camerini, Fowler *et al.*), 413.

—— —— .—Pt. V. (Carlson, Hooper and King), 701.

—— ——, primary, cut off in energy spectrum (Gething), 495.

—— ——, stars in emulsions, gap measurement (Hodgson), 725.

—— ——, protons and α particles in stars (Perkins), 138.

Cosmic rays, temporary increase in neutron component (Adams), 503; (Adams and Braddick), 505.
—— ——, double stars (Li), 1152.
—— ——, stars, latitude effect (Lattimore), 961.
—— ——, single protons, origin (Lattimore), 819.
—— ——, momentum and sign of fast particles (Moral), 1058.
Coster (D.) and Kiestra (S.), fine structure near the Fe K-absorption edges in various oxides of Fe, 144.
Cowling (T. G.), atmospheric absorption of heat radiation by water vapour, 109.
Curran (S. C.), Cockroft (A. L.) and Insch (G. M.), investigation of soft radiation.—VII. Energy per ion-pair for slow electrons in gases, 517.
Dainton (A. D.) and Kent (D. W.), heavy nuclei of cosmic radiation, 963.
Daish (C. B.), Fender (D. H.) and Woodall (A. J.), use of resistance thermometers for rapidly changing temperatures, 729.
Daniel (Vera), order disorder transitions in mixed ketones, 631.
Darwin (Sir C.), some conformal transformations involving elliptic functions, 1.
Davidson (I. A.), *see* Clegg and Davidson, 77.
Davies (I. L.), *see* Woodward and Davies, 1001.
Deformation, inhomogeneous, of a plastic lamina (Hill), 733.
——, textures in metals (Calnan and Clews), 1085.
Density variations in aluminium (Snoek), 1188.
Di-iso-electronic row (Richter), 983.
Dilworth (Miss C. C.), Goldsack (S. J.), Goldschmidt-Clermont (Y.) and Levy (F.), magnetic deflection of fast charged particles in the photographic emulsion, 1032.
Domb (C.), the statistics of correlated events.—I., 969.
Donovan (B.) and Conn (G. K. T.), electrical conductivity of bismuth fibres.—II. Anomalies in the magneto-resistance, 770.
Eddy viscosity, in turbulent shear flow (Townsend), 890.
—— ——, effect on ocean waves (Bowden, 907.
Elasticity, theory in general coordinates (Green and Zerna), 313.
Electrical conductivity of bismuth fibres.—II. (Donovan and Conn), 770.
—— noise, statistical analysis (MacDonald), 814.
Electromagnetic disturbances, propagation along thin wire (Coleman), 276.
Electron optics, potentials derived from axial values (Berz), 209.
—— streams, transit-time.—II. (MacDonald), 863.
Elliptic functions, conformal transformations involving (Darwin), 1.
Ellyett (C. D.), influence of high altitude winds in meteor trail ionization, 694.
Energy distributions behind decaying shocks.—I. (Lighthill), 1101.
—— release in reaction ^{7}Li(dp)^{8}Li (Paul), 942.
—— states, calculation by uncertainty relations (Soh), 851.
Evaporated layers, optical properties (Avery), 1018.
——, interferometric study (Faust), 1238.
Farnell (G. C.), Burton (P. C.) and Hallama (R.), fluorescence of silver halides at low temperatures.—Pt. I. The pure halides, 147.
——, ——.—Pt. II. Mixed halides, 545.
Faust (R. C.), interferometric study of evaporated silver films, 1238.
Fender (D. H.), *see* Daish *et al.*, 729.
Ferromagnetics, domain boundaries (Lilley), 792.
Field (G.), *see* Corinaldesi and Field, 364.
Fine structure near K absorption edges in oxides of Fe (Coster and Kiestra), 144.
Fission, search for negative proton (Scott and Titterton), 918.
——, spontaneous from natural uranium (Whitehouse and Galbraith), 429.

Fluids, quantum mechanics (Price), 948.
Fluorescence of silver halides.—Pts. I. and II. (Farnell, Burton and Hallama), 157, 545.
Fourth order meson - equation (Thirring), 653.
Fowler (P. H.), *see* Camerini *et al.*, 413.
——, nuclear transmutations produced by cosmic ray particles of great energy, 169.
Frank (F. C.), lattice sums for ionic crystals, 1287.
——, structure of a crystal surface, 200.
Franzinetti (C.), mass of charged particles of cosmic radiation, 86.
Freeman (Miss J. M.), *see* Burcham and Freeman, 337, 873.
——, emission of short range alpha particles.—IV. $^{19}F(p\alpha)^{16}0$, 1225.
Frölich (H.), Pelzer (H.) and Zieman (S.), properties of slow electrons in polar materials, 221.
Fürth (R.), the "velocity" of brownian movement, 1255.
Gabor (D.), communication theory and physics, 1161.
Galbraith (W.), *see* Whitehouse and Galbraith, 429.
Gamma radiation, production of pairs (Hooper and King), 1194.
Gardner (F. F.), use of atmospherics to study propagation of very long radio waves, 1259.
Garrett (C. G. B.), thermal conductivity of potassium chrome alum below 1° K., 621.
Gas containing soundwaves, force on moving body (Nabarro), 1270.
—— discharge, energy distribution of electrons (Haigh and Smith), 557.
Geomagnetic radial variation, experimental determination (Runcorn, Benson, Moore and Griffiths), 783.
Germanium dioxide, decay of current (Tillman and Yemm), 1281.
Gething (P. J. D.), cut off in energy spectrum of primary cosmic rays, 495.
Gisolf (J. H.), back current in blocking-layer rectifiers, 754.
Goldsack (S. J.), *see* Dilworth, *et al.*, 1032.
Goldschmidt-Clermont (Y.), *see* Dilworth *et al.*, 1032.
——, fields of spherical symmetry (Narliker and Singh), 152.
Gravitational sphere of fluid, thermal equilibrium (Buchdahl), 362.
Green (A. E.) and Zerna (W.), theory of elasticity in general coordinates, 313.
Greenhow (J. S.), fluctuation and fading of radio echoes from meteor trails, 682.
Griffin (L. J.), observations on unimolecular growth steps on crystal surfaces, 196.
Griffiths (D. H.), *see* Runcorn, Benson, Moore and Griffiths, 783.
Gross (B.), inversion of Laplace transform, 543.
Guest (P. G.), orthogonal polynomials in least squares fitting of observations, 124.
Haigh (C.) and Smith (T.), energy distribution of electrons in positive columns, 557.
Hallama (R.), *see* Farrell, Burton and Hallama, 157, 545.
Harding (J. B.), further evidence for the existence of τ-mesons, 405.
Hardness, effect of specimen size in measurement (Hill), 745.
de Heer (J.), influence of overlap integral in molecular-orbital calculations for alternant hydrocarbons, 370.
Helium II, velocity of flow in creeping film (Jackson and Henshaw), 1081.
——, transfer rates for surface films (Burge and Jackson), 205.
Henshaw (D. G.), *see* Jackson and Henshaw.
Herdmann (J.), scattering of 90 MeV. neutrons by alpha particles, 444.
Hodson (A. L.), Loria (A.) and Ryder (N. V.), control of Wilson cloud chamber by means of an internal counter, 826.
Hodgson (P. E.), gap measurement of cosmic ray stars in emulsions, 725.
Hooper (J. E.), *see* Carlson *et al.*, 701.
Hooper (J. E.) and King (D. T.), multiple processes in the production of pairs of electrons by γ radiation, 1194.

Hill (R.), the inhomogeneous deformation of a plastic lamina in a compression test, 733.
——, theoretical investigati ns of the effect of specimen size in the measurement of hardness, 745.
——, theory of plastic bulging of a metal diaphragm by lateral pressure, 1133.
Insch (G. M.), *see* Curran *et al.*, 517.
——, calibration of proportional counters by excitation of fluorescence radiation, 857.
Interaction of collodial particles.—III. (Levine), 53.
Intrinsic block structure and the strength of metals (Paterson), 410.
Ionic crystals, lattice sums (Frank), 1287.
Ionized gas, refractive index and radiactive processes (Westfold), 509.
Ionizing particles, energy losses in photographic plate (Messell and Ritson), 1129.
Jackson (L. C.) and Henshaw (D. G.), the velocity of flow of He II in the creeping film, 1081.
—— and Preston-Thomas (H), superconductivity of Niobium, 1284.
—— *see* Burge and Jackson, 205.
Jacobs (J. A.), relaxation methods applied to plastic flow.—I. Notched bar under tension, 349.
—— .—II., 458.
Jelley (J. V.), the radioactivity of F^{20}.—I., 1199.
Jones (H.), effect of electron concentration on lattice spacing in magnesium solid solids, 663.
Kent (D. W.), *see* Dainton and Kent, 963.
Kiestra (S.), *see* Coster and Kiestra, 144.
King (D. T.), *see* Carlson *et al.*, 701.
——, *see* Hooper and King, 1194.
Laminar boundary layer on solids of revolution (Whitehead and Canetti), 988.
Laplace transform, inversion (Gross), 543.
Lattimore (S.), latitude effect of cosmic ray stars, 961.
Lattimore (S.), origin of single cosmic ray protons, 819.
Leah (A. S.), Rounthwaite (C.) and Bradley (D.), resistance thermometry in the study of gaseous explosions, 468, 1289.
—— ——, atomic oxygen in CO explosions, 478.
Levine (S.), interaction of colloidal particles.—III. Free energy of double layers, 53.
Levy (F.), *see* Dilworth *et al.*, 1032.
Li (T. T.), double stars due to cosmic rays, 1152.
Liebmann (G.), method of mapping of vector potential distributions in axially symmetrical systems, 1143.
Lighthill (M. J.), energy distribution behind decaying shocks, 1101.
Lilley (B. A.), energies and widths of domain boundaries in ferromagnetics, 792.
Littauer (R. M.), the radioactivity of F^{20}.—II., 1214.
Lock (W. O.), *see* Camerini *et al.*, 413.
Loria (A.), *see* Hodson, Loria and Ryder, 826.
MacDonald (D. K. C.), the statistical analysis of electrical noise, 814.
——, transit-time phenomena in electron streams.—II., 863.
MacKay (D. M.), quantal aspects of scientific information, 289.
Magnesium, cohesive energy of metallic (Raines), 568.
—— solid solutions, effect of electron concentrations (Jones), 663.
Magnetic deflection of fast charged particles in the photographic emulsion (Dilworth *et al.*), 1032.
—— spectrometer (Rae), 525.
Mapping vector potential distributions (Liebmann), 1143.
Matthews (P. T.), S-matrix for meson-nuclear interactions, 185.
Meltzer (B.), noise in current-carrying ohmic conductors, 393.
Menon (M. G. K.), Muirhead (H.) and Rochat (O.), reactions produced by slow negative π-mesons, 583.
Mesons, further evidence for the existence of τ-mesons (Harding), 405.

Mesons, reactions by slow negative π (Menon *et al.*), 583.
——, π nature of neutral particle in decay (O'Ceallaigh), 838.
Messel (H.) and Ritson (D. M.), energy losses of particles at relativistic velocities in the photographic plate, 1129.
Meteor trails, fluctuation and fading of radio echoes (Greenhow), 682.
——, measurement of height (Clegg and Davidson), 77.
—— trail ionization, influence of wind (Ellyett), 694.
Mixed ketones, order disorder transitions (Daniel), 631.
Moore (A. F.), *see* Runcorn, Benson, Moore and Griffiths, 783.
Moyal (J. E.), momentum and sign of fast cosmic ray particles, 1058.
Muirhead (H.), *see* Camerini *et al.*, 413.
——, *see* Menon *et al.*, 583.
Nabarro (F. R. N.), force on body moving uniformly through gas containing sound waves, 1270.
Narliker (V. V.) and Singh (K. P.), gravitational fields of spherical symmetry, 152.
Noise in ionization chamber pulse amplifiers (Wilson), 66.
——, in ohmic conductors (Meltzer), 393.
Nucleus, position of lowest dipole-level (Touschek), 849.
O'Ceallaigh, nature of neutral particle in decay of the π-meson, 838.
Orthogonal polynomials in lead squares (Guest), 124.
Osborne (D. V.), *see* Atkins and Osborne, 1078.
Papapetrou (A.), four dimensional generalization of Wilson's hypothesis, 399.
Paterson (M. S.), intrinsic block structure and strength of metals, 410.
Paul (E. B.), energy release in the reaction ^{7}Li(dp)^{8}Li, 942.
——, *see* Baxter, Burcham and Paul, 937.
Pelzer (H.), *see* Fröhlich, Pelzer and Zienan, 221.
Perkins (D. H.), emission of protons and alpha-particles in high energy cosmic ray stars, 138.
Pippard (A. B.), kinetics of phase transition in superconductors, 243.
Plastic flow, relaxation methods (Jacobs), 349, 458.
——, bulging of metal diaphragm (Hill), 1133.
Preston-Thomas (H.), *see* Jackson and Preston-Thomas, 1284.
Price (P. J.), quantum mechanics of fluids, 948.
Properties of slow electrons in polar materials (Fröhlich, Pelzer and Zienan), 221.
Proportional counters, calibration (Insch), 857.
—— ——, in magnetic field (West and Rothwell), 873.
Protons, fast, loss of energy in matter (Taylor), 966.
Radar information, theory (Woodward and Davies), 1001.
Radioactive corrections in non-relativistic limit (Thirring), 1193.
Radioactivity of F^{20}.—I. (Jelley), 1199.
—— —— .—II. (Littauer), 1214.
Rae (E. R.), magnetic spectrometer of large solid angle, 525.
Raimes (S.), cohesive energy of metallic magnetium, 568.
Rectifiers, back current in blocking-layer (Gisolf), 754.
Resistance thermometry in rapidly changing temperatures (Daish *et al.*), 729.
—— —— in gaseous explosions (Leah *et al.*), 468, 1289.
Richter (A. F.), the di-iso-electronic row and effective charge in L isorows, 983.
Ritson (D. M.), *see* Messel and Ritson, 1129.
Rochat (O.), *see* Menon *et al.*, 583.
Rolled sheet in tension and cupping tests, directional properties (Bourne and Hill), 671.
Rothwell (Miss P.), *see* West and Rothwell, 873.
Rounthwaite (C.), *see* Leah *et al.*, 468, 478, 1289.

Runcorn (S. K.), Benson (A. C.), Moore (A F.) and Griffiths (D. H.), experimental determination of the geomagnetic radial variation, 783.
Ryder (N. V.), *see* Hodson, Loria and Ryder, 826.
Scattering of 90 MeV. neutrons by alpha particles (Heidmann), 444.
—— of pseudoscalar charged mesons (Corinaldesi and Field), 364.
Scientific information, quantal aspects of (Mackay), 289.
Scott (J. M. C.) and Titterton (E. W.), search for negative proton in fission, 918.
Second sound below 1° K., velocity (Atkins and Osborne), 1078.
Shannon (C. E.), programming a computor for playing chess, 256.
Singh (K. P.), *see* Narliker and Singh, 152.
S-matrix for meson-nuclear interactions (Matthews), 185.
Smith (T.), *see* Haigh and Smith, 557.
Snoek (J. L.), density variations in aluminium, 1188.
Soft radiations VII. (Curran, Cockroft and Insch), 517.
Soh (H. P.), calculation of energy states by uncertainty relations, 851.
Sound waves, propagation in an open-ended channel (Chester), 11.
Specific heat of free electrons in metals (Wohlfarth), 534.
Statistics of correlated events.—I. (Domb), 969.
Structure of a crystal surface (Frank), 200.
Superconductors, kinetics of phase transition (Pippard), 243.
Superconductivity of Niobium (Jackson and Preston-Thomas), 1284.
Taylor (A. E.), loss of energy of fast protons in matter, 966.
Tempest (R. K.), velocities and local Mach numbers in flow of compressible fluid, 382.
Thermal conductivity of potassium chrome alum below 1° K. (Garrett), 621.
Thirring (W.), fourth order meson-equation, 653.
——, radiative corrections in non-relativistic limit, 1193.
Thorum-232, binary and ternary photofission (Titterton and Brinkley), 500.
Tillman (J. R.) and Yemm (H.), decay of current in germanium dioxide, 1281.
Titterton (E. W.), *see* Scott and Titterton, 918.
—— and Brinckley (T. A.), binary and ternary photofission of Th-232, 500.
Touschek (B. F.), position of lowest dipole-level of a nucleus, 849.
Townsend (A. A.), eddy viscosity in turbulent shear flow, 890.
Unimolecular growth steps on crystal surfaces (Griffin), 196.
"Velocity" of brownian movement (Fürth), 1255.
West (D.) and Rothwell (Miss P.), proportional counters in magnetic field; isomerism of Br^{80}, etc., 873.
Westfold (K. C.), refractive index and classical radiative processes in an ionized gas, 509.
Whitehead (L. G.) and Canetti (G. S.), the laminar boundary layer on solids of revolution, 988.
Whitehouse (W. J.) and Galbraith (W.), energy spectrum from spontaneous fission of natural uranium, 429.
Wilkins (J. J.), betatron-starting in electron sychrotrons, 34.
Wilson cloud chamber, control (Hodson, Loria and Ryder), 826.
Wilson (R.), noise in ionization chamber pulse amplifiers, 66.
Wilson's hypothesis, four dimensional generalization (Papapetrou), 399.
Wohlfarth (E. P.), influence of exchange and correlation forces on specific heat of electrons in metals, 534.
Woodall (A. J.), *see* Daish *et al.*, 729.
Woodward (P. M.) and Davies (I. L.), theory of information, 1001.
Yemm (H.), *see* Tillman and Yemm, 1281.
Zerna (W.), *see* Green and Zerna, 313.
Zienan (S.), *see* Fröhlich, Pelzer and Zienan, 221.

END OF THE FORTY-FIRST VOLUME.

PRINTED BY TAYLOR AND FRANCIS, LTD., RED LION COURT, FLEET STREET, E.C.4

U. of Haw.